PENNSYLVANIAN DEPOSITIONAL SYSTEMS AND GEOLOGY OF THE PECOS RIVER CANYON, NORTHERN NEW MEXICO

by

Sonja Heuscher

A thesis submitted to the faculty of
The University of Utah
in partial fulfillment of the requirements for the degree of

Master of Science

in

Geology

Department of Geology and Geophysics

The University of Utah

December 2007

THE UNIVERSITY OF UTAH GRADUATE SCHOOL

SUPERVISORY COMMITTEE APPROVAL

of a thesis submitted by

Sonja Heuscher

This thesis has been read by each member of the following supervisory committee and by majority vote has been found to be satisfactory.

Chair: A. Chan

David A. Dinter

Cari L.

THE UNIVERSITY OF UTAH GRADUATE SCHOOL

FINAL READING APPROVAL

To the Graduate Council of the University of Utah:

I have read the thesis of Sonja Heuscher in its final form and have found that (1) its format, citations, and bibliographic style are consistent and acceptable; (2) its illustrative materials including figures, tables, and charts are in place; and (3) the final manuscript is satisfactory to the Supervisory Committee and is ready for submission to The Graduate School.

Date

Marjorie A. Chan
Chair: Supervisory Committee

Approved for the Major Department

Marjorie A. Chan
Chair/Director

Approved for the Graduate Council

David S. Chapman
Dean of The Graduate School

ABSTRACT

Stratigraphic, sedimentologic, and field mapping data from the Pecos River Canyon of northern New Mexico are used to interpret Pennsylvanian depositional systems, their relation to Ancestral Rocky Mountain paleogeography, the general geologic history, and Cenozoic geomorphic processes. The Pennsylvanian La Pasada and Alamitos Formations record primarily subtidal and shallow water marine sedimentation on the Pecos platform at the edge of an actively subsiding tectonic basin. The 203 m of strata in the study area consist of 59% siltstone, sandstone, and conglomerate, 25% carbonate, and 16% shale. Seven shoaling upward cycles and eight gravity flow pulses observed in the studied section reflect an interplay of intrabasinal and extrabasinal controls. Using existing stratigraphic data, subsidence history calculation based on an estimate of isostatic subsidence indicates that ~450 m of tectonic subsidence occurred at the Pecos platform throughout the Pennsylvanian (~165 m during the Desmoinesian). The large amount of tectonic subsidence during deposition of the studied interval and decrease in number of shallowing upward cycles proximal to the basin bounding fault show that tectonics had an influence on the succession of strata at Pecos. East to southeast lateral thinning of strata and south directed paleocurrents indicate that the Ancestral Rocky highland was located northwest of the study area. This highland location supports the idea that the Pecos-Picuris fault, a major fault approximately 6 km northwest of the study area, may have been an active Pennsylvanian basin-bounding fault.

Paleocurrents show bidirectional north and south transport in tabular and trough crossbedded mixed carbonate-siliciclastic sediment with mud drapes and reactivation surfaces indicating reworking by tidal currents. Stacked channels and large clasts in conglomerates indicate high-energy sediment pulses from flood

plumes and rapidly shifting channels in close proximity to the Uncompahgre Uplift. However, the presence of open marine Pennsylvanian invertebrate fossils and trace fossils in many of these conglomeratic deposits and interbedded carbonates shows deposition on a carbonate shelf. The arkosic composition of sandstones and abundance of granitic and metamorphic clasts in the conglomerates reveal basement uplift of igneous and metamorphic provenance. Thus, the clastic sediments are interpreted as tidal influenced fan-delta deposits on the carbonate Pecos platform, southeast of the Uncompahgre highlands of the Ancestral Rocky Mountains.

Geologic mapping revealed previously unmapped faults, folds, and surficial deposits. The folding and faulting are likely associated with the Laramide Orogeny and Rio Grande Rift respectively. A large anticline and smaller superimposed folds show northwest to southeast crustal shortening. Northeast striking steep normal faults with an average offset of ~9 m parallel major normal faults associated with formation of the Rio Grande Rift. Geologic structure exerts important controls on geomorphology of the Pecos River Canyon and surrounding area. The canyon is asymmetric with the east rim higher than the west rim due to a southwest structural dip across the canyon. Because the east rim of the canyon is ~60-150 m higher than the west rim, the east side of the canyon is subject to a higher rate of physical weathering. A large area (~1.9 km^2) below the east rim contains a combination of landslide, rockfall, and colluvial material. This study enhances our understanding of the sedimentology and stratigraphy of the Pennsylvanian Pecos shelf adjacent to the Ancestral Rocky Mountains in northern New Mexico and provides insight into geomorphic and structural styles of the Pecos River Canyon and the surrounding region.

CONTENTS

ACKNOWLEDGMENTS

I acknowledge several individuals for their contributions to this investigation. A special thanks to Tim McElvain for making this study possible through his financial support. An American Association of Petroleum Geologists Foundation 'Grant in Aid' provided financial support for field expenses. My advisor, Marjorie Chan, and committee members, David Dinter and Cari Johnson, provided helpful suggestions and research guidance. Tony Ekdale (University of Utah) and Bob Bereskin (Bereskin and Associates, Inc) assisted with identification of trace and body fossils. The help of Abraham Emond and Zach Heuscher as field assistants is greatly appreciated. GPR equipment was provided by Dr. Gerard Schuster, University of Utah. Travis Crosby provided expertise in operating the GPR equipment. Last, but not least, thanks to George Broome for providing field accommodations.

CHAPTER 1

GEOLOGY AND GEOMORPHOLOGY OF THE PECOS RIVER CANYON

1.1 Introduction

This chapter presents an interpretation of the geology and geomorphology of the Pecos River Canyon in northern New Mexico. A detailed sedimentologic interpretation is included in Chapter 2. Tim McElvain (personal communication, 2004) put forth the idea that brecciated surficial deposits in the canyon may have originated from a meteorite impact. Thus, a detailed geologic mapping and geomorphic study was completed to assess the potential of the area as a meteorite impact site. An understanding of geologic structure provided a framework for correlation of stratigraphic sections, thus, facilitating a stratigraphic and sedimentologic study of the area. The objectives of this research include the following:

1. Detailed geologic mapping and interpretation of geologic history.

2. Study of the geomorphology and surficial deposits to assess the potential of the area as a meteorite impact site.

3. Delineating facies, determining the Pennsylvanian depositional environment and paleogeography, discussed in Chapter 2.

The study area lies east of Santa Fe, New Mexico, and just north of the town of Pecos, New Mexico, along the Pecos River. The study area location is shown in Figure 1.1 (~8 by 5 km in area). Physiographically, the study area is just east of the Rio Grande Rift and at the southern end of the Sangre de Cristo Mountains (Figure 1.2).

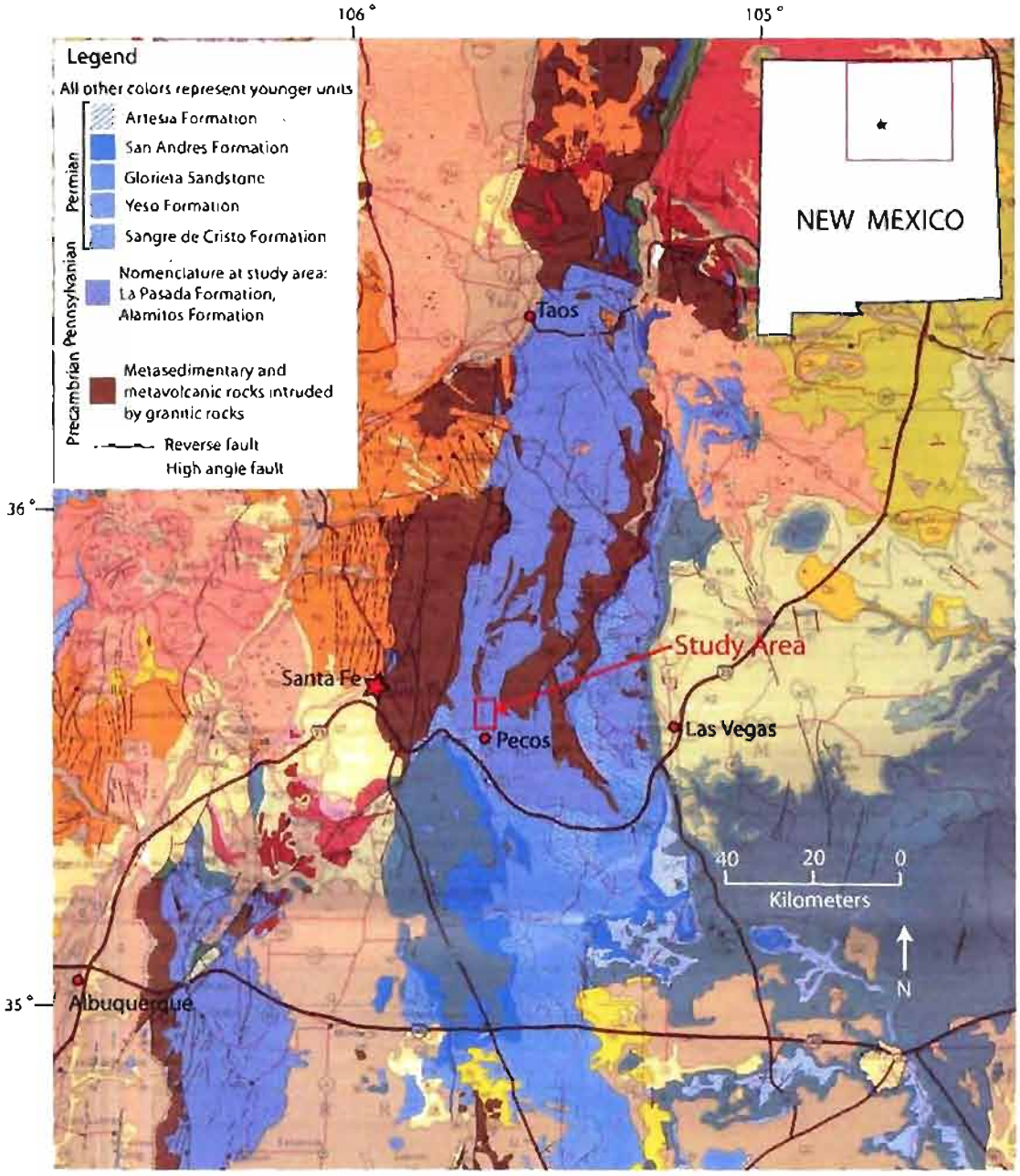

Figure 1.1. Generalized geologic map modified from *New Mexico Geological Society* [1996] with study area locality. The blue areas are Pennsylvanian and Permian sedimentary bedrock. Dark brown areas are Precambrian rock. Other colors represent younger geologic units.

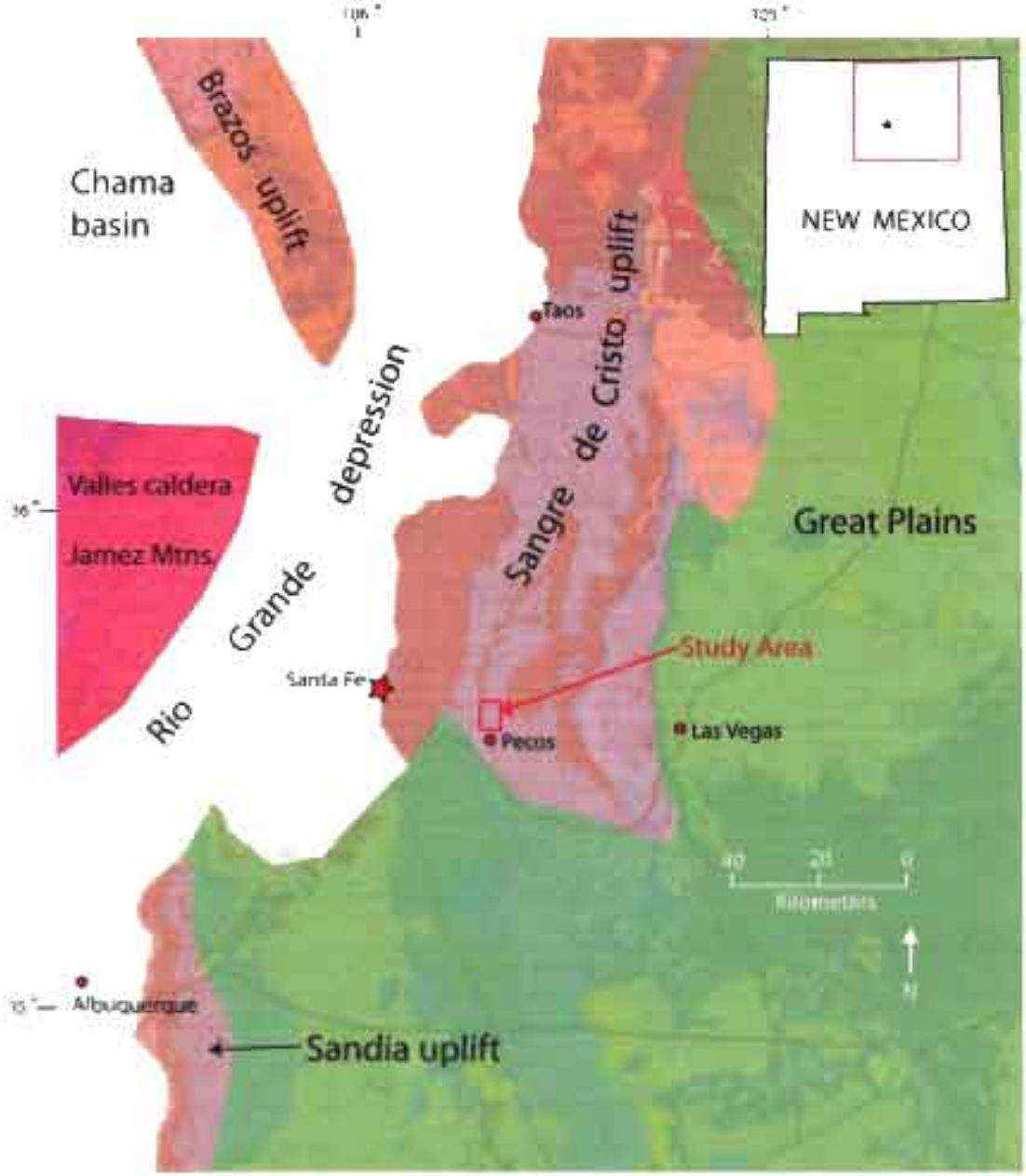

Figure 1.2 *Generalized physiographic map after New Mexico Geological Society (1996), overlain on Figure 1.1*

Outcrop in the study area consists of Middle Pennsylvanian sedimentary rocks of the Alamitos Formation and La Pasada Formation. Pennsylvanian outcrop covers a large area of the Sangre De Cristo mountains in northern New Mexico (Figure 1.1). The map area consists of approximately 26 km^2 surrounding brecciated surficial deposits at the potential meteorite impact site shown in Figure 1.3. The study site is located in the Santa Fe National Forest and on private land. The elevation varies from 2134 to 2560 m (7000 to 8400 ft), and vegetation consists primarily of ponderosa pine, juniper, and scrub oak.

This area lies in the Pecos Quadrangle, which was mapped previously by the United States Geologic Survey (USGS) [*Johnson*, 1973] and the New Mexico Bureau of Geology and Mineral Resources [*Reed and Rawling*, 2002]. Figure 1.4 shows a section of the USGS quadrangle map at the study area. A large region just north of the study area was mapped by *Miller et al.* [1963].

Stratigraphic nomenclature of Pennsylvanian rocks in this area has been controversial, primarily due to rapid lateral facies changes and variations in unit thicknesses. Several systems of stratigraphic nomenclature have been proposed for the Pennsylvanian outcrop in the region; three for the Pecos area alone [*Brill*, 1952; *Sutherland*, 1963; *Johnson*, 1973; *Baltz and Myers*, 1984] (Figure 1.5). The nomenclature system proposed by *Sutherland* [1963] was used in the most recent geologic map of the Pecos Quadrangle [*Reed and Rawling*, 2002] and the type sections for the Alamitos and La Pasada Formations are located within a few kilometers of the study area. Thus, the nomenclature system of *Sutherland* [1963] was chosen for this study.

In assessing the potential of the locality as a meteorite impact site, previously unmapped faults, folds, river terraces, and large landslides were documented. In addition, study of the stratigraphy and sedimentology reveals information about the Middle Pennsylvanian depositional environments in the area, depositional processes, and regional paleogeography.

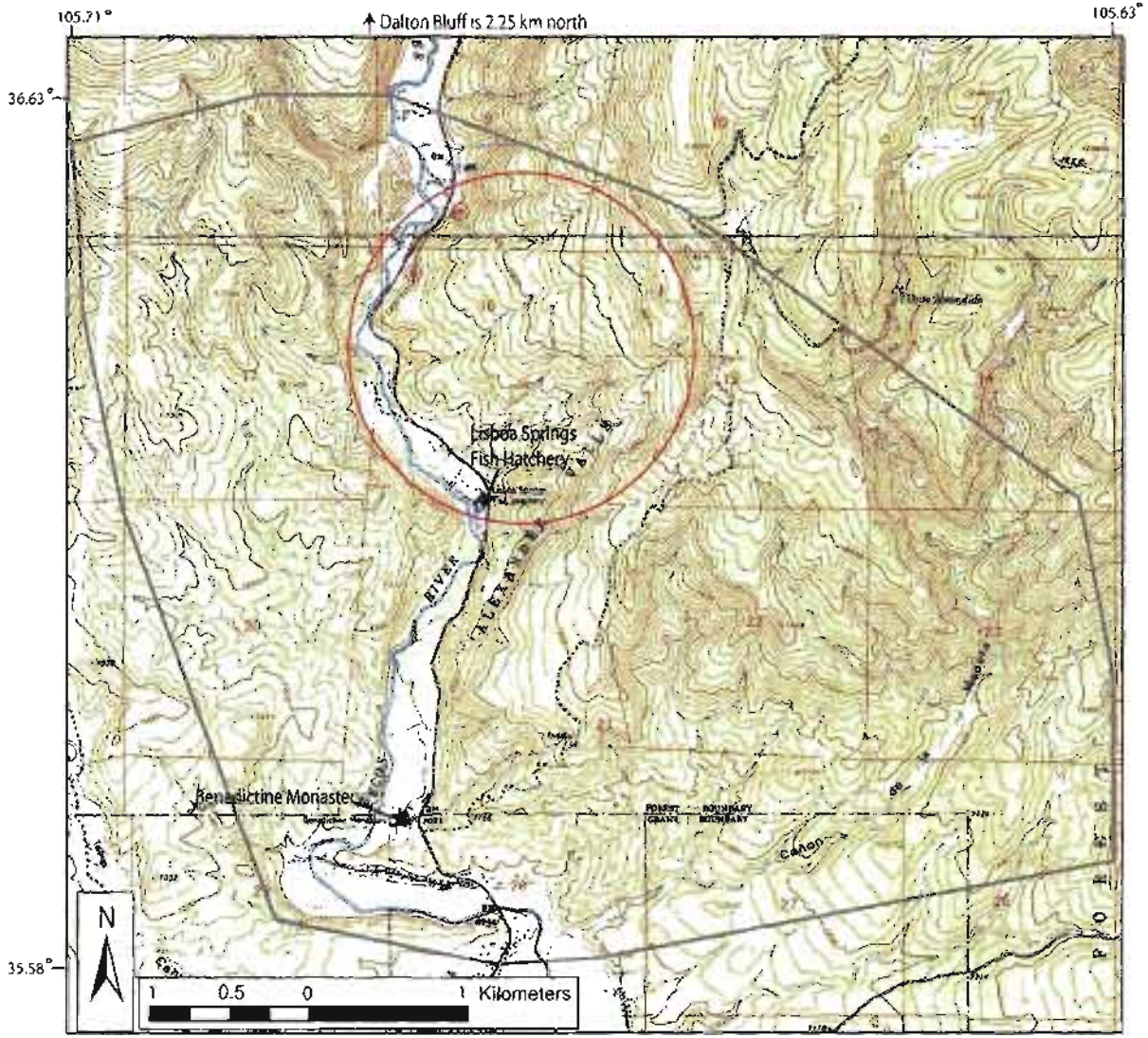

Figure 1.3. Topographic map showing mapped area boundary (gray line), proposed meteorite impact site and brecciated surficial deposits (red circle), and important place names. *United States Geological Survey* [1961] base map.

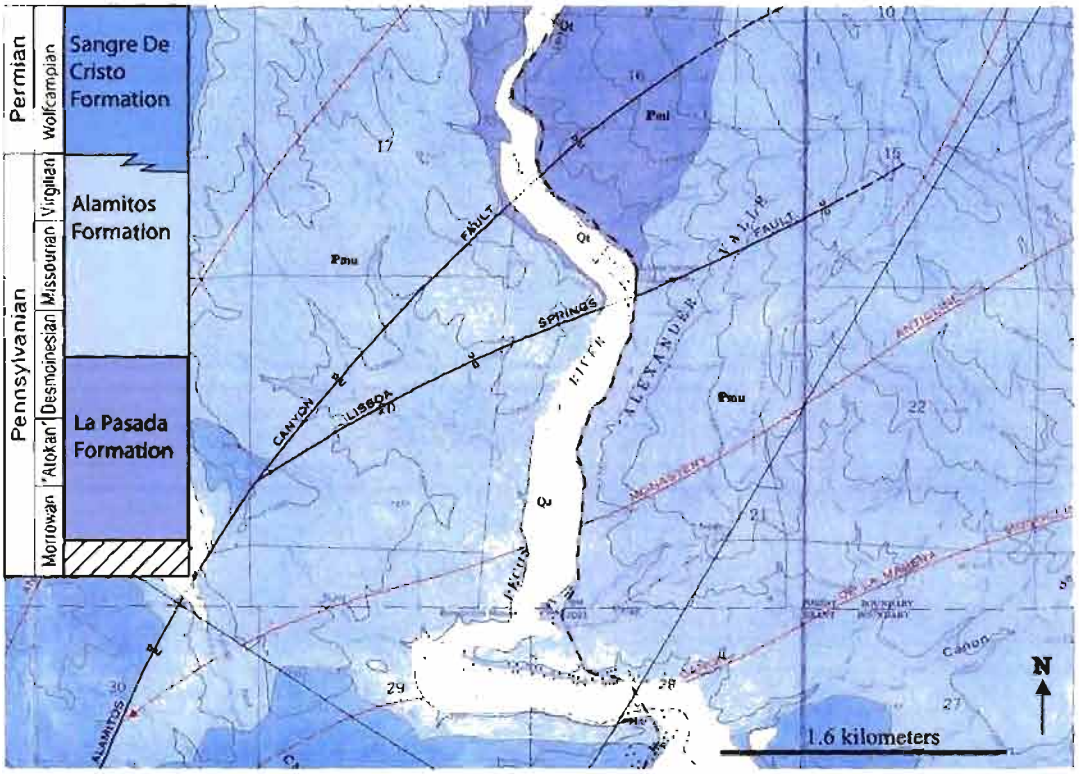

Figure 1.4. Stratigraphic nomenclature used in this study color-coded to the USGS geologic map of part of the study area [*Johnson*, 1973]. Figure 1.5 summarizes nomenclature history in the Pecos area.

	Pennsylvanian					Permian
	Morrowan	Atokan	Desmoinesian	Missourian	Virgillian	
Brill, 1952	Sandia Formation		Gray Limestone Member	Arkosic Limestone Member / Madera Formation		Sangre de Cristo Formation
Johnson, 1973	Sandia Formation		Lower Madera Formation (Pml)	Upper Madera Formation (Pmu)		
Sutherland, 1963	La Pasada Formation cliff 2, cliff 3, cliff 4 ..... cliff 7			Alamitos Formation cliff 8		
Terminology used for this study	La Pasada Formation (P_{lp}) cliff 2, cliff 3, cliff 4 ..... cliff 7			Alamitos Formation (P_{al}) Lower and upper cliffs		

Figure 1.5. Stratigraphic nomenclature for the Pecos area and terminology used in this study. Time interval of the section mapped in this study is indicated by the blue dashed box.

1.2 Methods

Methods for the geologic and geomorphic study of the area include geologic field mapping with a Brunton compass and topographic map, measuring stratigraphic sections, field notes and sketches, Global Positioning System (GPS) waypoints, airphoto analysis, a Ground Penetrating Radar (GPR) survey, thin section analysis, and study of surficial deposits in man-made cuts. Bedrock and surficial deposits were mapped on a topographic base and digitized using ArcGIS 9.1. The La Pasada and Alamitos Formations were subdivided into smaller informal mappable units to create a detailed geologic map and to aid stratigraphic study. Six GPR line surveys were collected with either a 50 or 100 MHz antenna at 0.5 m sample spacing.

Geologic mapping in the area is challenging. The following list describes several challenges and how they were addressed:

- Because the area is forested, outcrop is limited. However, there are several cliffs and tributary canyons with excellent outcrop. Exposed beds were traced along cliffs whenever possible.

- Mapping in a forested area can often cause difficulties in finding an exact location on a topographic map due to the inability to see reference landmarks. To overcome this problem, coordinates from a hand-held GPS unit were occasionally used to locate a position on a map. GPS waypoints proved useful for organizing data in addition to marking locations. Five hundred and eleven waypoint locations were marked in this study (Figure 1.6). A detailed waypoint map and annotated list of waypoints are included in Appendix A.

- The stratigraphy of the area has several repetitive rock types as well as lateral facies changes; thus, determining stratigraphic level and correlations can be challenging. To overcome these problems, beds were physically walked out where possible, and where walking out beds was not possible, detailed observations and notation of the stratigraphy aided in mapping the adjacent areas. Marker beds and fossils (e.g., chert, reworked rugose coral, brachiopod-rich arkose) were useful for correlating strata.

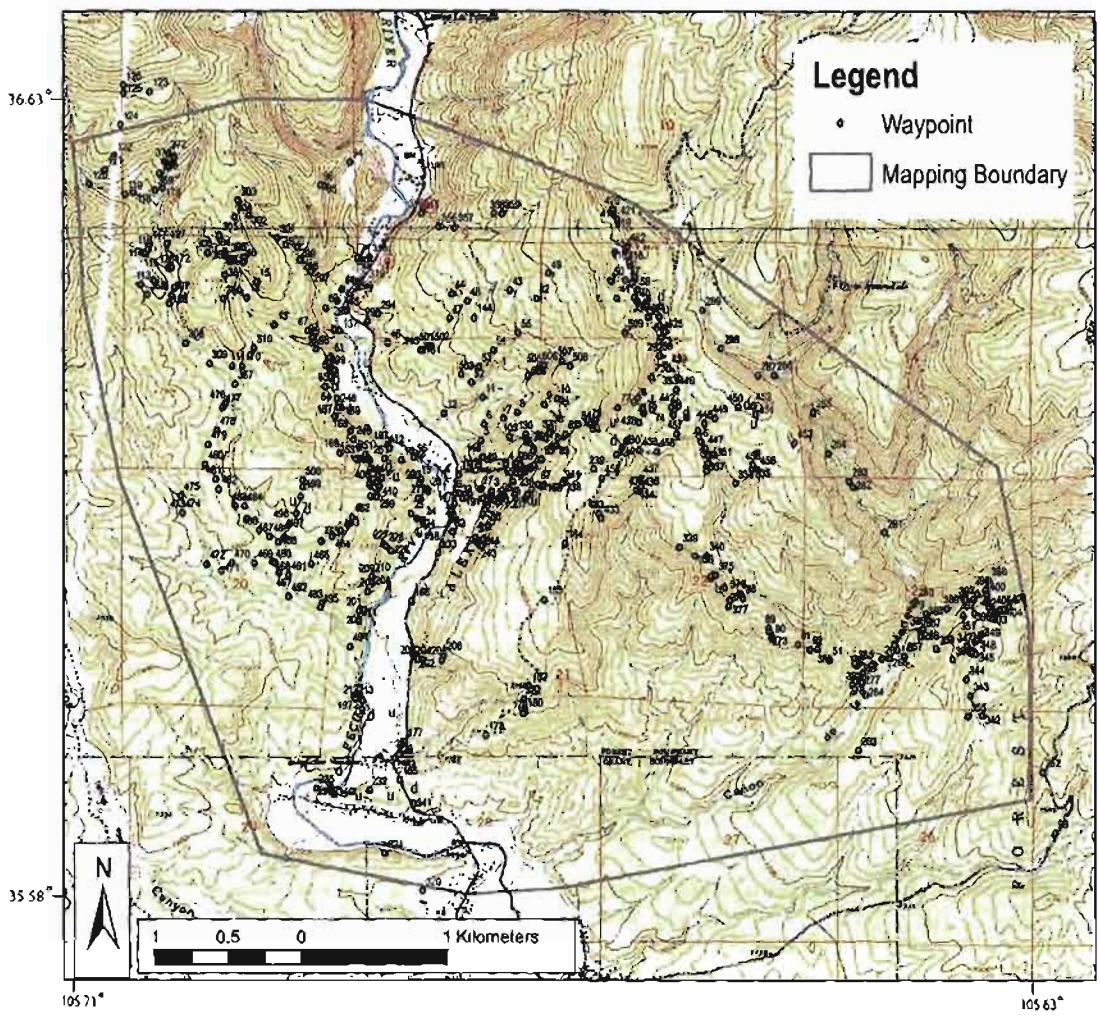

Figure 1.6. Waypoint locations (511) on *United States Geological Survey* [1961] topographic map. A detailed waypoint map is included in Appendix A.

1.3 Results and Discussion

1.3.1 Geology

In this study, the upper 140 m of the La Pasada Formation and all of the Alamitos Formation (388 m) were mapped (Figure 1.5). At the type localities, the La Pasada Formation consists of 67% limestone, 24% shale and siltstone, and 9% sandstone and conglomerate [*Miller et al.*, 1963]. The Alamitos Formation consists of 21% limestone, 50% shale and siltstone, and 29% sandstone and conglomerate [*Miller et al.*, 1963]. These sediments were deposited throughout the Pennsylvanian Period on a carbonate platform adjacent to the Ancestral Rocky Mountains [*Miller et al.*, 1963; *Casey*, 1980; *Ude*, 1992; *Gong*, 1992; *Baltz and Myers*, 1999]. The overlying latest Pennsylvanian to Permian Sangre De Cristo Formation consists of alluvial arkoses and redbeds. Permian, Triassic, Jurassic, and Cretaceous sediments (Yeso, Glorieta, San Andres, Artesia, Moenkopi, Santa Rosa, Chinle, Entrada, Todilto, Morrison, Dakota, Graneros, Greenhorn, and Carlie Formations) were deposited in the area and then eroded or partially eroded during the Laramide orogeny (~80-55 Ma) [*Tweto*, 1980; *Reed and Rawling*, 2002; *Baltz and Myers*, 1999].

Figures 1.7, 1.8, and 1.9 show the detailed geologic map and cross section produced as a result of this study. A CD-ROM containing the geologic map and waypoint data is included in Appendix A. The upper part of the La Pasada Formation was subdivided into three informal units (P_{lp1}, P_{lp2}, P_{lp3} in ascending stratigraphic order) and the Alamitos Formation was subdivided into three units as well (P_{al1}, P_{al2}, P_{al3} in ascending stratigraphic order). These subdivisions are based on stratigraphic breaks that can be traced throughout the study area. The exact stratigraphic breaks for these units are shown in Chapter 2 of this study. *Sutherland* [1963] measured the type stratigraphic section for the La Pasada Formation at Dalton Bluff, 2.4 km north of the north boundary of the study area. Sutherland numbered the cliffs on the bluff sequentially, cliff 1 through cliff 8 (Figure 1.5). Since these cliffs are laterally continuous, cliffs 4-8 dip south from Dalton Bluff

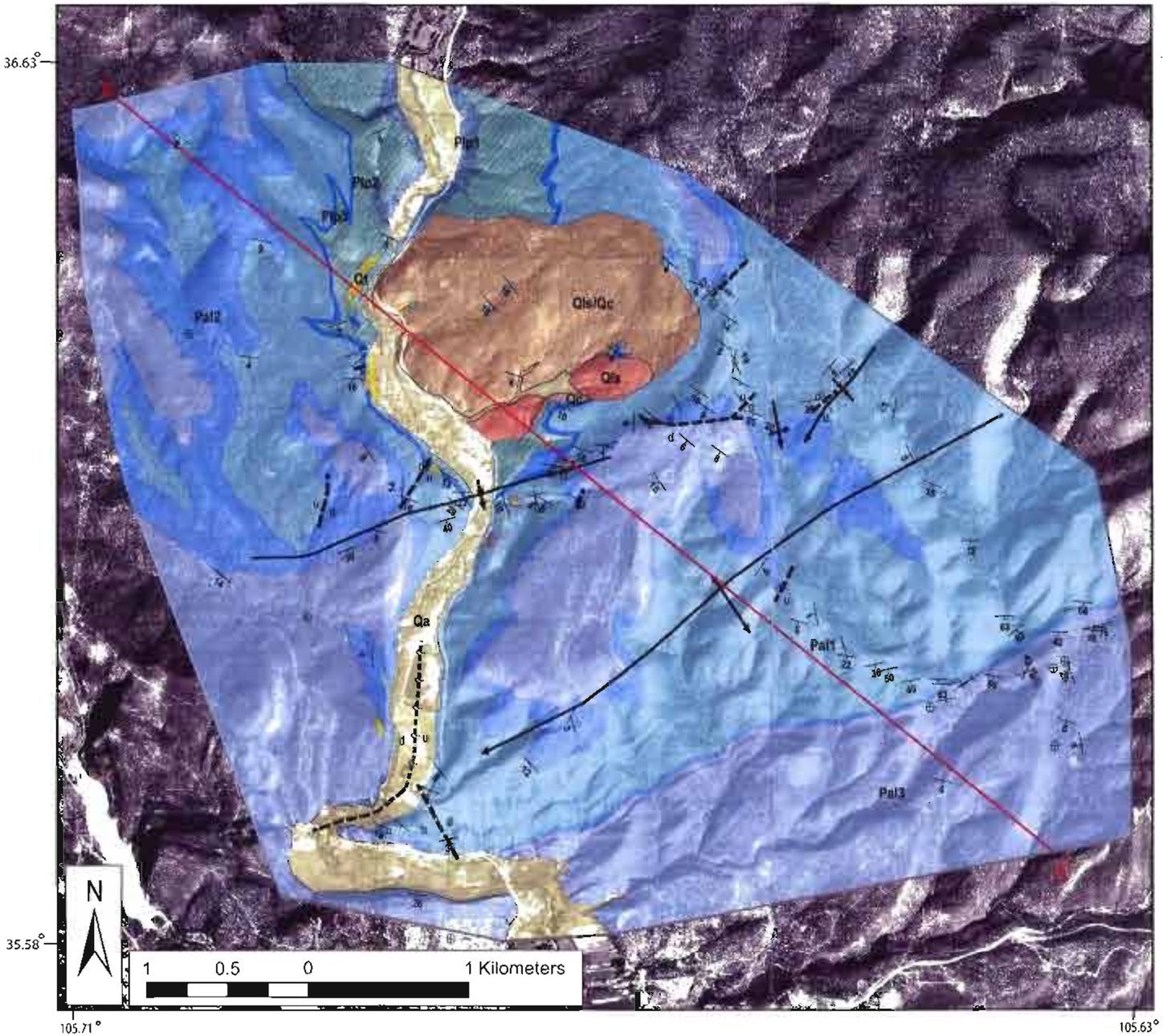

Legend

Mapped units

Quaternary

- Q_a Quaternary alluvium
- Q_c Quaternary colluvium
- Q_{ls} Quaternary landslide
- Q_{ls}/Q_c Quaternary landslides and colluvium
- Q_t Quaternary terrace

Pennsylvanian

- P_{al3} Pennsylvanian Alamitos Formation, outcrop above the top of the upper cliff
- P_{al2} Pennsylvanian Alamitos Formation, outcrop below the top of the upper cliff and above the top of the lower cliff
- P_{al1} Pennsylvanian Alamitos Formation, outcrop below the top of the lower cliff
- P_{lp3} Pennsylvanian La Pasada Formation, outcrop above the top of the chert in cliff 7
- P_{lp2} Pennsylvanian La Pasada Formation, outcrop below the top of the chert in cliff 7 and above cliff 4
- P_{lp1} Pennsylvanian La Pasada Formation, outcrop below the top of cliff 4

- Anticline, plunging, asymmetric
- Monocline
- Anticline, plunging, symmetric
- Syncline, plunging
- u / d Fault, 'u' on upthrown side, 'd' on downthrown side
- Fault, uncertain
- Approximate contact location
- Map area boundary
- 10 Strike and Dip
- Horizontal bed
- 80 Overturned bed, showing dip
- Vertical bed
- Line of cross section

Figure 1.7. Photogeologic map of the Pecos Canyon study area. USGS air photo base.

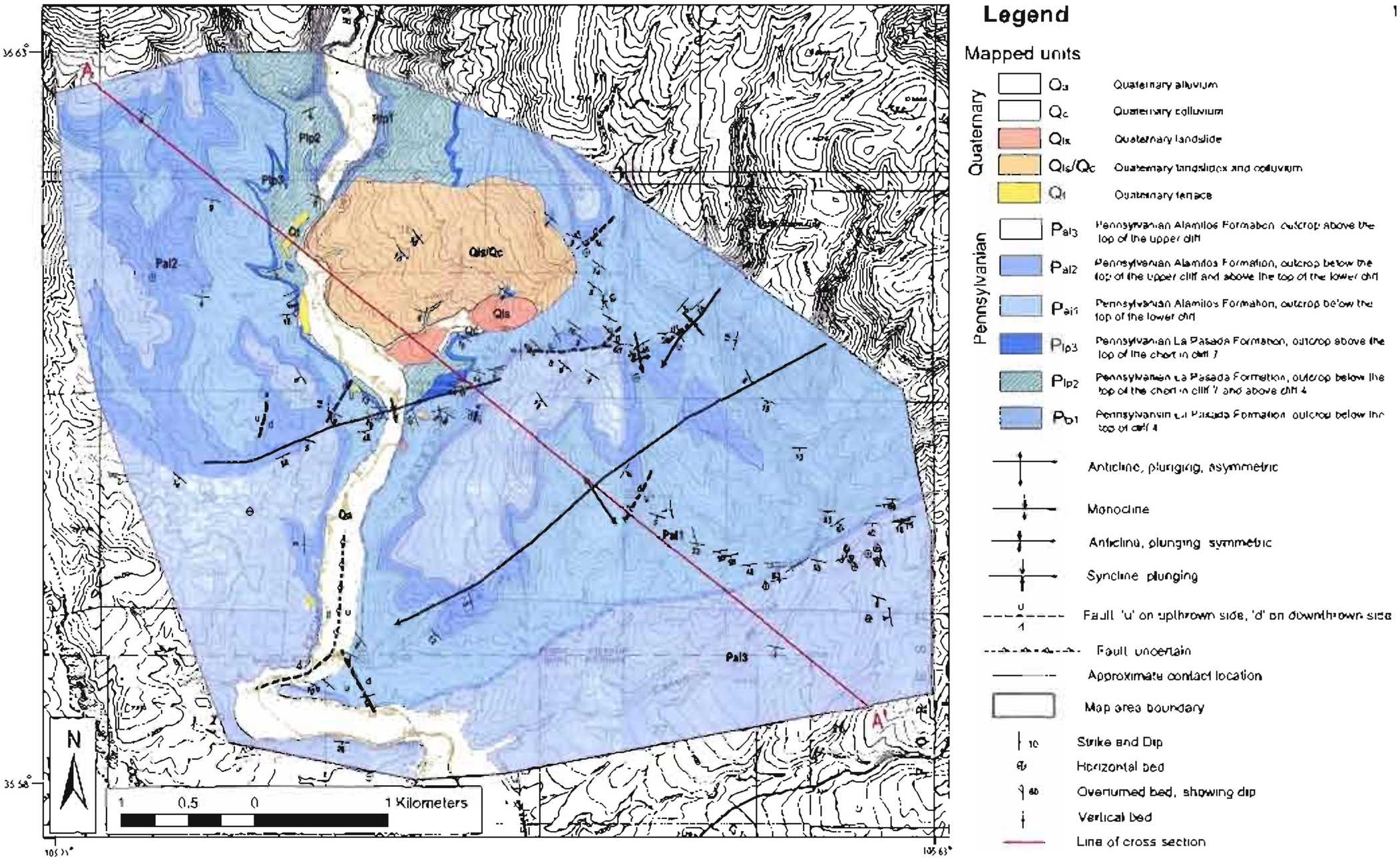

Figure 1.8. Geologic map of the Pecos Canyon study area. Topographic base with 40 ft contour interval.

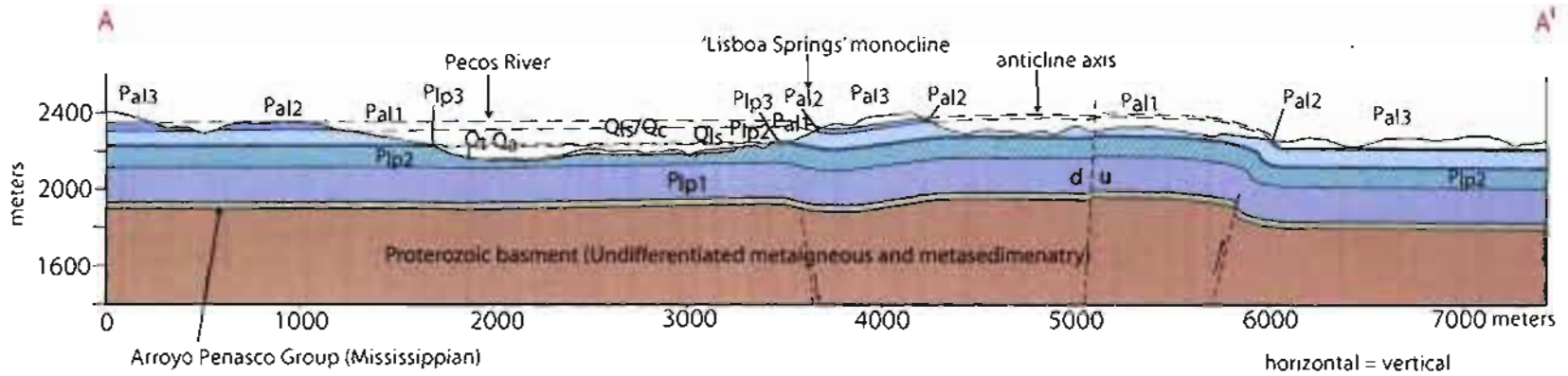

Figure 1.9. Geologic cross section of Pecos Canyon study area. Legend and line of section are shown on Figures 1.7 and 1.8.

into the study area. Prominent cliff 4 and cliff 7 are notated on the geologic map produced in this study.

The largest structure in the field area is a southwest-plunging anticline with a northeast to southwest axial orientation, located in the southeast portion of the map area (Figures 1.7 and 1.8). The anticline is asymmetric; beds on the southeast limb become vertical to slightly overturned, whereas beds on the opposite limb dip at 10 to 15°(Figure 1.9). The axial length of the anticline is at least 4.7 km. This anticline was mapped previously by the the USGS [*Johnson*, 1973] and New Mexico Bureau of Geology [*Reed and Rawling*, 2002]. *Miller et al.* [1963] mapped a similar shaped and sized anticline at Elk Mountain ~44 km to the north. The orientation of the Elk Mountain anticline is also similar to the one at Pecos, with a north-northeast axial orientation and a south-southwest plunge. Small folds and monoclines (< 0.5 km in axial length) in the study area also show northeast to southwest or a north to south axial orientation. This structure likely developed during the Laramide orogeny (late Cretaceous to early Tertiary) because *Miller et al.* [1963] attributed similar folds to Laramide deformation in their study of the region just north of this study area. They noted that Cretaceous rocks are involved in north-south axial folding on the east side of the Sangre de Cristo Mountains and that west of the mountains on the east edge of Santa Fe, steeply tilted Pennsylvanian rocks are overlain by the undeformed Miocene Santa Fe Group. Thus, deformation in the Pennsylvanian rocks appears to be post-Cretaceous and pre-Miocene (Laramide). *Baltz and Myers* [1999] also documented Laramide folding and faulting ~25 km east of the study area.

The folded structure in the Pecos study area is dissected by a number of small high-angle normal faults that may be associated with formation of the Rio Grande Rift (<27 Ma) because they parallel major normal faults in the region. The faults strike north-northeast, offsets range between 6 and 21 m (20 and 70 ft), and the offset on most faults is ~9.1 m (~30 ft). *Miller et al.* [1963] documented similar faults in the Sangre De Cristo Mountains over 40 km north of the study area.

The interplay among Cenozoic uplift, climate fluctuation, and erosion has resulted in incision of the Pecos River, forming the present canyon and surficial deposits. River terrace deposits consist of subrounded Precambrian boulders and cobbles in a sand-silt matrix. Two river terraces were documented in the study area at 12 m (40 ft) and 24 m (80 ft) above the present river. The terrace deposits were identified at a total of six map locations (Figure 1.8). *Miller et al.* [1963] documented well-defined terraces along the Rio Santa Barbara 6.7-10.3 m (22-34 ft) and 18.2-21.3 m (60-70 ft) above the stream and presented several lines of evidence that the terrace gravels are Pleistocene and related to glaciation. The Rio Santa Barbara and Pecos River share the high peaks of the Sangre de Cristo Mountains at their headwaters. The Rio Santa Barbara is a drainage on the north side of the mountains and the Pecos River drains the south side of these mountains. The similarity of heights of the Pecos and Santa Barbra terraces above the respective present river levels indicates that the two areas were affected by the same two Pleistocene glacial events.

There are some notable differences between the map produced in this study and previously published maps in part due to a more detailed study of the area. Previously unmapped faults, folds, landslides, and river terraces are now documented (Figure 1.7). Data collected in this study show that the previously mapped Lisboa Springs Fault, shown on the map in Figure 1.4, does not exist. In multiple places, unfaulted beds were physically traced across the previous mapped location of the fault. A monocline was documented along over half (i.e., a 2 km long section) of the previous mapped location of the Lisboa Springs fault. At a road-cut along Highway 63 across from the Lisboa Springs Fish Hatchery (shown in Figure 1.3) (waypoint 146 - 147) beds in the center of the monocline have been eroded away by a tributary drainage. Without knowing that the beds on the north side of the tributary correspond stratigraphically to the beds on the south side of the tributary, it looks as though there might be a fault at this road-cut. Measured sections and thin sections of a rusty brown trilobite wackestone marker bed on either side of the

tributary confirm that outcrop on the north side of the tributary correlates to a section of outcrop on the south side of the tributary.

A 2-D GPR survey was conducted along the road at this tributary location in attempt to confirm the 'Lisboa Springs' monocline structure with geophysics. The exact location of the survey is labeled 'Monocline GPR Survey' in Figure 1.10. A 70 m long profile was collected with a 50 MHz antenna at 0.5 m sample spacing. Assuming a radar velocity of 0.1 m/ns, a depth of penetration of 7 m was achieved. The survey results (Figure 1.11) indicate that the steeply dipping beds on the north side of the tributary gradually level toward the south side of the tributary, supporting the monocline interpretation. The approximate dip of beds on the north side of the tributary calculated from the GPR data matches the measured dip of beds in outcrop at this location.

1.3.2 Geomorphology

Geologic structure in the area shows some control on the morphology of the canyon. The canyon has formed asymmetrically with the east rim higher than the west rim due to the southwest structural dip in the area. Because the east rim of the canyon is higher than the west rim (~60-150 m or ~200-500 ft higher), the east side of the canyon is subject to a higher rate of physical weathering. This has resulted in the canyon taking an asymmetric shape in plan view, with the east side of the canyon having a greater area below the rim than the west side of the canyon. The southwest structural dip across the canyon may be somewhat variable because there is a stratigraphic offset between the east and west sides of the canyon in several places. This offset amount varies. From south to north it ranges from 49 m (160 ft) at the Benedictine Monastery to 0 m at the Lisboa Springs Fish Hatchery to 61 m (200 ft) 2.4 km north of the Lisboa Springs Fish Hatchery to 24 m (80 ft) at Dalton Bluff (see topo and geologic maps, Figures 1.3 and 1.8). A questionable fault is shown in the river valley at the Benedictine Monastery on the geologic map of the Pecos Canyon study area (Figure 1.8), but another explanation for the variable offset is a variable amount of Laramide folding. Regardless, since the east

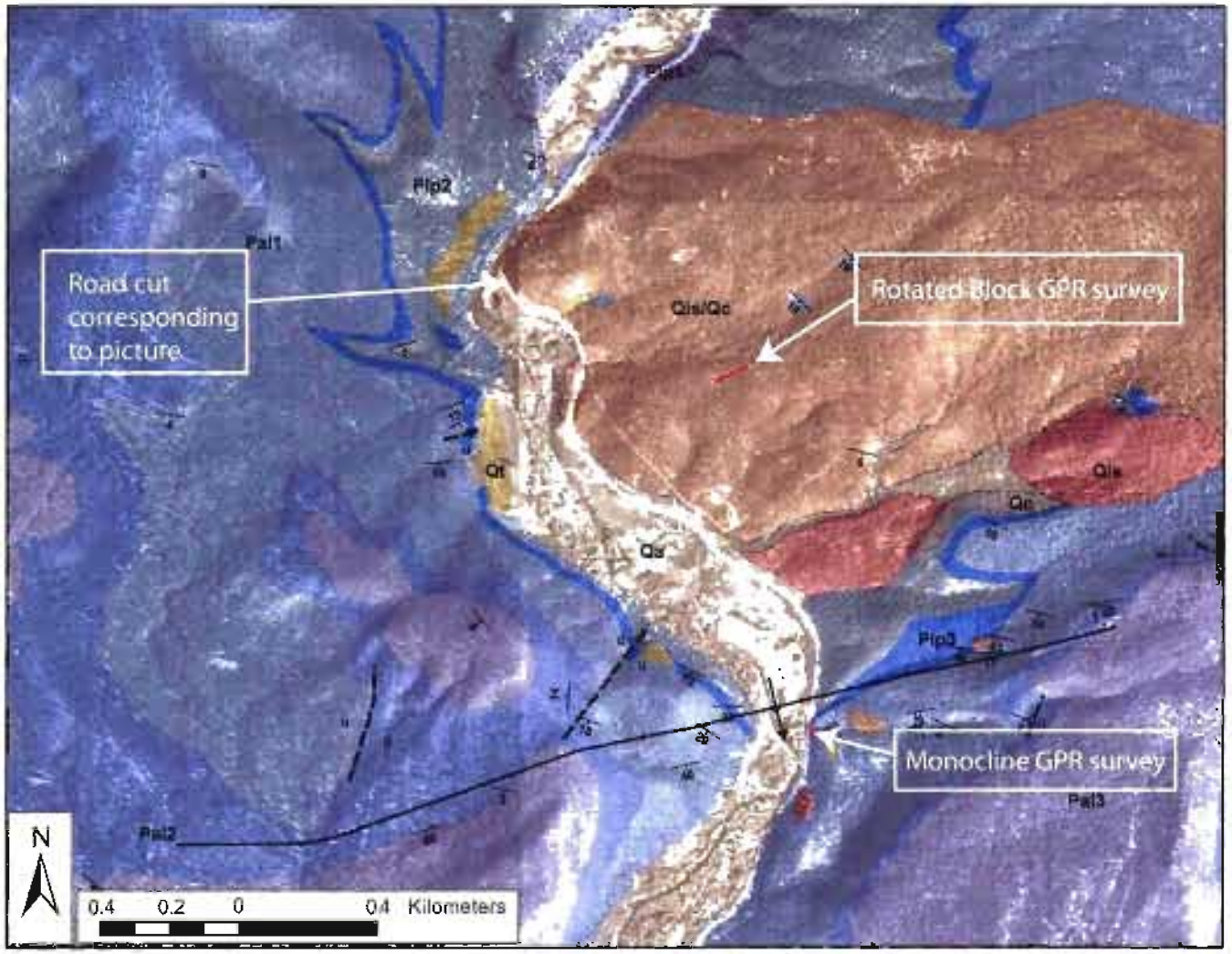

Figure 1.10. Airphoto with geology overlay showing the location of the two GPR survey lines and locations of the road cut and surficial deposit shown in Figure 1.14 and evaluated in Table 1.1. For color legend see Figure 1.7.

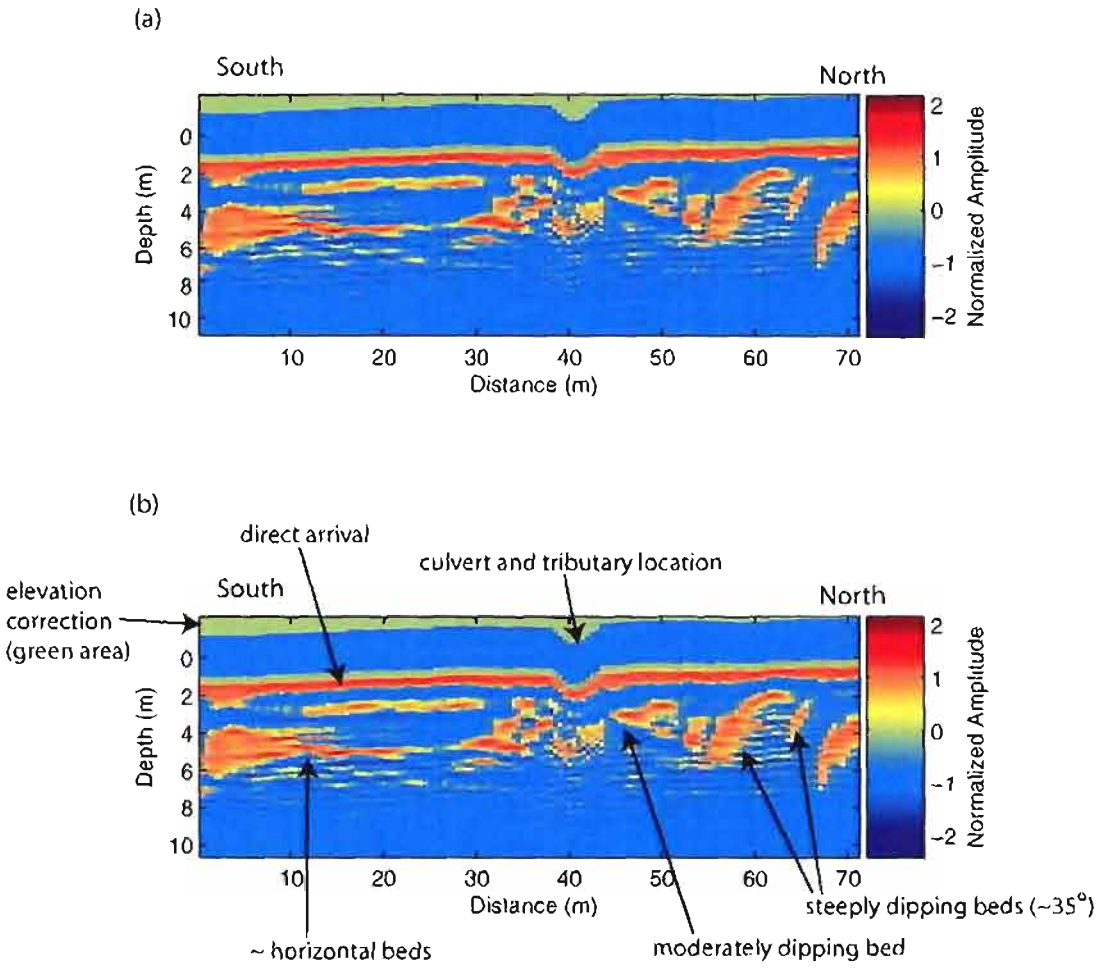

Figure 1.11. GPR survey results for 'Monocline' survey line at the road-cut along highway 63 across from the Lisboa Springs Fish Hatchery. The survey location is shown in Figure 1.10. 2X vertical exaggeration. (a) Elevation corrected data; (b) interpreted data.

rim of the canyon is much higher than the west rim, there are more landslides, rockfall, and colluvial material on the east side of the canyon (orange areas on geologic map). There are large rotated blocks in these areas, such as the one shown in Figure 1.12, ranging in size from 3 to >50 m. The largest blocks are composed of cherty limestone. The cherty limestone forms a prominent cliff in the area that is stratigraphically equivalent to cliff 7 in the study by *Sutherland* [1963]. There is a thick (>12 m) sequence of shale and mudstone stratigraphically below cliff 7 that forms a good slide plane.

A GPR line survey was completed on the east side of the canyon in this area in attempt to determine the depth and geometry of the landslide area. The exact location of the survey is labeled 'Rotated Block GPR Survey' in Figure 1.10. A 60 m long profile was collected with a 50 MHz antenna at 0.5 m sample spacing (Figure 1.13). Assuming a radar velocity of 0.1 m/ns, a depth of penetration of 5 to 6 m was achieved. Unfortunately, this depth of penetration was insufficient to characterize the landslide depth and a larger survey plan was abandoned. The

Figure 1.12. A large tilted and rotated block interpreted as a landslide block at waypoint 509 (Figure 1.6). The block is composed of black-green siltstone and shale interbedded with limestone (east view).

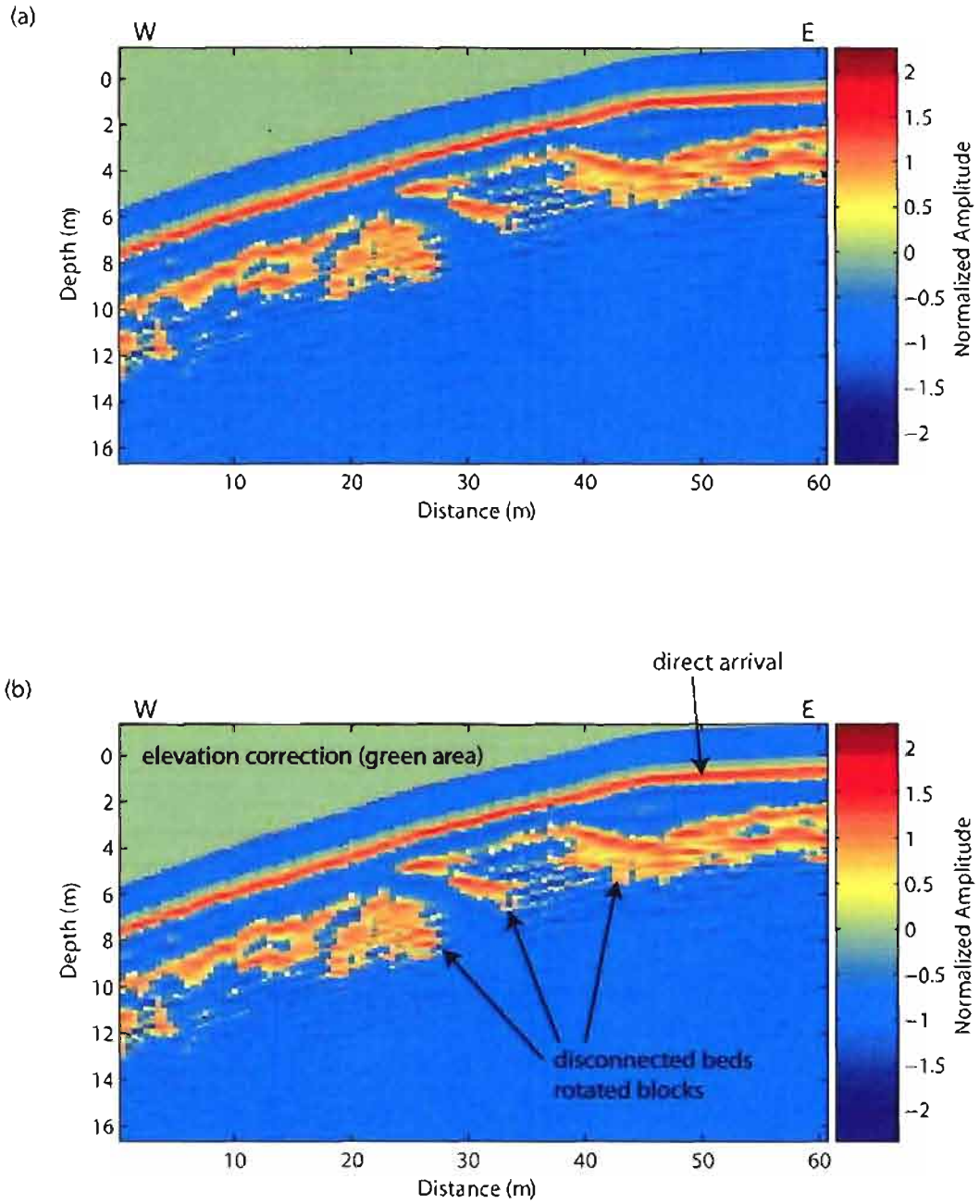

Figure 1.13. GPR survey results for the 'Rotated Block' line survey just east of Hwy 63 and ~1 km north of the Lisboa Springs Fish Hatchery. The survey location is shown in Figure 1.10. 2X vertical exaggeration. (a) Elevation corrected data; (b) interpreted data.

survey data from the single profile (Figure 1.13) show large rotated blocks, some of which crop out at the surface at various orientations along the survey line. The data also show that the surficial deposit at this location is at least 5 m deep.

An excellent exposure of a surficial deposit that is common in the study area occurs at a large road cut located at waypoint 45 (Figure 1.10). The deposit contains large (up to 6 m) angular blocks in a sandy matrix (see photograph, Figure 1.14). Table 1.1 shows a list of characteristics of this deposit that are both present and lacking for four potential interpretations of its origin: alluvial fan, landslide, colluvium, and impact. The characteristics present under the impact column of Table 1.1 are characteristics that can be found in crater-fill deposits [*French*, 1998]. Examination of thin sections from the study area did not reveal shocked produced mineral deformation features.

The comparison table indicates that the landslide interpretation is the best match as the deposit has more characteristics in common with a landslide than with the other three interpretations. If the deposit is a landslide, it is lacking an

Figure 1.14. East looking view of the surficial deposit at the road cut shown in Figure 1.10 and evaluated in Table 1.1.

Table 1.1. List of comparative characteristics for four potential interpretations of the surficial deposit exposed at the road cut on state Hwy 63 shown in Figures 1.14 and 1.10 and other similar surficial deposits in the vicinity. [*French*, 1998](Jerry Higgins, personal communication, 2006)

Landslide	Alluvial Fan	Colluvium	Impact
Characteristics Present			
- large brecciated blocks, sand matrix	- brecciated rock, sand matrix	- brecciated rock, sand matrix	- large brecciated blocks, sand matrix
- deposit composed of materials found upslope	- deposit composed of materials found upslope	- deposit is composed of materials found upslope	- deposit composed of materials found upslope
- significant vertical relief above deposit	- significant vertical relief above deposit		- significant vertical relief above deposit
- lens-shape morphology in cross section	- lens-shape morphology in cross section		
- potential river diversion as a result of deposition	- potential river diversion as a result of deposition		
- highly erodible lithologic units beneath thick units resistant to weathering			
- hummocky terrain			
Characteristics Lacking			
- scarp (possibly degraded due to age)	- debris-flow channels	- uniform morphology	- impact melt rocks
	- internal stratification	- thinner deposit	- shocked produced mineral deformation features
			- obvious impact crater
			- central uplift
			- circular morphology visible at many different map scales
			- shatter cones

obvious scarp. However, the landslide may be old enough that the scarp has eroded away. Large juniper trees are present in the landslide area, and age dating of tree rings denotes that the deposit is over 100 years old. River terraces are not present in the landslide areas, indicating that the landslides occurred after terrace formation.

Rock units dip to the southwest 10-15° steeper than the gradient of the river (0.48°), which flows south; thus, the oldest formation, the La Pasada Formation, crops out in the north, followed by the Alamitos Formation and Sangre De Cristo Formation. The southward structural dip causes the canyon to narrow where the river intersects more resistant rock units. Points where the river narrows due to these units are shown in Figure 1.15. The units correspond to cliffs 4 and 7 in the stratigraphic section by *Sutherland* [1963] at Dalton Bluff 2.4 km (1.5 miles) north of the north boundary of the study area.

The southeast side of the map area contains another example of geologic structure controlling geomorphology. Here a series of steeply dipping ridges and hogbacks are visible in airphotos (see airphoto in Figure 1.7). The ridges were formed by erosion of the steeply dipping limb of the large asymmetric anticline discussed previously (Section 1.3.1).

1.4 Conclusions

Study of the geology of Pecos River Canyon just north of Pecos, New Mexico reveals previously unmapped faults, folds, and surficial deposits. Large Laramide folds ($\sim$2.3 - $>$ 4.7 km in axial length) with smaller superimposed folds ($<$ 0.5 km in axial length) possibly indicate northwest to southeast crustal shortening. The largest structure, located in the southeast part of the map area, is an asymmetric southwest plunging anticline. With the exception of this anticline, the strata generally dip southwest 10-15°. The folded Laramide structure is dissected by northeast striking high-angle faults with an average offset of $\sim$9 m that are likely associated with formation of the Rio Grande Rift $<$27 Ma [*Cather et al.*, 2004](see cross-section, Figure 1.9). GPR, stratigraphic, and thin section data show that a monocline exists where the previously mapped Lisboa Springs Fault is located. A

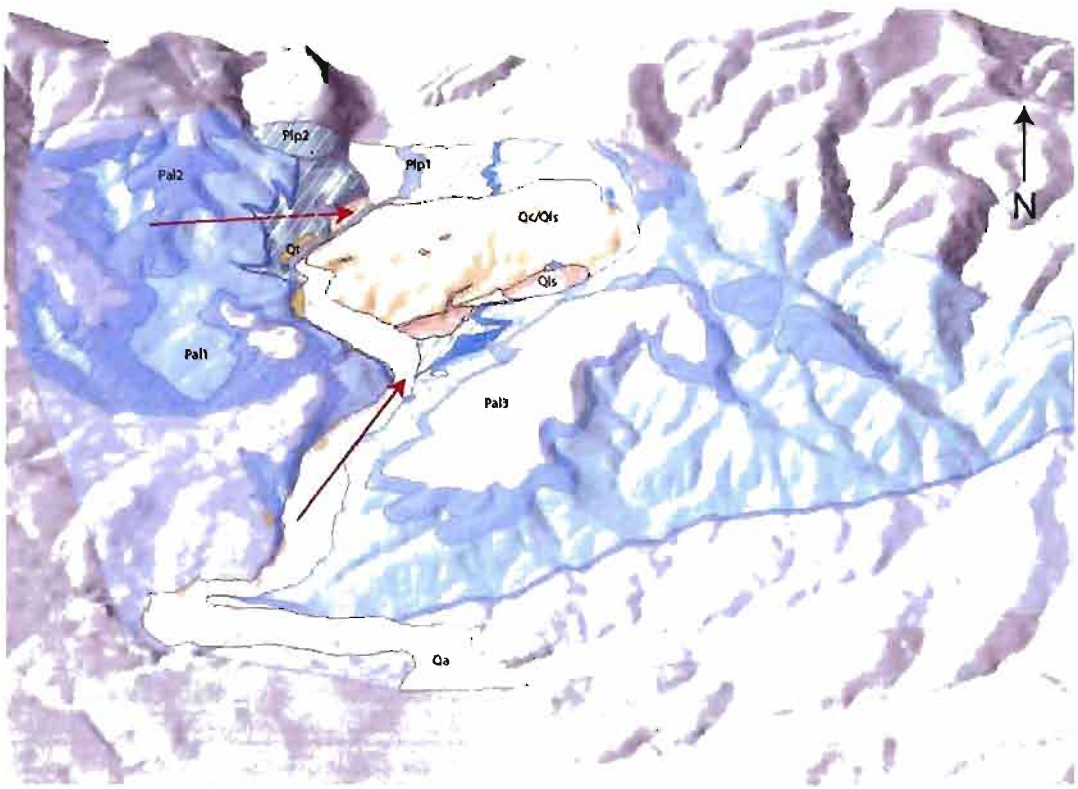

Figure 1.15. 3D oblique view of geologic map units (Figure 1.7) draped on Digital Elevation Model (DEM). Arrows show where the river intersects southward-dipping resistant rock units causing the canyon to narrow.

detailed study of the geology greatly facilitated study of stratigraphic relationships discussed in Chapter 2. Likewise, a detailed understanding of the stratigraphy facilitated geologic mapping.

The study area contains several examples of geologic structure controlling geomorphology. Because rock units dip more steeply than the gradient of the river, the Pecos Canyon briefly narrows where the river intersects resistant rock units. Geologic structure results in an asymmetric canyon shape, with the east side of the canyon much wider in area then the west side, and the east rim 60 to 150 m higher than the west rim. Thus, the east side of the canyon is subject to a higher rate of erosion and mass wasting. A large area below the east rim of the canyon contains large rotated blocks 3 to >50 m in size. Assessment of the physical characteristics

of this area (Table 1.1) indicate that it is not a meteorite impact site due to a lack of impact melt rocks, a central uplift, shocked produced mineral deformation features, and other features diagnostic of meteorite impacts. The area is interpreted as a combination of landslide, rockfall, and colluvial material.

The interplay between Cenozoic uplift, climate fluctuation, and erosion have resulted in incision of the Pecos River forming the present canyon and surficial deposits. River terraces in the study area at 12 and 24 m above the river likely formed as a result of Pleistocene climate fluctuation, i.e., two glacial advance/retreat cycles. Alluvial sedimentation, colluvial creep, rockfall, and landslides are processes that continue in the canyon today. This study demonstrates how detailed geologic mapping provides insight into regional geomorphic and structural styles.

1.5 Future Directions

Additional geologic mapping of surficial deposits, faults, and folds will lead to an increased understanding of the geologic history and will aid correlation of strata in future stratigraphic studies. A seismic survey in the colluvial-landslide area on the east side of the canyon in the study area might provide additional characterization of landslide geometry. Age dating of surficial deposits could reveal information about the age of the canyon and incision rates. River terraces in the study area likely formed as a result of Pleistocene climate fluctuation. Age dating could be used to validate this conclusion and determine if the terraces correlate in age to the glacial deposits in the Sangre De Cristo Mountains north of the study area. *Miller et al.* [1963] documented a thick surficial deposit more than 300 m above the river less than 2 km northwest of the study area. The age and origin of this deposit is unknown and may be considerably older than the surficial deposits documented in this study. The high surficial deposit likely originated from the earlier stages of uplift of the southern Sangre De Cristo Mountains because the Pecos River Canyon was significantly incised after its deposition. Thus, age dating of this deposit allows estimation of the canyon's age and incision rate. Useful age dating methods may

include beryllium, aluminium, and helium cosmogenic nuclides, optical stimulated luminescence, lichenometry, and diffusion age dating for old river terraces.

CHAPTER 2

PENNSYLVANIAN FACIES, DEPOSITIONAL SYSTEMS, AND PALEOGEOGRAPHY OF THE PECOS PLATFORM

2.1 Introduction

2.1.1 Purpose

This chapter presents a detailed sedimentologic study of the upper 43 m of the La Pasada Formation and lower 160 m of the Alamitos Formation in the Pecos River Canyon of northern New Mexico. The studied stratigraphic interval is Middle Pennsylvanian (Desmoinesian) in age. More specifically, objectives of this study include facies analysis, interpretation of depositional processes, and paleogeographic reconstruction. Results of this study are compared to previous regional and detailed studies. In addition, modern and ancient analogs are utilized to help interpret the characteristics and spatial relationships of the sedimentary units in the Pecos study area.

2.1.2 Background

The Ancestral Rocky Mountains formed during the collision of North America and Gondwana at a stage in the formation of the supercontinent Pangea. The Ancestral Rockies sourced much of the clastic sedimentation in western North America during the Pennsylvanian (Figure 2.1). The Pecos platform lies at the southern end of the Taos Trough, which is one of several Pennsylvanian basins associated with the formation of the Ancestral Rocky Mountains (Figure 2.2). The Taos Trough was bounded to the west by the Uncompahgre Uplift along the

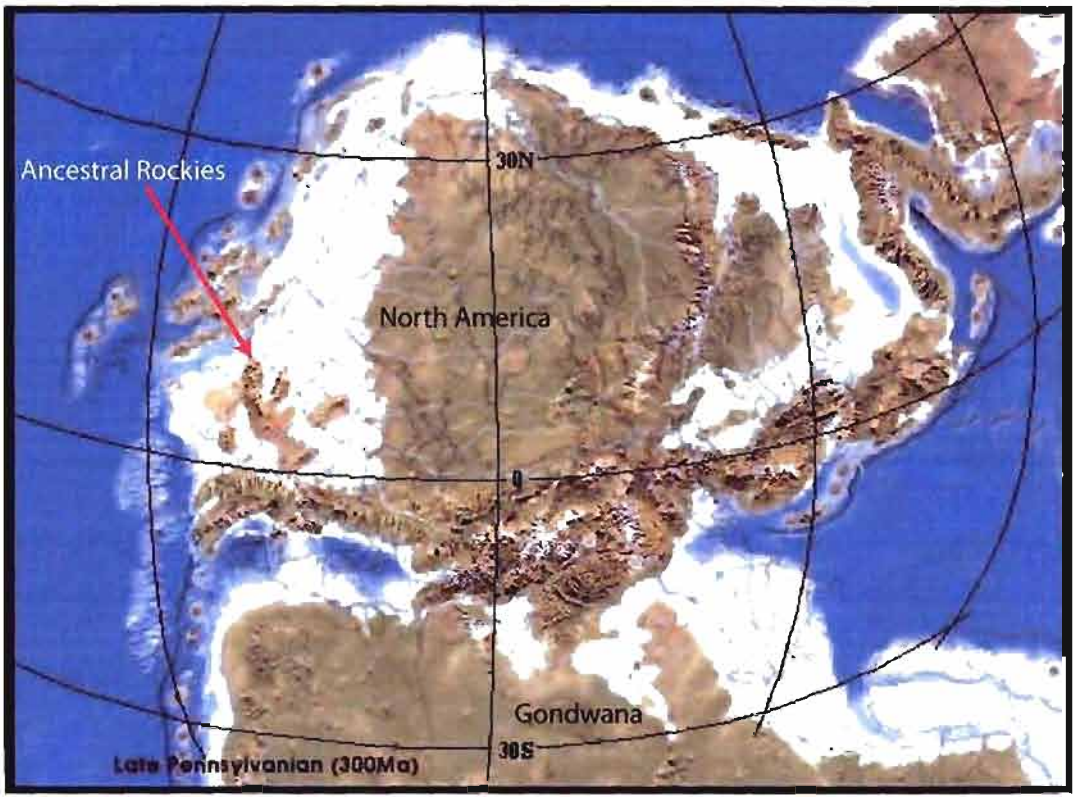

Figure 2.1. Paleogeography of the Ancestral Rocky Mountains during the collision of North America and Gondwana during the formation of Pangea, Late Pennsylvanian. From *Blakey* [2006] with permission.

north-south striking Pecos-Picuris fault and on the south by the Pennsylvanian Pedernal Uplift as shown in Figure 2.3.

The Pecos-Picuris fault was originally active in the Precambrian as a right-lateral strike-slip fault, reactivated with vertical movement in the Pennsylvanian (upthrown to the west) and reactivated again during the Laramide Orogeny with vertical dip-slip movement (upthrown to the west) [*Miller et al.*, 1963]. *Bauer and Ralser* [1995] also document Precambrian strike-slip activity for the Pecos-Picuris fault. *Bauer et al.* [1997] do not discount possible Pennsylvanian activity. They speculate that the fault was reactivated during the Laramide Orogeny with strike-slip and dip-slip movements, and conclude that it was reactivated again

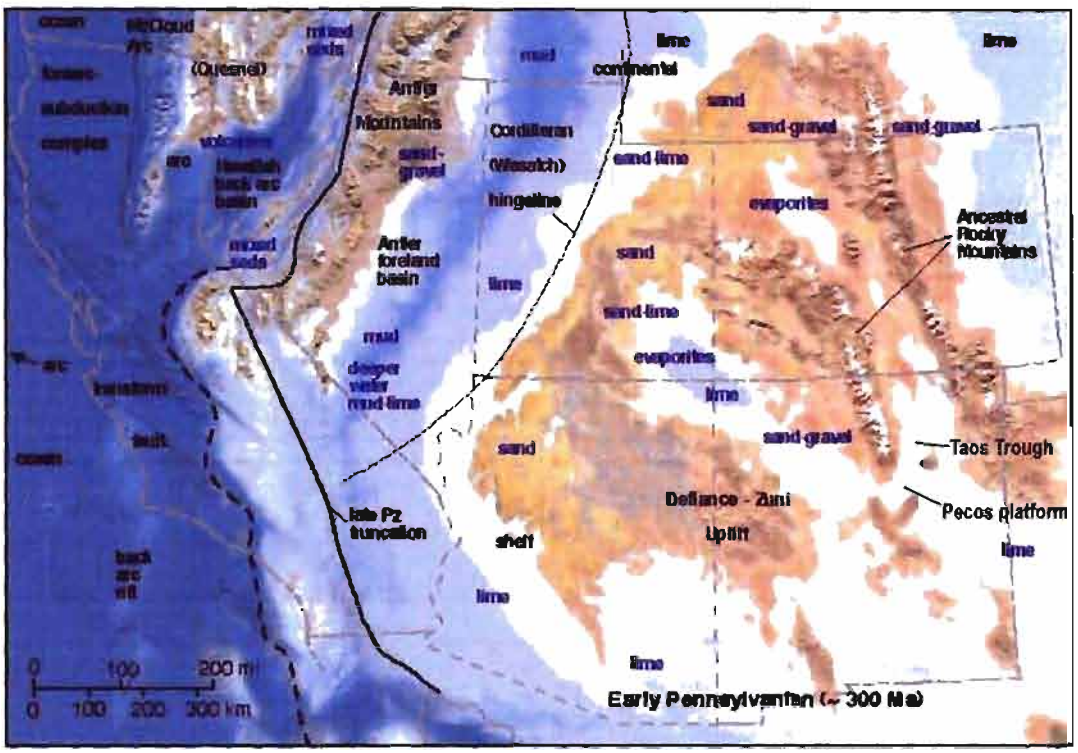

Figure 2.2. Paleogeography of southwestern North America, Early Pennsylvanian. From *Blakey* [2006] with permission.

with Neogene vertical rift related movement based on fission-track data [*Bauer and Ralser*, 1995].

The Uncompahgre Uplift provided a major source of siliciclastic sediment to the Taos Trough in the region surrounding Taos, New Mexico. Here, the Taos Trough contains ~2000 m of alluvial fan, fan-delta, and braided stream deposits [*Casey*, 1980]. Further south, sedimentary rock of the La Pasada and Alamitos Formations on the Pecos platform consists of cyclic deposits of both open marine carbonates and submarine siliciclastics [*Sutherland*, 1963; *Casey*, 1980; *Gong*, 1992; *Ude*, 1992].

2.1.3 Previous work

Previous work on the stratigraphy and sedimentology of the Taos Trough region has been presented by *Reed and Wood* [1947]; *Brill* [1952]; *Baltz and Bachman* [1956]; *Miller et al.* [1963]; *Casey and Bachman* [1979]; *Casey* [1980]; *Baltz and*

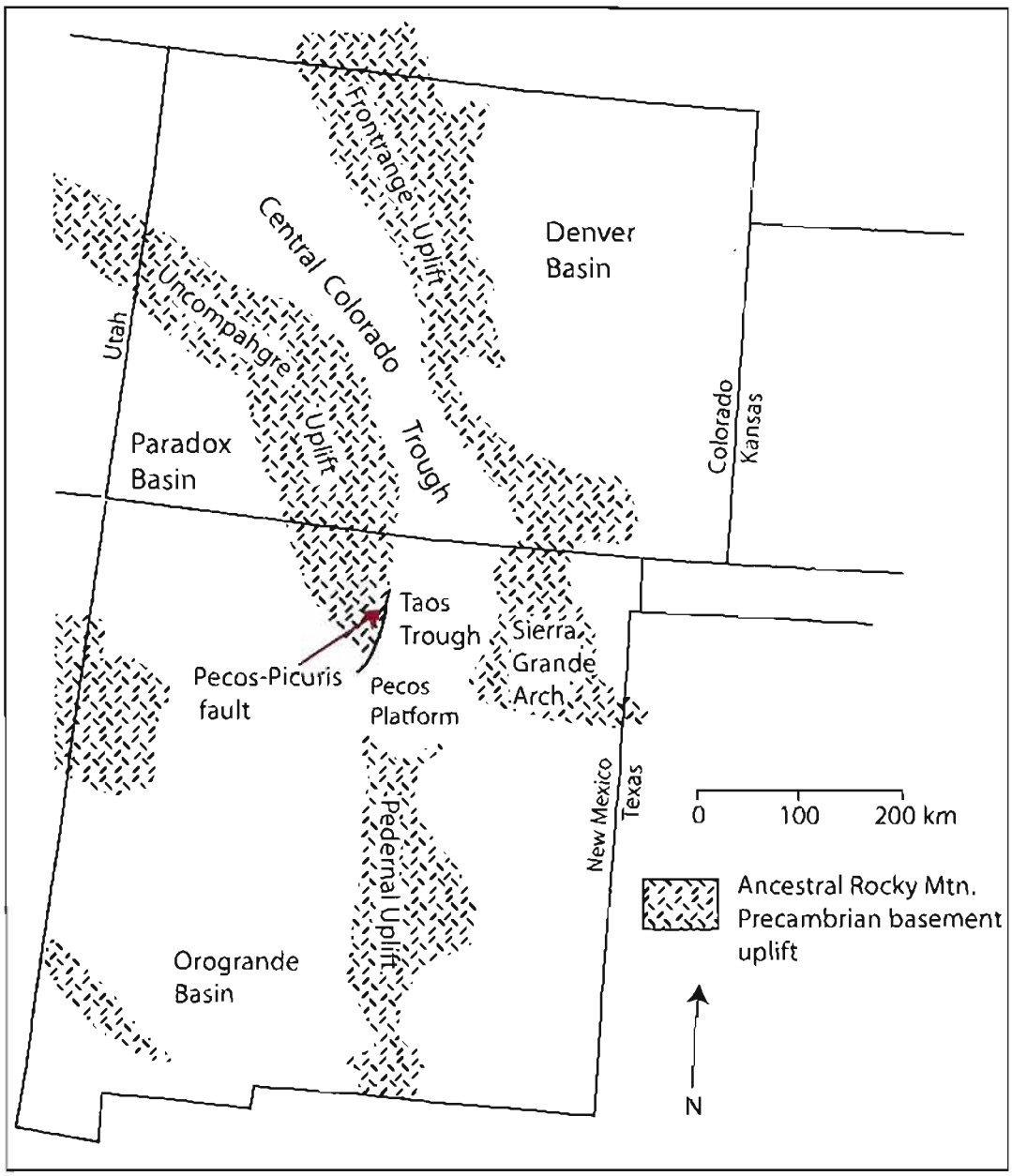

Figure 2.3. Pennsylvanian paleogeography of New Mexico showing Ancestral Rocky Mountain tectonic elements. Modified from *Soegaard* [1990].

Myers [1984]; *Soegaard* [1990]; *Gong* [1992]; *Ude* [1992]; *Baltz and Myers* [1999]. The outcrop studied by *Ude* [1992] lies within the area of this study. Specifically, Ude studied an 0.5 km^2 area near the Benedictine Monastery (Figure 1.3, Chapter 1). Biostratigraphy of the region was established by *Thompson* [1942], *Young Jr.* [1945], and *Sutherland and Harlow* [1973]. Stratigraphic sections in the study area are correlated with sections measured by *Sutherland* [1963], allowing placement of the studied interval in his biostratigraphic framework.

Stratigraphic nomenclature of Pennsylvanian rocks in this area has been controversial, primarily due to rapid lateral facies changes and variations in unit thicknesses. Three main systems of stratigraphic nomenclature have been proposed for the Pennsylvanian outcrop in the region [*Brill*, 1952; *Miller et al.*, 1963; *Baltz and Myers*, 1984] (Figure 2.4). The nomenclature system proposed by *Miller et al.* [1963] was used in the most recent geologic map of the Pecos Quadrangle [*Reed and Rawling*, 2002]. It is important to note that in the study area, the Upper Madera Formation mapped by the USGS [*Johnson*, 1973] is equivalent to the Alamitos Formation [*Miller et al.*, 1963] mapped by the New Mexico Bureau of Geology

<table>
<tr><td></td><td colspan="5">Pennsylvanian</td><td>Permian</td></tr>
<tr><td></td><td>Morrowan</td><td>Atokan</td><td colspan="2">Desmoinesian</td><td>Missourian</td><td>Virgillian</td><td rowspan="5">Sangre de Cristo Formation</td></tr>
<tr><td>Brill, 1952</td><td colspan="2">Sandia Formation</td><td>Gray Limestone Member</td><td colspan="3">Arkosic Limestone Member
Madera Formation</td></tr>
<tr><td>Johnson, 1973</td><td colspan="2">Sandia Formation</td><td>Lower Madera Formation (Pml)</td><td colspan="3">Upper Madera Formation (Pmu)</td></tr>
<tr><td>Sutherland, 1963</td><td colspan="3">La Pasada Formation
cliff 2, cliff 3, cliff 4 ..... cliff 7</td><td colspan="3">Alamitos Formation
cliff 8</td></tr>
<tr><td>Terminology used for this study</td><td colspan="3">La Pasada Formation (P_{lp})
cliff 2, cliff 3, cliff 4 ..... cliff 7</td><td colspan="3">Alamitos Formation (P_{al})
Lower and upper cliffs</td></tr>
</table>

Figure 2.4. Stratigraphic nomenclature for the Pecos area and terminology used in this study. Time interval of the composite stratigraphic section evaluated in this study is indicated by the red dashed box.

[*Reed and Rawling*, 2002] and to the upper arkosic limestone member of the Madera formation in the nomenclature of *Brill* [1952]. The type sections for the La Pasada and Alamitos formations are located within a few kilometers of the area mapped in this study (Figure 1.3). Thus, the nomenclature system of *Sutherland* [1963] was chosen for this study. According to *Sutherland* [1963], the total thickness of the Alamitos Formation is 388 m (1275 ft), and the total thickness of the La Pasada Formation is 297 m (973 ft).

2.2 Methods

Primary methods for the sedimentologic part of this study include the following: measuring detailed stratigraphic sections, study and comparison to previously measured sections, sample collection, outcrop photographs, field sketches and notes of crossbedding and stratigraphic relationships, paleocurrent measurements, examination of thin sections, and literature review. The strata in the study area were divided into descriptive facies. Criteria to characterize facies include the following:

1. Composition
2. Grain size, shape, and sorting
3. Color
4. Bedding geometry and extent
5. Primary sedimentary structures
6. Paleocurrent characteristics
7. Fossil and trace fossil content

A total of 150 samples was collected in the study area, including several from the region surrounding the study area. A sample map, listing of samples, and photos of several samples are included in Appendix A.

Thin sections were used to augment the lithologic description of facies. A total of 42 thin sections was analyzed under a petrographic microscope. Grain composition,

average grain diameter, sorting, shape, cements, and fossil content are described from thin sections. Point counts were used to classify several samples using >150 counts. The classification scheme developed by *Mount* [1985] was employed for mixed carbonate-siliciclastic sediment with the aid of thin section data.

Ude [1992] conducted a facies analysis of part of the stratigraphic section in this study. Some of his raw data were used to supplement several facies descriptions. Figure 2.5 shows the locations of detailed measured sections. Sections were measured with a meter stick and Brunton compass. Lithology, fossils, trace fossils, bioturbation, average and maximum clast size, and sedimentary structures were described for stratigraphic units in the sections. Carbonate rocks were initially described and classified in the field by visual examination of hand sample with the nomenclature of *Dunham* [1962].

Appendix C contains copies of the four original detailed stratigraphic sections used for the composite section. Over 10 additional sections consisting of a brief lithologic description and/or approximate thicknesses were completed. These additional sections were useful for mapping as well as for understanding lateral facies relationships. Six sections in an approximate east-west line across the study area (Figure 2.6 red line) were used to construct a stratigraphic cross-section.

2.3 Results

Study area outcrops consist of siliciclastics, carbonates, and mixed carbonate-siliciclastic rocks. A 203 m composite section was created by combining the four measured sections discussed previously (Figure 2.5). Stratigraphic symbols are illustrated in Figure 2.7. The composite section (Figure 2.8) reveals stratigraphic breaks used for creating the geologic map discussed in Chapter 1 and shown in Figure 2.6. Cliffs 4 and 7 refer to cliffs 4 and 7 of the La Pasada Formation in the study of *Sutherland* [1963]. The 'upper cliff' and 'lower cliff' are part of the Alamitos Formation and are informal terms created for use in this study (Figure 2.4). These two cliffs form a distinctive doublet that can be traced throughout much of the study area; thus, facies and thickness changes of this part of the section were noted

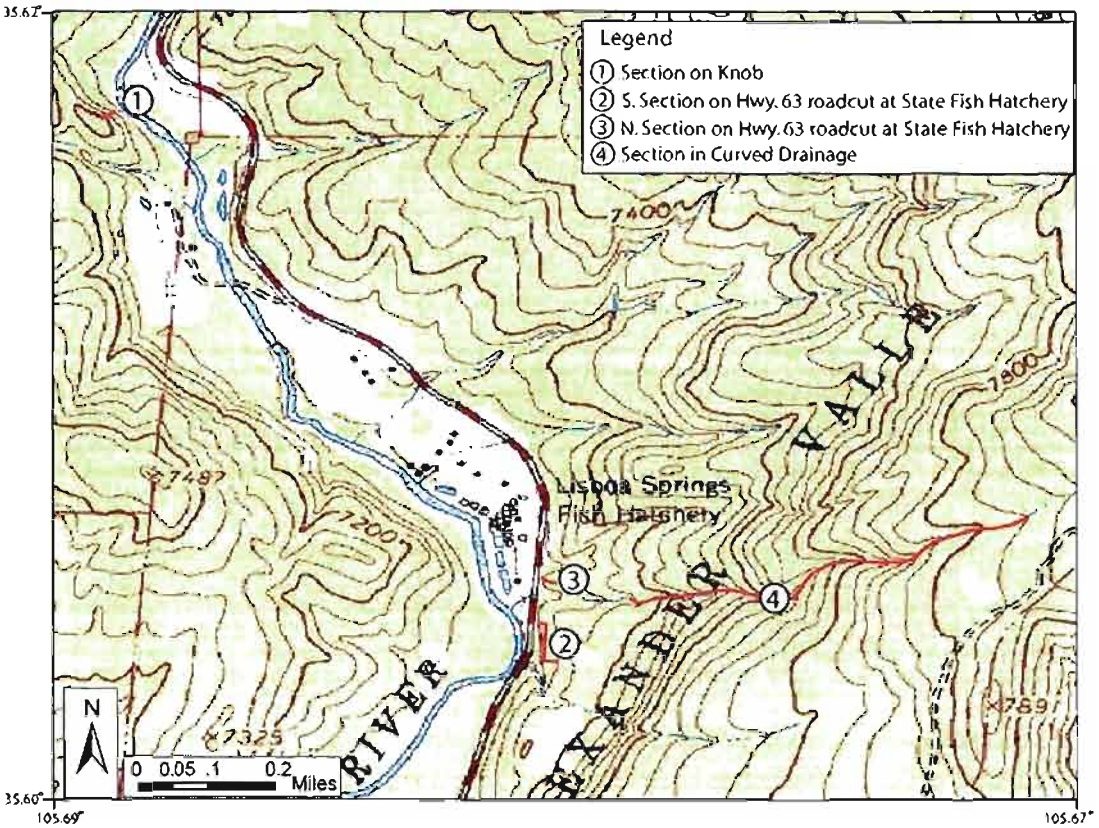

Figure 2.5. Locations of measured sections used for composite section. *United States Geological Survey* [1961] topographic map with contours in feet.

while mapping. The upper and lower cliffs are commonly present at or near the Pecos Canyon rim in the study area. Their stratigraphic locations are also shown on the composite section (Figure 2.8).

The composite section contains 59% siltstone, sandstone, and conglomerate, 25% carbonate, and 16% shale. However, it is important to note that 42% of the sandstone portion (25% of the total composite section) is of mixed carbonate-siliciclastic composition. Stratigraphic rock units were aggregated into descriptive facies. Tables 2.1 and 2.2 summarize the results of facies analysis for the 10 predominately carbonate rock types. Tables 2.3, 2.4, and 2.5 summarize the characteristics and interpretation of the seven predominately clastic facies. Additional facies

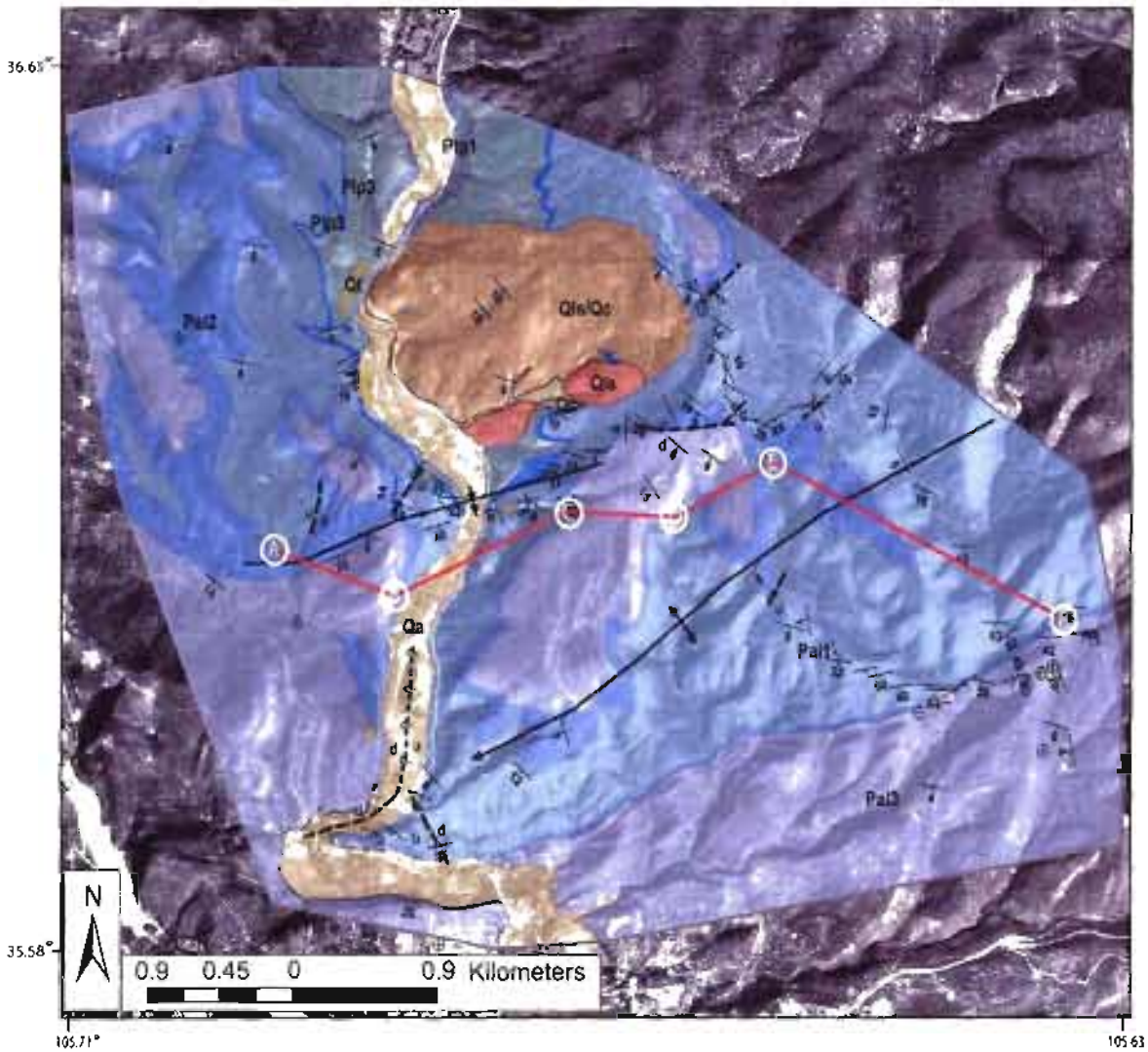

Figure 2.6. Photogeologic map of Pecos study area. Red line shows location of correlated sections.

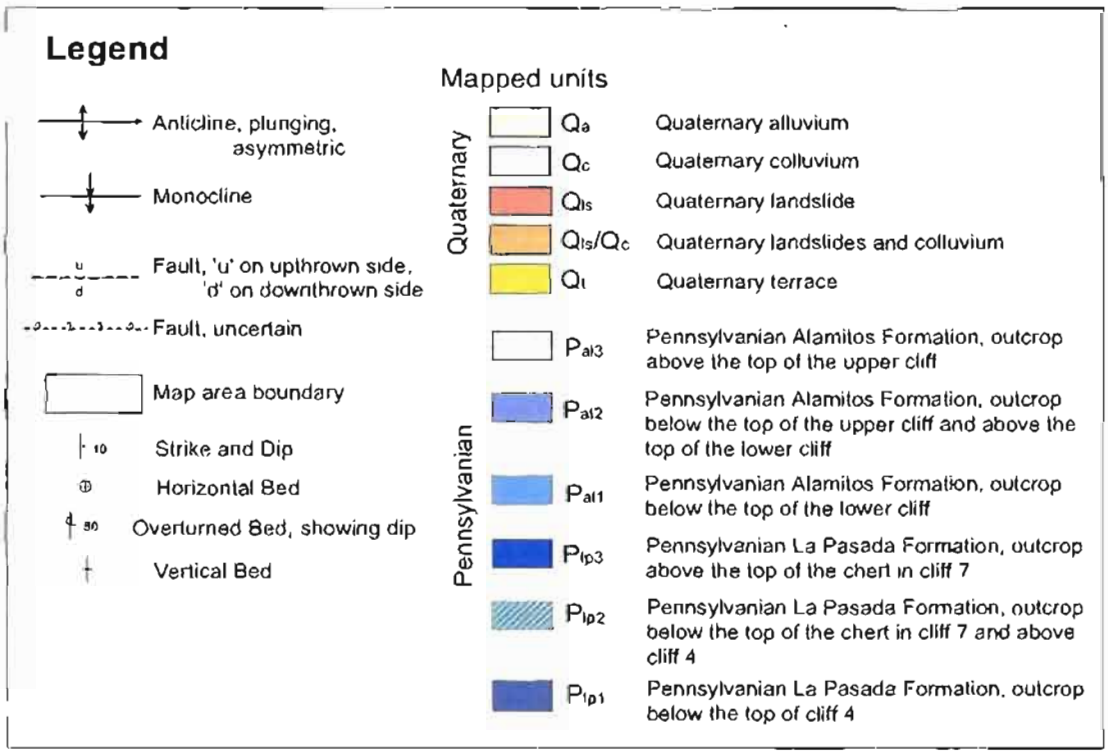

Figure 2.6. (continued).

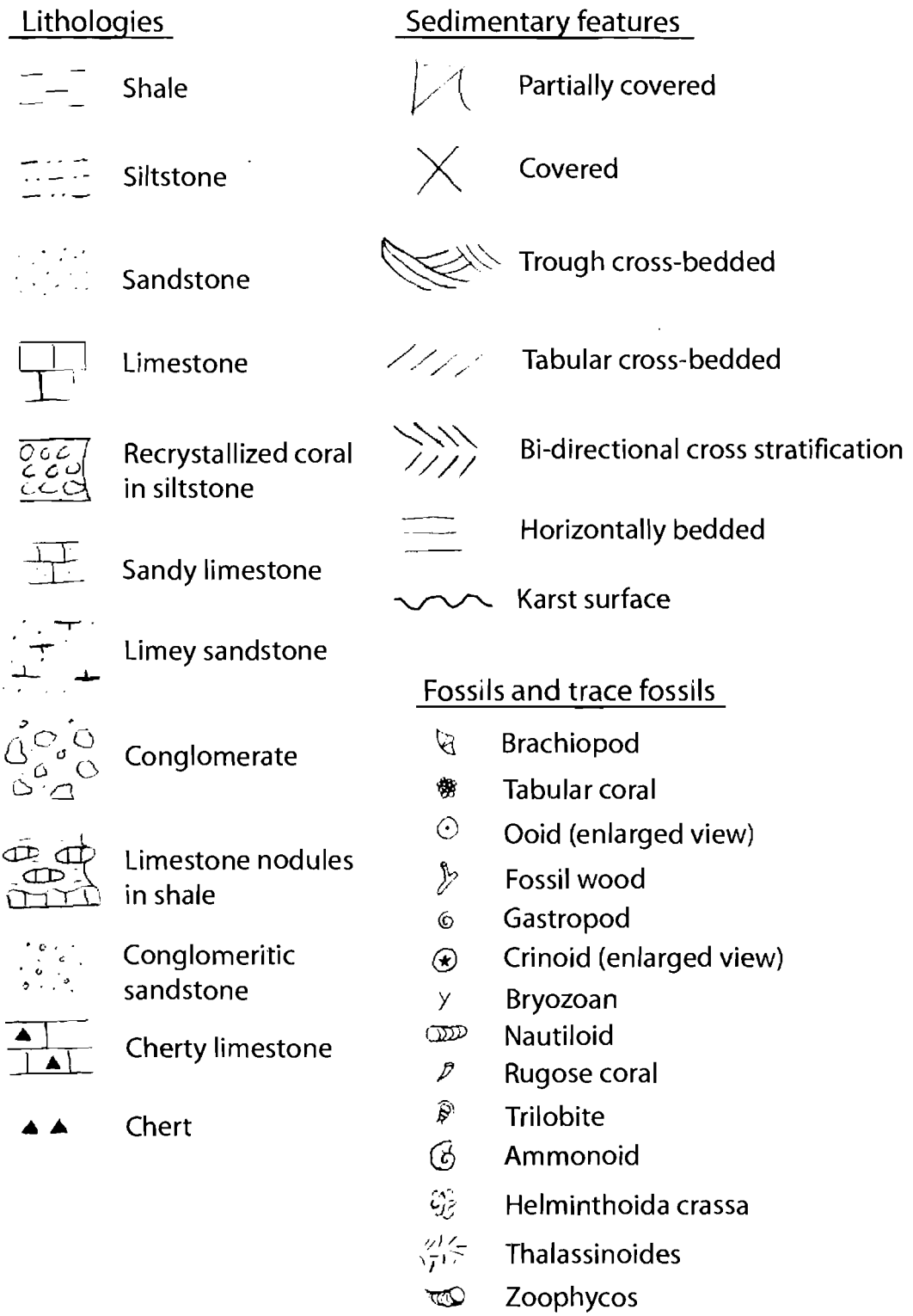

Figure 2.7. Legend for stratigraphic sections.

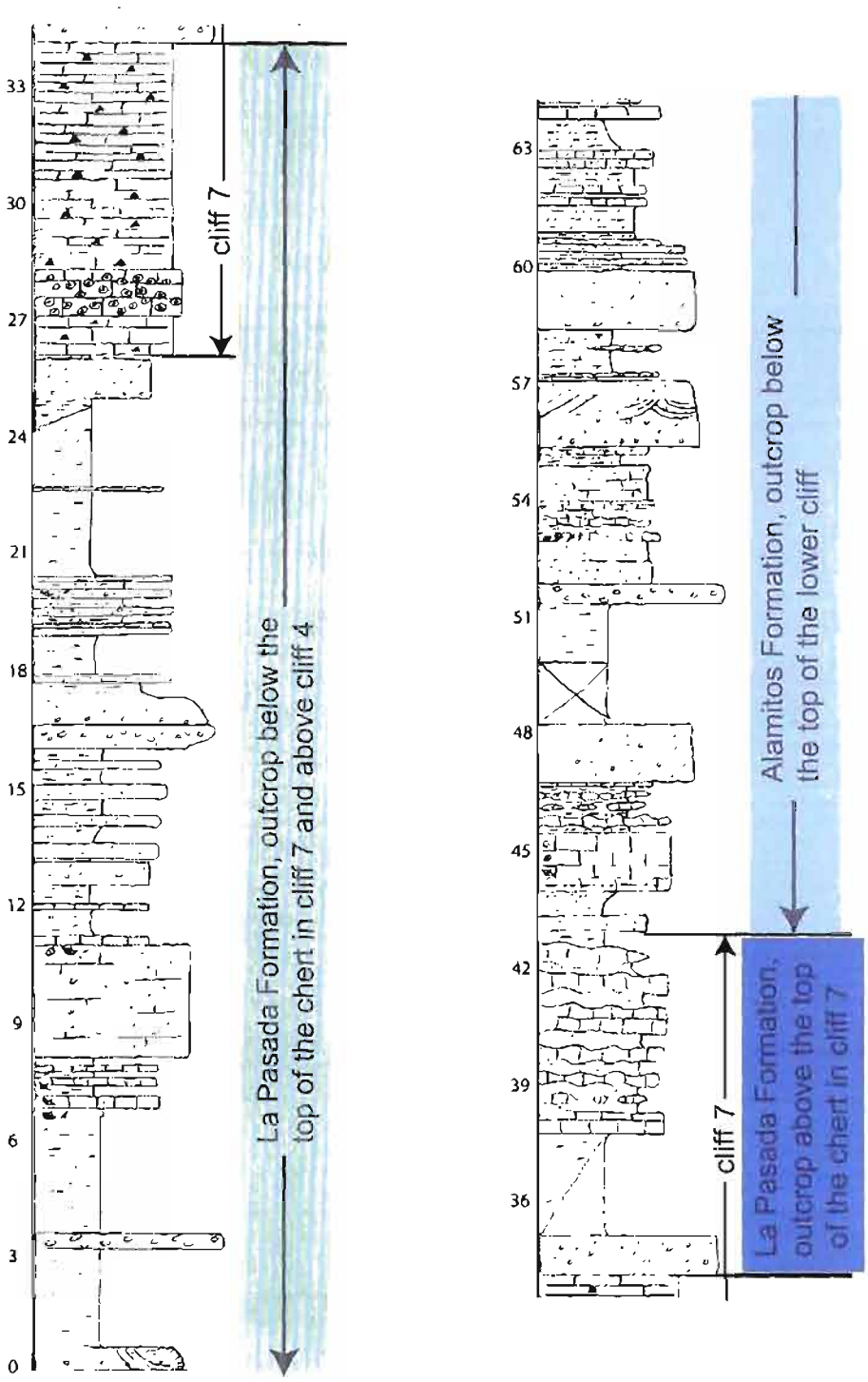

Figure 2.8. Composite section showing stratigraphic breaks used for creating the geologic map shown in Figure 2.6. Section height is marked in meters.

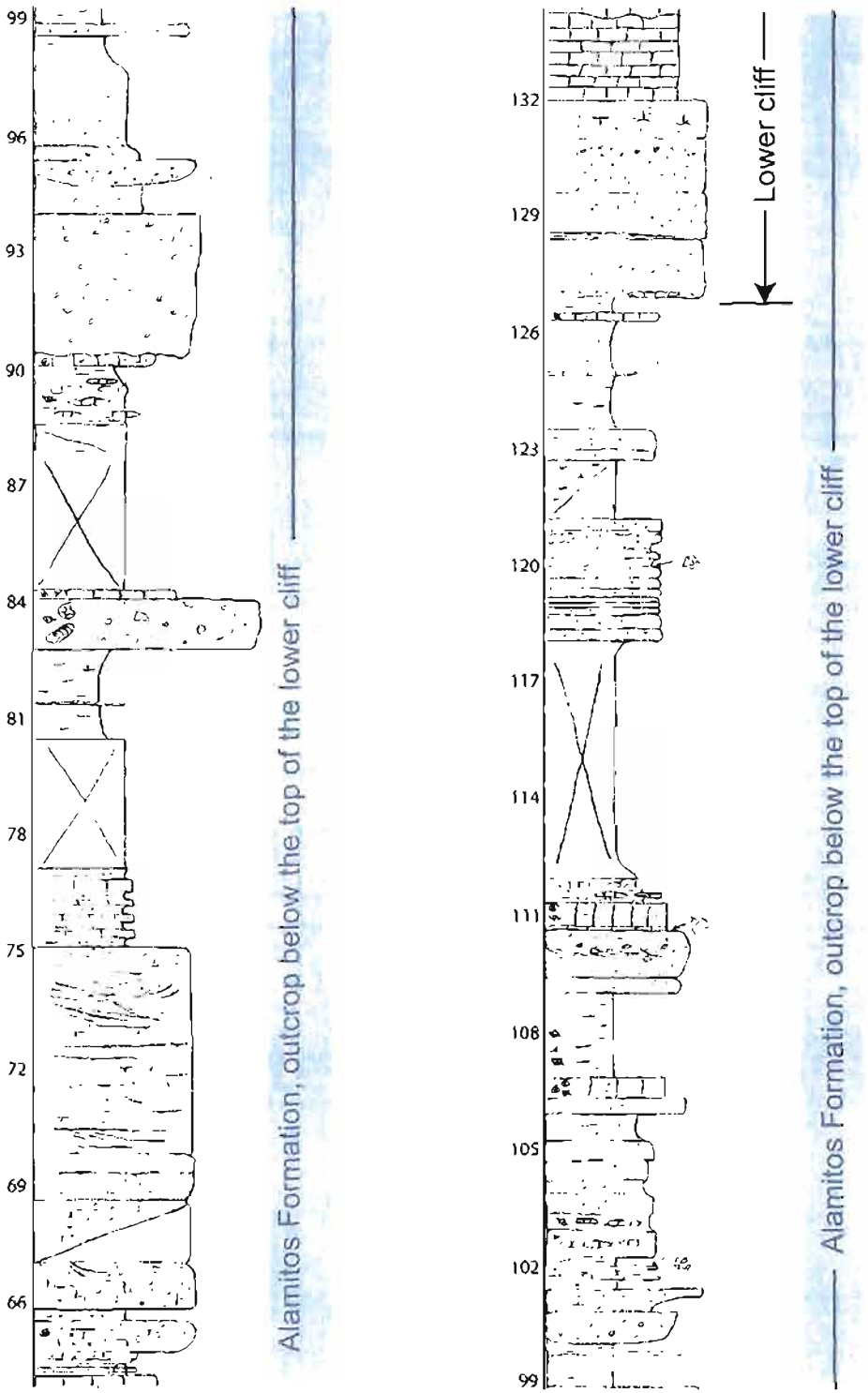

Figure 2.8. (continued).

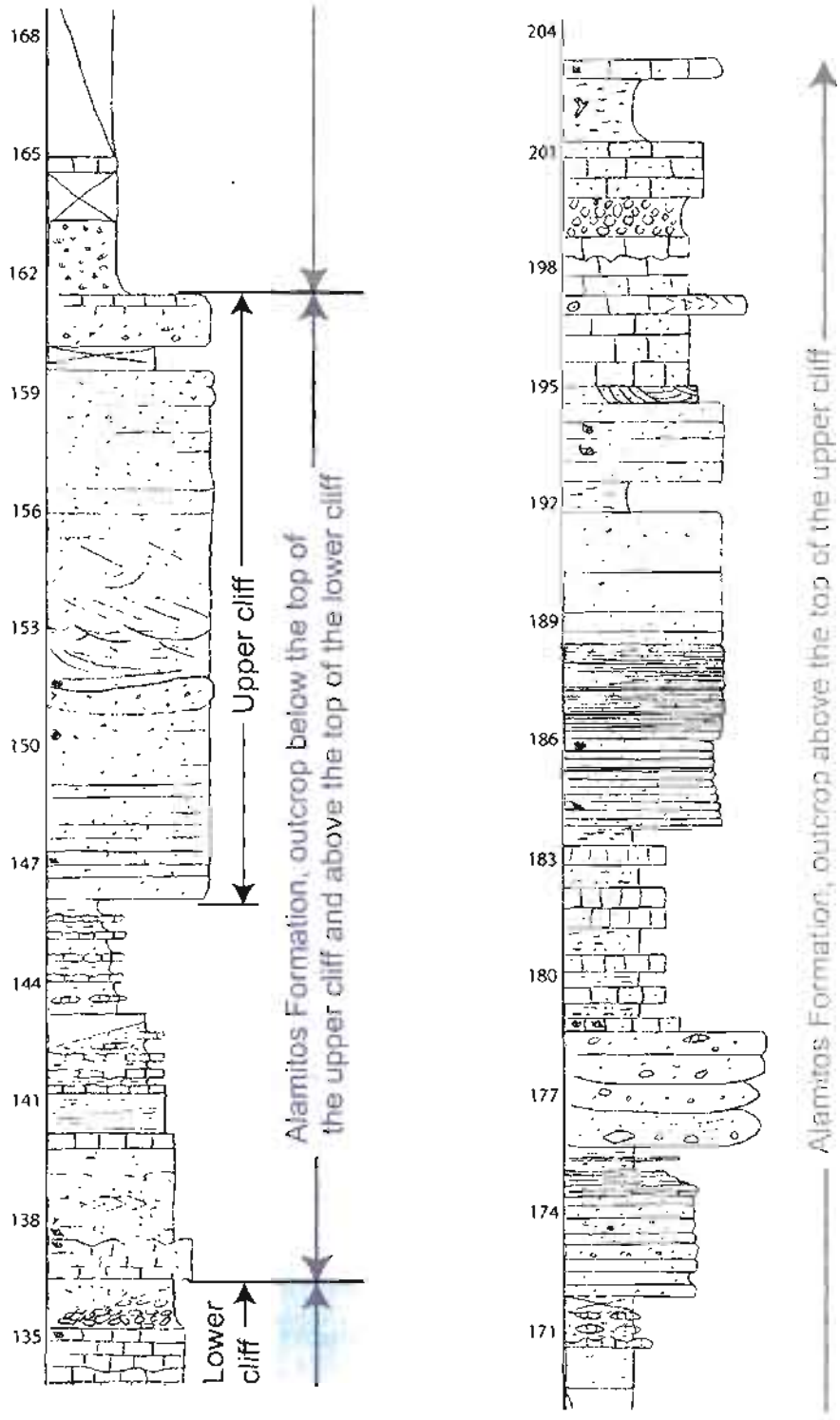

Figure 2.8. (continued).

Table 2.1. Carbonate Facies Characteristics

Facies Name	Composition	Fossils and Trace Fossils*	Lateral Extent
lime mudstone and shale	boudinage lime mudstone interbedded with organic rich black shale	benthic forams, calcispheres, ostracodes	varies, can be < 200 m or > 500 m
boundstone and coral packstone	rugose coral boundstone and corals in siltstone, corals often recrystallized	rugose coral	laterally extensive over 100's of m
wackestone	lime wackestone	brachiopods, gastropods, crinoids, trilobite frags., forams, bryozoans, ostracodes	varies, can be < 200 m or > 100's of m
phylloid packstone	phylloid algal packstone, recrystallized	phylloid algae, possibly *Archaeolithophyllum*	< 60 m
cherty wackestone-packstone	chert (siliceous sponge spicules), siltstone, and limestone, wackestone-packstone	sponge spicules, brachiopods	laterally extensive over 100's of m
siltstone with lime mudstone nodules	siltstone (may be silicified) with nodular limestone (fossiliferous and concretionary)	brachiopods, conularids (jellyfish), bryozoans, sponge spicules, *Planolites**	grades laterally to burrowed limestone facies
burrowed wackestone	nodular limestone with thin layers of siltstone or silty micrite[a], mottled appearance from vertical and horizontal burrows	brachiopods, fusulinids, gastropods, crinoid and bryozoan frags., ostracods, intensely burrowed by *Thalassinoides**	grades laterally to siltstone with limestone nodules facies
skeletal packstone	crinoidal-brachiopod packstone, crinoidal packstone, bryozoan packstone, or conglomeratic crinoidal-brachiopod packstone with 0.5-6 cm mudstone, igneous, and metamorphic clasts	crinoids, brachiopods, bryozoan	< 100 m
sandy limestone	arenitic sandy micrite[a]	*Zoophycos*, bryozoan, brachiopod fragments, crinoid fragments, fusulinids	laterally extensive over 100's of m
ooid grainstone	ooid grains composed of fusulinids, skeletal frags., quartz	fusulinids, echinoderm, gastropod, bryozoan, and brachiopod frags., bivalves	< 100 m

*Trace fossils marked with asterisks., frag. = fragments

[a]Classified according to *Mount* [1985].

Table 2.2. Carbonate Facies Interpretation

Facies Name	**Interpretation**
lime mudstone and shale	restricted, subtidal, distal to sediment source
boundstone and coral packstone	high energy shallow marine, corals form a biostrome that may reflect incipient reef development, corals reworked by wave action or wave generated currents
wackestone	moderate energy shelf
phylloid packstone	shelf, algal mat that forms a biostrome, no significant depositional relief, lateral growth on the sea floor, grew on the shelf below normal wave base (~5 m) and within the photic zone (5-25 m in the Paradox Basin)
cherty wackestone-packstone	subtidal shelf
siltstone with lime mudstone nodules	low-moderate energy shelf
burrowed wackestone	low-moderate energy shelf
skeletal packstone	shallow carbonate shoals, redeposited by gravity flow currents where packstone is gradational to, or at the top of the green conglomerate facies
sandy limestone	low energy shelf
ooid grainstone	shallow carbonate shoals

Table 2.3. Clastic Facies Characteristics

Facies Name	Composition	Fossils and Trace Fossils*	Lateral Extent/Geometry
green conglomerate	matrix supported polymictic conglomerate, matrix composition is equivalent to the green sandstone lithofacies	nautiloids, ammonoids, gastropods, brachiopods, crinoids	can occur unchannelized or as lenticular channels 1 m depth, 2-3 m wide, transitions laterally into green sandstone, green and red mudstone, and lime packstone facies
green sandstone	f. - vc. arkose with allogenic chlorite and igneous lithic fragments	*Zoophycos**, *Planolites**, brachiopods, *Helminthoida crassa**, sponge (*Girtyocoelia*)	transitions laterally rapidly (10-100 m) into green and red mudstone and green conglomerate facies
green and red mudstone	chlorite rich calcareous clay		rapid lateral transitions into green sandstone and green conglomerate facies
conglomeratic arkose	grain supported vc. conglomeratic arkose	sparse crinoids (<10%)	rarely transitions laterally into green conglomerate
fossiliferous arkose	grain supported vc. fossiliferous conglomeratic arkose, arkosic allochemic sandstone[a] (>50% sand, <50% allochems) or sandy allochem limestone[a] (<50% sand, >50% allochems)	fossil content varies (10-95%), fossil (95% allochems) or siliciclastic layers (70% siliciclastics) can occur in beds as little as ~1 cm thick, containing brachiopods, crinoids, bryozoan, trilobite frags., tabular coral, gastropods, fusulinids	laterally extensive over 100's of m
burrowed arkose	vertical burrows in f. ss, zones of c. or vc. arkose	*Arenicolites** (moderately burrowed)	grades laterally to limestone in less than 400 m
black shale	calcareous black shale containing muscovite	brachiopods (some in growth position), pelecypods, bryozoans, gastropods, *Planolites**	laterally extensive over 100's of m, transitions into siltstone

c. = coarse, vc. = very coarse, m. = medium, f. = fine, vf. = very fine
*Trace fossils marked with asterisks.
[a]Classified according to *Mount* [1985].

Table 2.4. Additional Clastic Facies Characteristics

Facies Name	Average grain size, Shape and Sorting	Grain Size Range	Clast Composition	Internal Structures
green conglomerate	c. grained matrix, most clasts are 2-5 cm, subangular, poorly sorted	silt - 15 cm clasts	predominately granite, metagranite, metarhyolite, vein quartz, quartzite; minor amphibolite, schist, and chert; one bone clast; intraclasts of siltstone, mudstone, sandstone, and limestone	generally massive, little trough cross stratification, no imbrication
green sandstone	c. grained, angular - subangular, poorly sorted	silt - conglomeratic (pebble)	N/A	inverse and normal grading
green and red mudstone	clay	clay - silt rich zones	contains abundant fossilized wood in one locality	parallel lamination or no lamination
conglomeratic arkose	vc. grains, 0.5-3 cm clasts, subrounded - angular, very poor to moderate sorting, grains have point to linear contact	silt - 7 cm clasts	predominately granite, metagranite, metarhyolite, vein quartz, quartzite, minor siltstone, amphibolite, sandstone, schist, chert	generally massive, occasional tabular planar and trough cross stratification, no imbrication, rare normal grading
fossiliferous arkose	m.-c. grained, subrounded - subangular, poor to well sorted	f. grained - 3 cm	granite, metagranite, metarhyolite, vein quartz, minor chert, minor petrified wood and limestone intraclasts	tabular cross beds, massive, horizontal beds, trough cross beds, bidirectional tabular cross beds, mud drapes, reactivation surfaces
burrowed arkose	predominately f. grained, arkose is well sorted, subrounded	clay - vc. sand	N/A	inverse and normal grading
black shale	clay	clay - silt	N/A	parallel lamination

c. = coarse, vc. = very coarse, m. = medium, f. = fine, vf. = very fine

Table 2.5. Clastic Facies Interpretation

Facies Name	Depositional Process	Environment Interpretation
green conglomerate	unconfined sediment gravity flow deposits and confined (where channelized) gravity flow deposits from flood plumes of a fan delta or braid delta, largest clasts entrained by a critical current velocity of 5 m/sec according to Hjulstrom's diagram as modified by Sundborg [*Hjulstrom*, 1939]	flood plumes onto a carbonate platform/ subtidal fan delta slope
green sandstone	unconfined gravity flow deposits, fan delta or braid delta, more distal to sediment source, critical current velocity of 1.5 m/sec	flood plumes onto a carbonate platform/ subtidal fan delta slope
green and red mudstone	mudflows or subtidal hemipelagic sedimentation, deposited from suspension	shelf mudstone, flood plumes onto a carbonate platform/ subtidal fan delta slope
conglomeratic arkose	unconfined grain flows from a fan delta or braid delta, in places reworked by tidal and ocean currents, critical current velocity of 3.5 m/sec	fan delta front
fossiliferous arkose	originally deposited by unconfined grain flows by a fan delta or braid delta into or adjacent to areas of carbonate production, reworked by tidal and other ocean currents (including storm currents) in areas of carbonate production producing a mixed sediment, critical current velocity of 2.5 m/sec	shelf sandstone, tidal and shallow marine current reworked deltaic
burrowed arkose	mod. energy, burrowed deltaic or shoreface sand	near shore, possibly shoreface or beach
black shale	hemipelagic sedimentation, low energy	subtidal shelf

characteristics are included in Appendix B. Several facies are described in the following section. Facies that account for less than 3 % of the composite section are not described in detail.

2.3.1 Facies

2.3.1.1 Green conglomerate facies

The green conglomerate facies accounts for 11 m or 5.6% of the composite section. The green conglomerate is a polymictic, matrix-supported conglomerate with a matrix composition of up to 60% fine to very coarse-grained arkose. Allogenic and authigenic chlorite constitutes up to 10% of the conglomerate matrix [*Ude*, 1992] and is responsible for the olive-green color of siliciclastic sediments in the study area. Subangular pebble and cobble sized clasts of the green conglomerates range in diameter from 1 to 15 cm, with an average of 2 to 5 cm. Figure 2.9a shows the polymictic nature of the conglomerate. Approximately 85% of the clast composition consists of granite, metagranite, metarhyolite, vein quartz, and quartzite. Amphibolite, schist, and chert compose ~10% of the total clast composition. Intraclasts of siltstone, mudstone, sandstone, and limestone are also present. At waypoint 224, a 7 cm bone clast was discovered. The bone may be a fragment of a rib or nondiagnostic skull bone (Terry Gates, personal communication, 2006). At several locations, the conglomerates incorporate Pennsylvanian fauna. Nautiloids (Figure 2.9b), ammonoids (Figure 2.9c and d), gastropods, brachiopods, and crinoids are present in the conglomerates. The conglomerates are generally massive with little trough cross stratification and no imbrication. The green conglomerate facies can occur unchannelized or as lenticular channels 1 m in depth and 2 to 3 m wide. Figure 2.9e is a photograph of several stacked channels of green conglomerate. The green conglomerate facies transitions vertically and laterally into green sandstone, green and red mudstone, and lime packstone facies (Figure 2.10).

The green conglomerate facies is interpreted to represent unconfined submarine sediment gravity flow deposits and confined (where channelized) submarine sediment gravity flow deposits from flood plumes of a fan delta or braid delta.

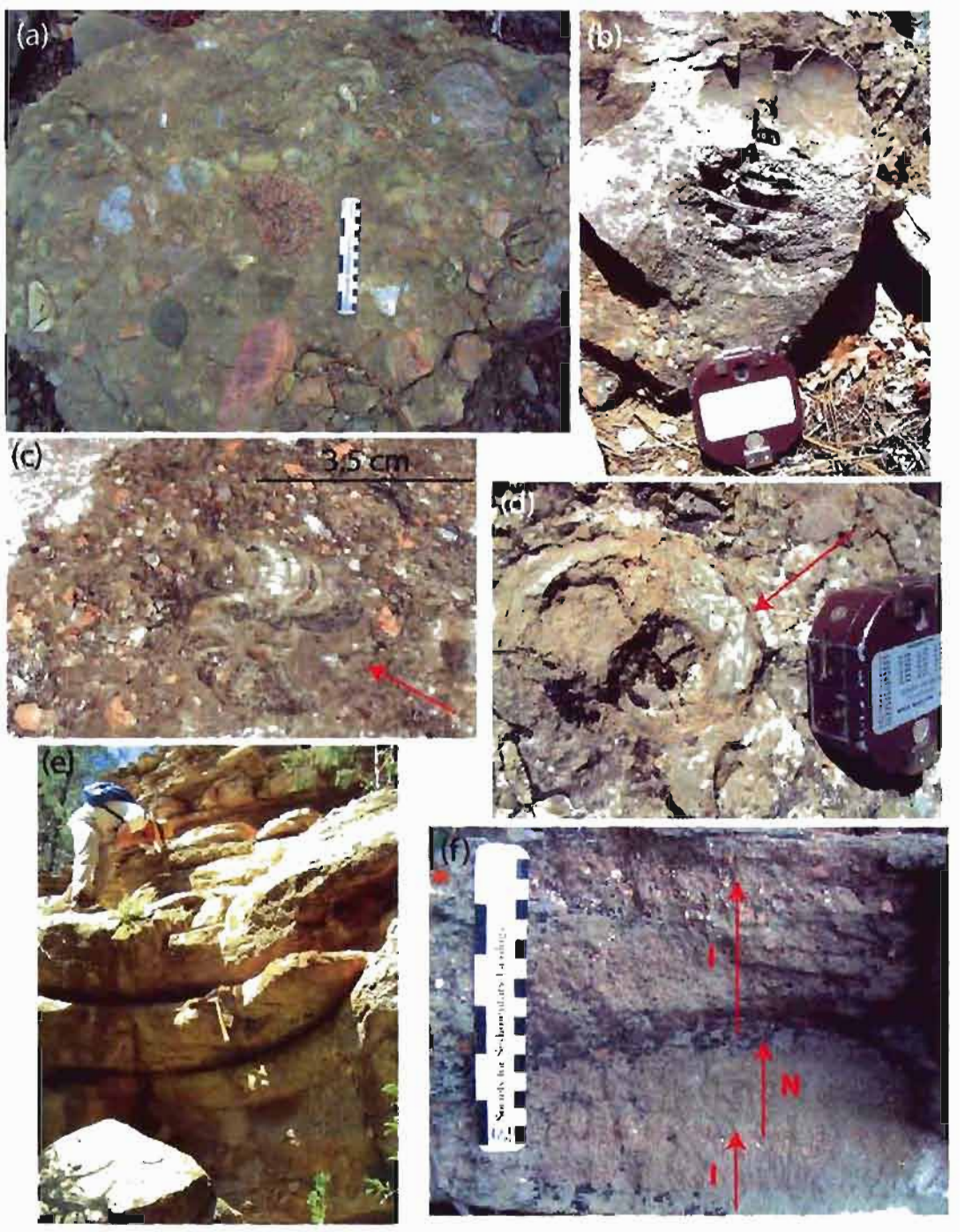

Figure 2.9. Outcrop photographs of the green conglomerate facies: (a) matrix supported clasts in the green conglomerate, (b) nautiloid fossil, (c) Pennsylvanian ammonoid (arrow), (d) Pennsylvanian ammonoid *Pseudoparalegoceras* (arrow points to suture pattern), (e) stacked channels of green conglomerate, and (f) inverse (I) and normal (N) grading in conglomeratic green sandstone.

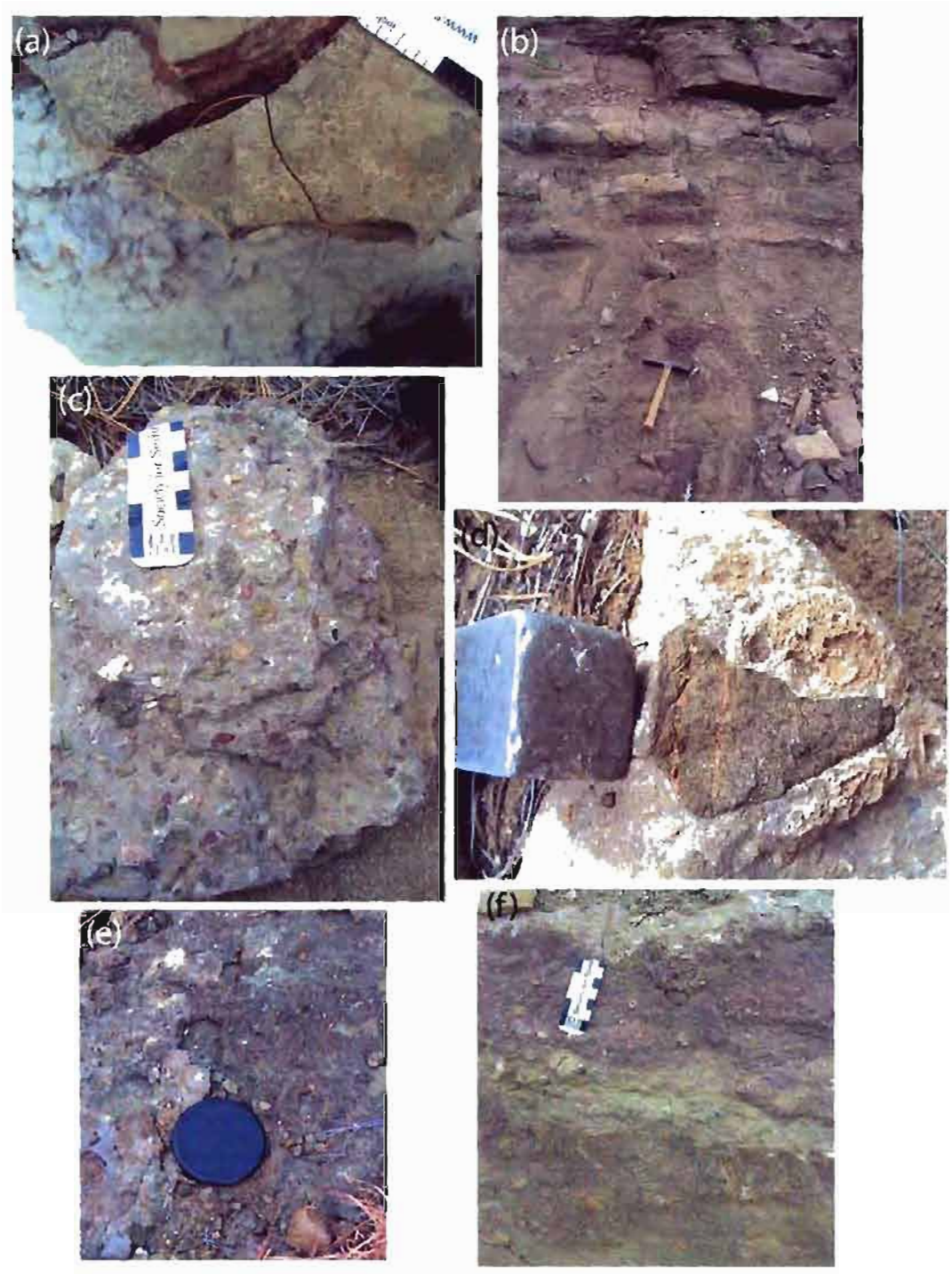

Figure 2.10. Green sandstone, mudstone, and packstone conglomerate facies: (a) *Helminthoida crassa* in the green sandstone facies, (b) green and red mudstone facies, (c) packstone conglomerate, (d) diorite clast in packstone, (e) lateral gradational contact between the packstone conglomerate and green conglomerate, and (f) vertical gradational contact between packstone conglomerate and green conglomerate.

These gravity flows may have originated from debris flows entering the ocean via delta channels. Presence of marine fauna, occasional interbedded limestone, and lateral and vertical gradation into facies with abundant trace fossils indicative of a low energy marine environment implies that the green conglomerate facies was deposited in a low energy marine setting. Lack of oxidation, rooting, or other evidence of subaerial exposure, as well as textural immaturity and presence of up to 40% lithic pebbles and cobbles indicating rapid deposition without subsequent reworking, all suggest that the conglomerates were deposited below wave base. The largest clasts were entrained by a critical current velocity of 5 m per second according to Hjulstrom's diagram as modified by Sundborg [*Hjulstrom*, 1939]. The nested channel complexes represent major conduits for transportation and deposition of conglomeratic flood plumes onto a carbonate platform or fan delta slope.

2.3.1.2 Green sandstone facies

The green sandstone facies accounts for 26 m, which is 13% of the composite statigraphic section. Sandstone composition consists of fine to very coarse arkose with allogenic chlorite and abundant (~25%) igneous lithic fragments. The sandstones are dominately coarse-grained, angular to subangular, poorly sorted, and commonly conglomeratic. Both inverse and normal grading are present (Figure 2.9f). The average sandstone composition consists of 40% quartz, 22% feldspar, 8% metamorphic and sedimentary lithic fragments, 10% allogenic and authigenic chlorite, up to 27% calcite cement, and 1 to 3% micaceous minerals and skeletal fragments [*Ude*, 1992]. The green sandstone facies commonly occurs between conglomeratic channel complexes. The facies exibits poor lateral continuity and transitions laterally into the green and red mudstone and green conglomerate facies.

The green sandstone facies was deposited by unconfined submarine sediment gravity flows from flood plumes of a fan delta or braid delta. *Ude* [1992] suggests that this facies is deposited from currents ranging from sandy high-density turbidity to liquefied flow. Evidence indicative of liquefied flows includes normal grading and flat, unscoured bases of tabular beds [*Lowe*, 1982]. Acceleration of liquefied

flows generates high-density turbidity currents [*Lowe*, 1982] capable of depositing the coarse-grained to conglomeratic fraction of the green sandstone facies. The largest clasts were entrained by a critical current velocity of 1.5 m/sec [*Hjulstrom*, 1939]. Between the passing of submarine gravity flows, low-energy conditions allowed development of horizontal trace fossils on the upper surfaces of sandstone beds. The genetic relationship of the green sandstone and conglomerate facies and the presence of Pennsylvanian brachiopods and sponges (Girtyocoelia), as well as *Zoophycos*, *Planolites*, and *Helminthoida crassa* (Figure 2.10a), suggest that the green sandstone faces was deposited below wave base by flood plumes onto a carbonate platform or a delta slope.

2.3.1.3 Green and red mudstone facies

The green and red mudstone facies consists of chlorite-rich calcareous clay and commonly contains silt. This facies accounts for 34 m (17.5%) of the composite stratigraphic section. Alternating ~0.1 to 0.3 m layers of green and red mudstone are common (Figure 2.10b). At several locations, the green and red colors both crosscut one bed, indicating that the color difference is the result of diagenesis. Thin sections across the color boundary in a siltstone show that the color difference is the result of the quantity of hematite. Red beds have an abundance of hematite; only a small amount of hematite is found in the green beds. The mudstone either lacks lamination or has well-developed parallel lamination. Upper and lower contacts of the mudstone facies are generally sharp. The green and red mudstone facies rapidly transitions vertically and laterally into green sandstone, green conglomerate facies, and black shale facies. The mudstone is commonly interbedded with the green sandstone and green conglomerate facies.

The green and red mudstone facies is interpreted as a subtidal delta derived mudflow deposit where it is associated with green sandstones and conglomerates, and is interpreted as a shelf mudstone where gradational with black shales. There are two methods by which the mudstone facies was deposited, by mud flows or from suspension by subtidal hemipelagic sedimentation. Deposition in a subtidal

environment by mud-rich flood plumes is evidenced by the mudstones' genetic relationship with the green conglomerate and green sandstone facies, as well as with an abundance of randomly oriented fossilized wood pieces (up to 15 cm) in the mudstone at one locality. Although burrows are not distinguishable, extensive bioturbation may be responsible for destroying intervals of parallel lamination in the mudstones. *Ude* [1992] put forth the idea that deposition by turbidity currents may explain the lack of parallel lamination. Deposition by hemipelagic sedimentation is evidenced by parallel lamination and the vertical and lateral gradational relationship of the green and red mudstone facies with the black shale facies.

2.3.1.4 Fossiliferous arkose facies

The fossiliferous arkose facies accounts for 50 m (25%) of the composite stratigraphic section. The fossiliferous arkose facies is a coarse-grained, grain-supported, fossiliferous conglomeratic arkose (Figure 2.11a and b). The fossil content varies between 10 and 95%. Fossil-rich layers (up to 95% allochems) or siliciclastic layers (up to 70% siliciclastics) can occur in beds as thin as ~1 cm. The fossil content consists of abraded brachiopods, crinoids, bryozoans, trilobite fragments, tabular corals, gastropods, and fusulinids. Clasts in the conglomeratic portion of the fossiliferous arkose facies consist of granite, metagranite, metarhyolite, and vein quartz. Clasts of chert, limestone intraclasts, and petrified wood are not as abundant. The fossiferous arkose facies has several types of bedding (in order of relative abundance): horizontal (Figure 2.11c), tabular crossbedded (Figure 2.11d and e), massive, trough crossbedded, and bidirectional tabular crossbedded. Massive and horizontal beds grade vertically and laterally into crossbedded units with the same or very similar grain size and composition. At several locations, tabular crossbedding was traced laterally into "massive" bedding where the visible crossbedding gradually disappeared. This is an indicator that "massive" or "homogeneous" sandstones of the fossiliferous arkose facies may have crossbedding that is not readily visible. This phenomenon has been observed and studied by

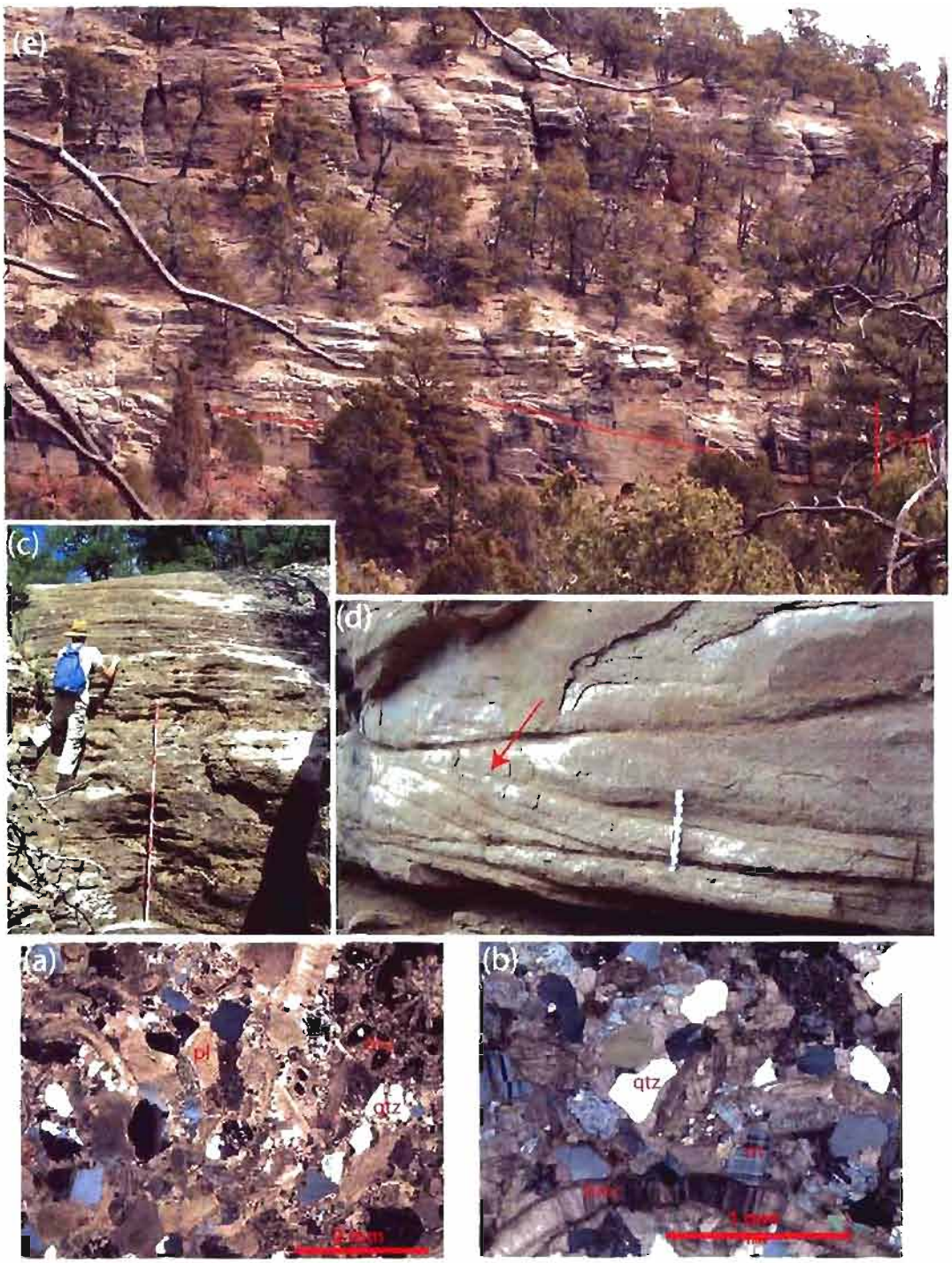

Figure 2.11. Fossiliferous arkose facies: (a) and (b) thin sections of the fossiliferous arkose facies (qtz = quartz, m = microcline, pl = pelmatozoan, brac = brachiopod, bry = bryozoan), (c) thin bedded fossiliferous arkose facies, (d) tidal bundles in the upper cliff, note mud drapes and reactivation surface from current reversal (arrow), and (e) large scale tabular cross bedding in upper and lower cliff (east view).

Hamblin [1965]. Using x-ray pictures of rock slices from samples that appear homogenous Hamblin observed internal structures in 87% of the "homogenous" sandstone samples. Thus, *Hamblin* [1965] concluded that most "homogeneous" sandstones do not represent a special sedimentary environment and suggests that "homogeneous" sandstones occur when variation in composition, texture, fabric, color, or cementation between structural units is slight.

Tabular crossbeds in the fossiliferous arkose facies are dominately tabular tangential, bundled, laterally extensive over 500 m, contain reactivation surfaces, and are commonly draped with a thin layer of mud (Figure 2.11d). Tabular tangential cross bed sets range in size from less than 10 cm thick up to 5 m (Figure 2.11e). North - south bimodal-bipolar paleocurrent trends (measured from crossbedding) in the fossiliferous arkose facies are observed in several places within the study area. The fossiliferous arkose exibits a sharp contact with underlying shale, is commonly capped by limestone, and becomes lime rich (>80% lime) at the top of a sequence (illustrated in 'upper cliff' and 'lower cliff' intervals of Figure 2.8). *Ude* [1992] observed a minor subaerial exposure surface at the top of an ooid grainstone bed at the top of an outcrop of the fossiliferous arkose where a thin peloidal horizon with circum-granular and intragranular cracking indicating repeated wetting and drying. The fossiliferous arkose facies is laterally extensive throughout the study area but varies in thickness.

The presence of abundant abraded and fragmented marine fauna implies that beds of fossiliferous arkose facies were deposited in a marine setting. The presence of rhythmic consistent mud drapes and reactivation surfaces from current reversal in tabular tangential crossbedding are diagnostic of deposition by tidal currents in a subtidal environment [*Nio and Yang*, 1991]. In studies of modern tidal deposits, deposits with these characteristics are called megaripple bundles [*Nio and Yang*, 1991]. Laterally extensive tabular tangential crossbeds at Pecos developed during migration of straight crested sand dunes (megaripples). Variations of tidal flow (asymmetric to symmetric) may account for the different types of crossbedding observed in the fossiliferous arkose facies. The large-scale tabular

tangential crossbedding (up to 5 m) suggests that parts of the shelf were subject to strong unidirectional tidal currents, whereas medium to small-scale bidirectional tabular crossbedding and interbedded trough crossbedding may have formed as a result of more symmetrical tidal currents [*Allen*, 1980; *Nio and Yang*, 1991]. Bimodal-bipolar paleocurrent trends are observed from bidirectional crossbedding and reversal in the dip direction of tabular tangential crossbedding (tidal bundles)(Figure 2.11a). Dip direction reversal in tidal bundles reflects the reversal of dominance of either flood or ebb currents [*Nio and Yang*, 1991].

The presence of ooid grainstones with minor subaerial exposure at the top of the fossilferous arkose facies indicates places where the shelf sandstone built slightly above sea level. Massive beds of the fossiliferous arkose facies contain crossbedding that is not readily visible. Massive beds resulted from deposition of akosic sediment into an area of carbonate production and were likely affected by tidal, storm, or other ocean currents resulting in a mixed carbonate-clastic sediment. Siliciclastic and carbonate-rich horizontal interbeds may represent carbonate shelf storm and fairweather deposits, respectively.

Ude [1992] concluded that the compositional differences between the green conglomerate/green sandstone facies and the fossiliferous arkose facies were due to different depositional processes rather than provenance. He proposed that the depositional matrix of chlorite clay present in the green sandstones and conglomerates has been winnowed from the fossiliferous arkoses by shallow-marine processes. If Ude is incorrect, then the chlorite rich sediments may indicate a more mafic provenance (Section 2.4.3). Ude's evidence for this conclusion is that the quartz-feldspar-lithic (QFL) composition of fossiliferous arkoses and green sandstones is very similar. This similarity is also observed in this study. In addition, Ude's conclusions are supported by the observation that the clast composition of the fossiliferous arkose facies is very similar to the green conglomerate facies. Thus, the fossiliferous arkose is interpreted as a reworked deltaic, shelf sandstone. It was probably originally deposited by unconfined grain flows by a fan delta or braid delta into or adjacent to areas of carbonate production, then reworked by tidal, storm,

and ocean currents in areas of carbonate production, producing a mixed sediment. The largest clasts in the fossiliferous arkose facies (3 cm) were entrained by critical current velocity of 2.5 m/sec [*Hjulstrom*, 1939].

2.3.1.5 Conglomeratic arkose facies

Only 2.2% (4 m) of the composite stratigraphic section is composed of the conglomeratic arkose facies. This facies is compositionally the same as the fossiliferous arkose facies except that it contains few fossils (<10% crinoid fragments) and has a larger maximum clast size (7 cm). The conglomeratic arkose facies shows sharp contacts with underlying shale. The conglomeratic arkose facies is very coarse-grained, grain-supported, conglomeratic, generally massive with occasional tabular planar and trough cross stratification, no imbrication, and rare normal grading.

The conglomeratic arkose facies is interpreted as deposits of unconfined grain flows at a fan delta or braid delta front (frontal splays). The presence of marine fauna implies that the conglomeratic arkose facies was deposited in a marine setting. Rare bidirectional tabular crossbedding and a low percentage of marine fossils indicate limited reworking by tidal, wave, and ocean currents. A sharp contact with the underlying black shale facies supports a grain-flow origin [*Gong*, 1992].

2.3.1.6 Black shale facies and lime mudstone interbedded with shale facies

The black shale facies and lime mudstone interbedded with shale facies account for 9.8% and 6.2% (31 total m) of the composite stratigraphic section, respectively. The black shale facies is calcareous, commonly contains fossils, and is commonly silty with abundant muscovite. Fossils in the black shale facies include brachiopods (some in growth position), pelecypods, bryozoans, and gastropods. The trace fossil *Planolites* is also present. In several places it has a greenish color and is gradational with the green mudstone facies.

The lime mudstone interbedded with shale facies consists of "'boudinage"' lime mudstone interbedded with organic rich black shale. Bed thickness varies between 10 and 30 cm. Fossils in this facies include benthic forams, calcispheres, and ostracodes.

The black shale facies and lime mudstone interbedded with shale facies are interpreted as deposits of low energy subtidal hemipelagic sedimentation in a shelf environment. In the southern part of the study area, both facies pinch out toward the north. Deposition in a lagoonal or estuarine environment protected by a barrier bar of the fossiliferous arkose facies is a possibility, but the unknown lateral extent of both facies leaves this interpretation in question.

2.3.1.7 Sandy limestone facies

Limestones in the study area are typically sandy or silty (Figure 2.12). The sandy limestone facies contains almost 50% very fine sand in lime mud. The facies is an arenitic sandy micrite according to Mount's classification [*Mount*, 1985] and accounts for 3.9% (7.6 m) of the composite stratigraphic section. The sandy limestone facies contains <20% allochem material, including bryozoan, brachiopod fragments, pelmatozoan fragments, and fusulinids. *Zoophycos* trace fossils are found in this facies (Figure 2.12a).

The presence of *Zoophycos* and the fine-grained nature of the sandy limestone facies is indicative of a low energy shelf environment. *Zoophycos* appeared to change its ecological setting from a shelf environment during the Paleozoic to a basinal environment during the Mesozoic (Tony Ekdale, personal communication, 2006).

2.3.1.8 Siltstone with lime mudstone facies and burrowed wackestone facies

The siltstone with lime mudstone facies and burrowed wackestone facies make up 4.3% and 2.7% of the composite stratigraphic section, respectively. The facies are laterally gradational with each other. The siltstone with lime mudstone facies (Figure 2.12b) is composed of siltstone with nodular limestone (fossiliferous and

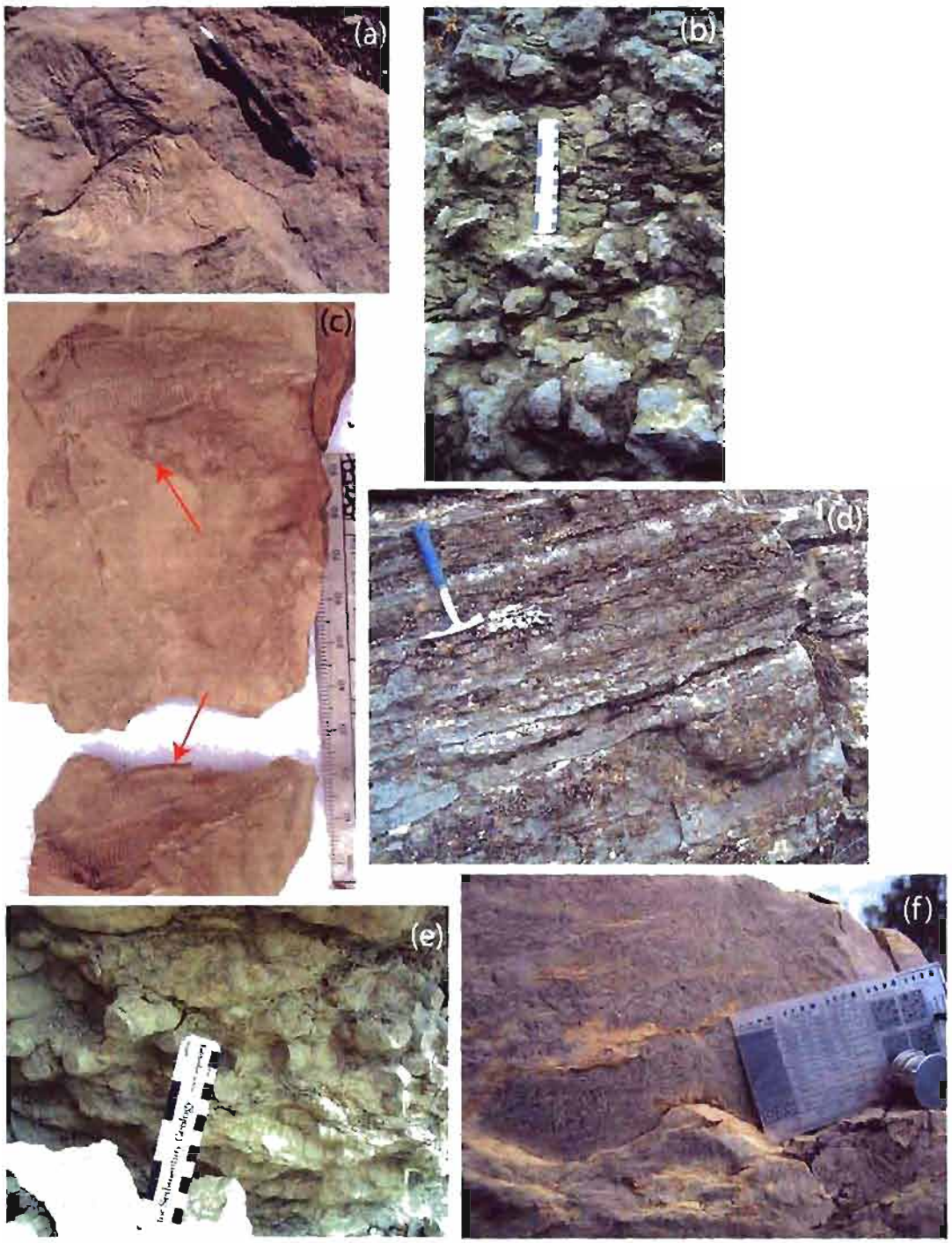

Figure 2.12. Carbonate facies: (a) *Zoophycos* in sandy limestone facies, (b) siltstone with limestone nodules facies, (c) two conularia in siltstone (arrows), (d) *Thalassinoides* burrows in burrowed wackestone facies, (e) rugose corals in siltstone, and (f) phylloid algae packstone.

concretionary). Fossils present in this facies include brachiopods, conularids, bryozoan, and sponge spicules. *Conularia* (Figure 2.12c) is a type of ancient jellyfish observed in the siltstone with limestone nodules facies. A *Planolites* trace fossil also occurs along bedding planes. The burrowed wackestone facies consists of nodular limestone with thin layers of siltstone or silty micrite. A mottled appearance results from vertical and horizontal *Thalassinoides* burrows (Figure 2.12d). Fossils of abundance in the facies include brachiopods, fusulinids, gastropods, crinoids, bryozoans, and ostracods.

The trace fossil and fossil assemblage of the siltstone with lime mudstone facies and burrowed wackestone facies indicates deposition in a low to moderate energy shelf environment. The diverse faunal assemblage implies that open marine conditions prevailed during sedimentation.

2.3.1.9 Cherty wackestone-packstone facies

Three and a half percent or 6.8 m of the composite stratigraphic section is composed of the cherty wackestone-packstone facies. The facies consists of spiculitic chert (siliceous sponge spicules), siltstone, and limestone. The facies is laterally extensive throughout the study area and maintains a constant thickness of 6 to 7 m. A 1 m thick crinoid packstone bed occurs 1 m above the base. The chert is resistant to weathering and forms a prominent cliff. This cliff is stratigraphically equivalent to cliff 7 at Dalton Bluff in the study by *Sutherland* [1963].

The cherty wackestone-packstone facies is interpreted as a subtidal shelf deposit. Wave-generated bottom currents may have concentrated the sponge spicules. Abundant silt and a lack of coarse grains suggest sedimentation distal to the clastic source area. Given this interpretation, the crinoid packstone interbed may represent the product of redeposition from a shallow water environment.

2.3.1.10 Other carbonate facies

The ooid grainstone, skeletal packstone, and boundstone/coral packstone facies make up only 0.3%, 2.1%, and 0.7% of the composite stratigraphic section,

respectively. However, all of these carbonate lithologies are good indicators of a high energy shallow open marine environment. The ooid grainstone and skeletal packstone facies formed on shallow carbonate shoals. The boundstone/coral packstone is composed of rugose coral boundstone and rugose corals in siltstone (Figure 2.12e). In several places the corals are recrystallized beyond recognition. The facies is laterally extensive throughout most of the study area; thus, the corals form a biostrome. The corals are commonly draped with siltstone and are not bound together with aligned long axes. This coral packstone may indicate reworking by wave action or wave-generated currents.

The skeletal packstone facies can occur as a conglomerate composed primarily of skeletal carbonate grains with abundant intraclasts of green and red mudstone (Figure 2.10c) and large (up to 6 cm) igneous and metamorphic clasts (Figure 2.10d). This conglomerate is gradational vertically and laterally with the green conglomerate facies (Figure 2.10e and f). It was likely deposited by high energy currents of low turbidity water that passed through carbonate shoals, thereby picking up and redepositing the carbonate material. The packstone's relationship with the green conglomerate facies suggests that it was deposited during the same flood events responsible for deposition of the green conglomerate.

2.3.2 Measured sections

Figures 2.13 through 2.16 are the four measured sections used to create the composite section. The sections show interpreted facies and depositional environment, as well as shallowing upward cycles (arrows with circled numbers) and gravity flow pulse intervals (arrows with boxed numbers). Cycles were defined based on changes in interpreted depositional environment. On the Pecos platform, a shallowing upward cycle consists of a conformable repetitive succession of strata that represent a shallowing of depositional environment. The Pennsylvanian-Permian cycles meeting this criterion are termed 'cyclothems' in other studies [*Gong*, 1992; *Klein and Kupperman*, 1992; *Tankard*, 1986; *Miller and West*, 1993]. In sequence stratigraphic terminology, the shallowing upward cycles at Pecos could be called

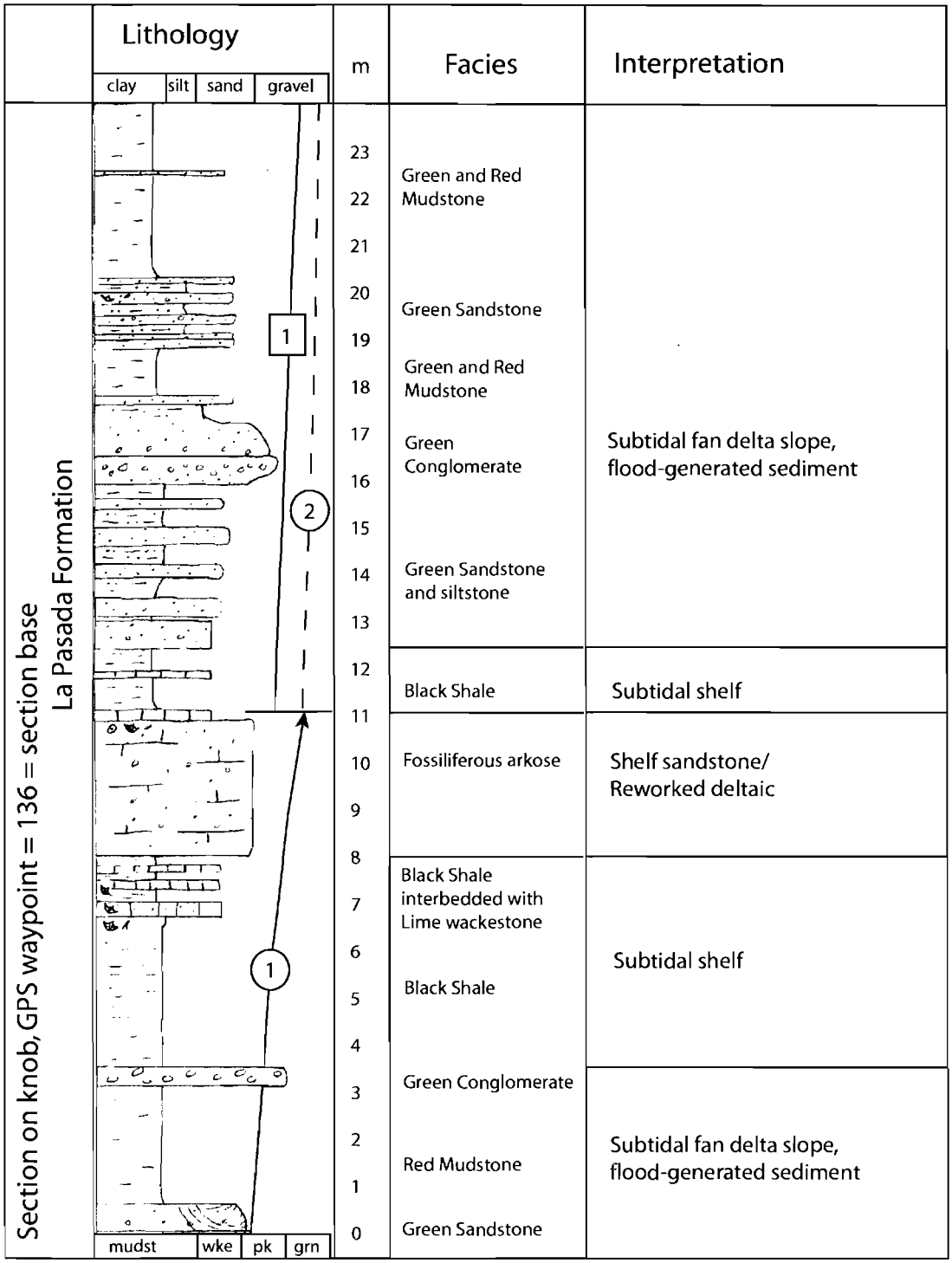

Figure 2.13. Section on Knob. Arrows with circled numbers indicate shallowing upward cycles. Dashed line shows interval where the shallowing cycle is not well defined. (Dashed line continues upward in the section.) Arrows with boxed numbers indicate gravity flow pluse intervals.

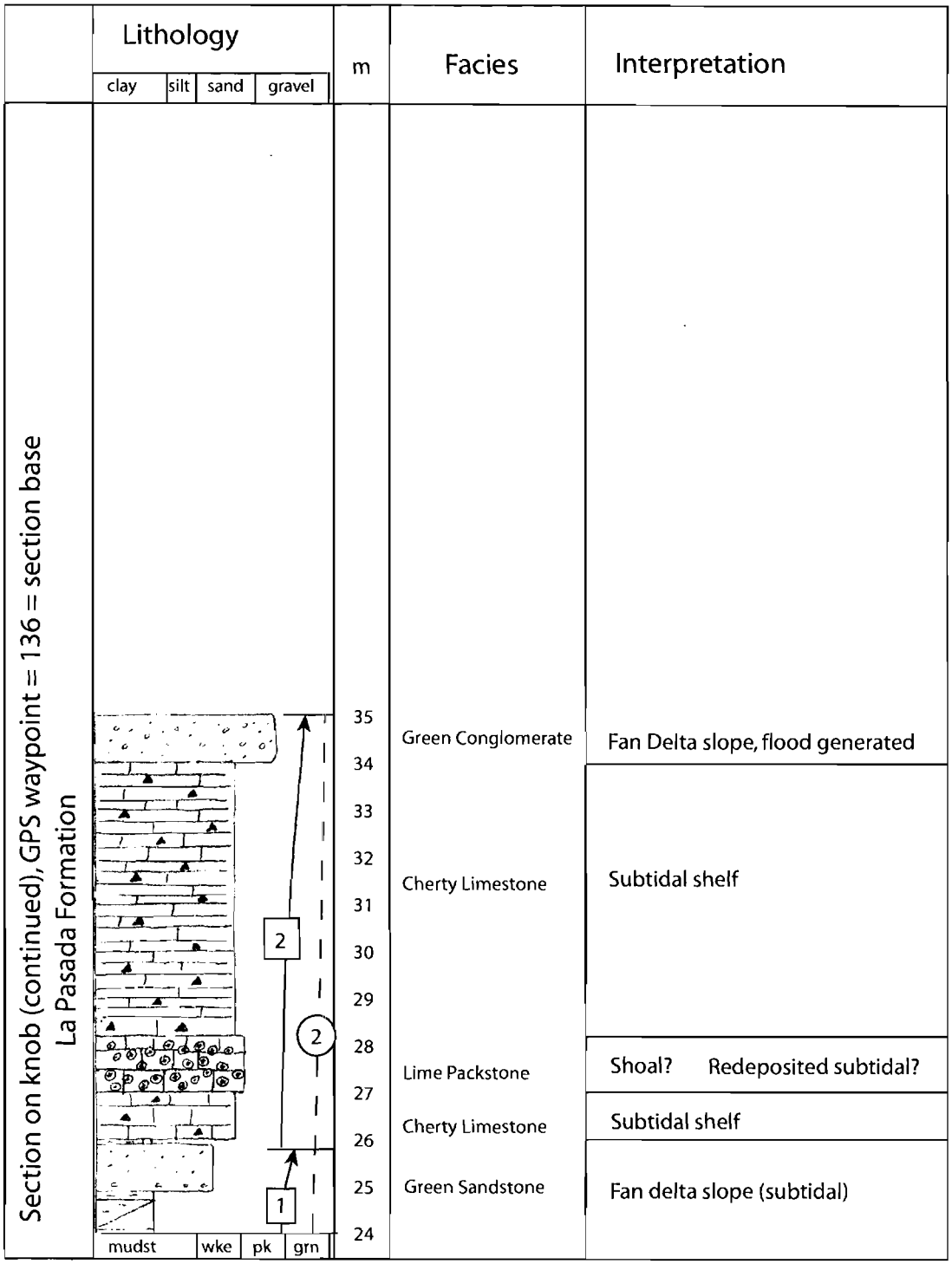

Figure 2.13. (continued).

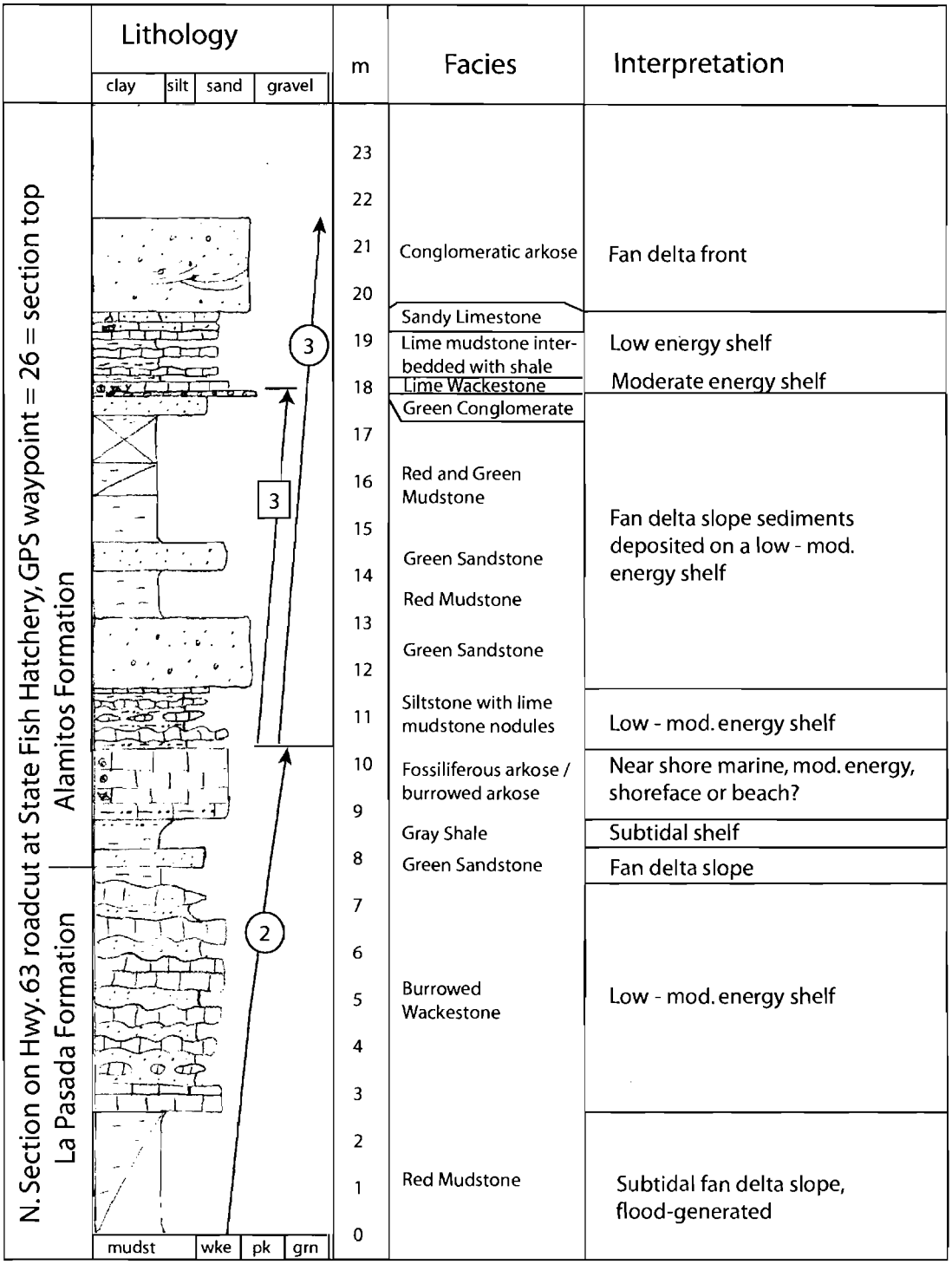

Figure 2.14. North Section on Hwy. 63 Roadcut. Arrows with circled numbers indicate shallowing upward cycles. Dashed line shows interval where the shallowing cycle is not well defined. (Dashed line continues upward in the section.) Arrows with boxed numbers indicate gravity flow pluse intervals.

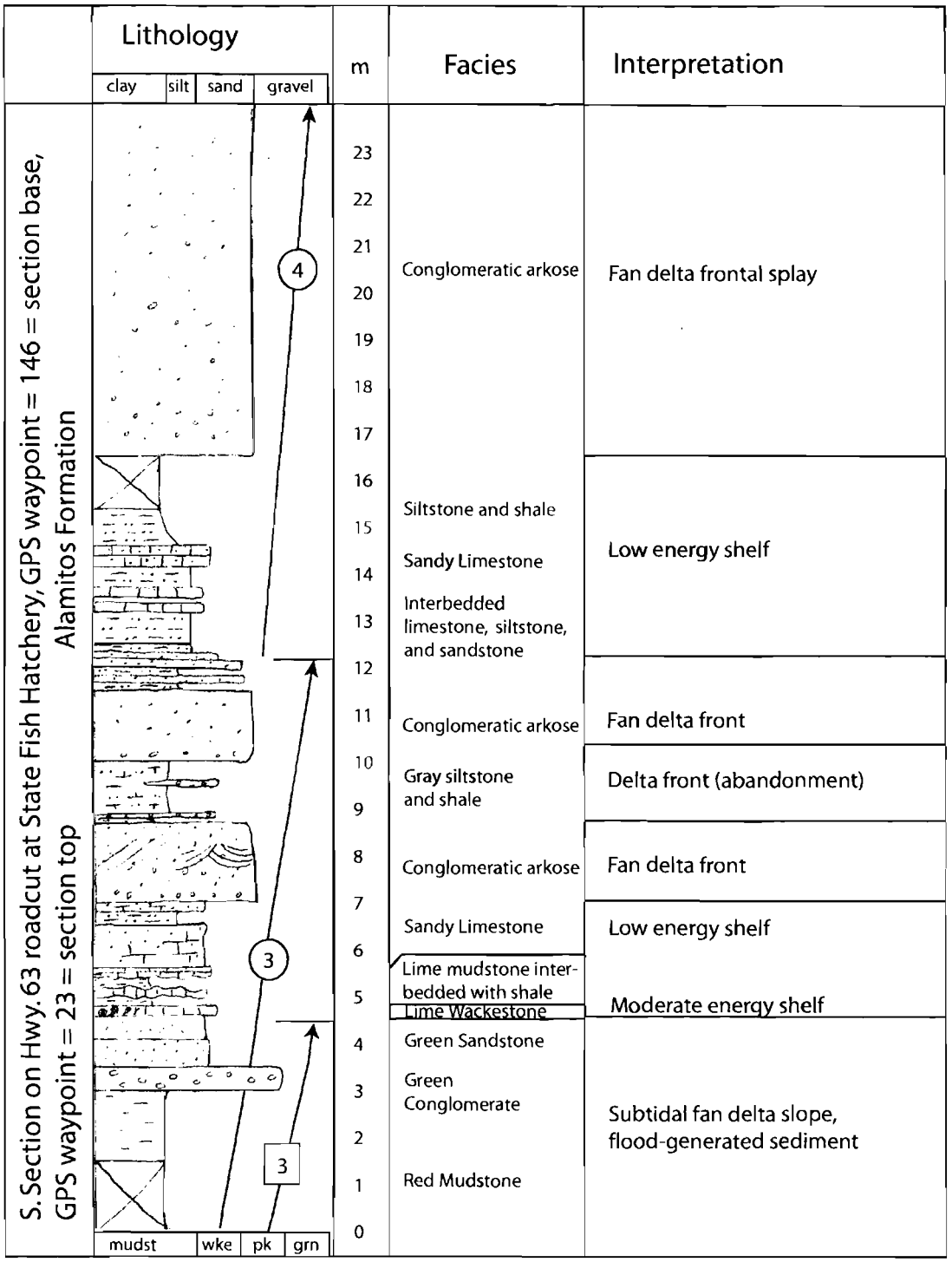

Figure 2.15. South Section on Hwy. 63 Roadcut. Arrows with circled numbers indicate shallowing upward cycles. Arrows with boxed numbers indicate gravity flow pluse intervals.

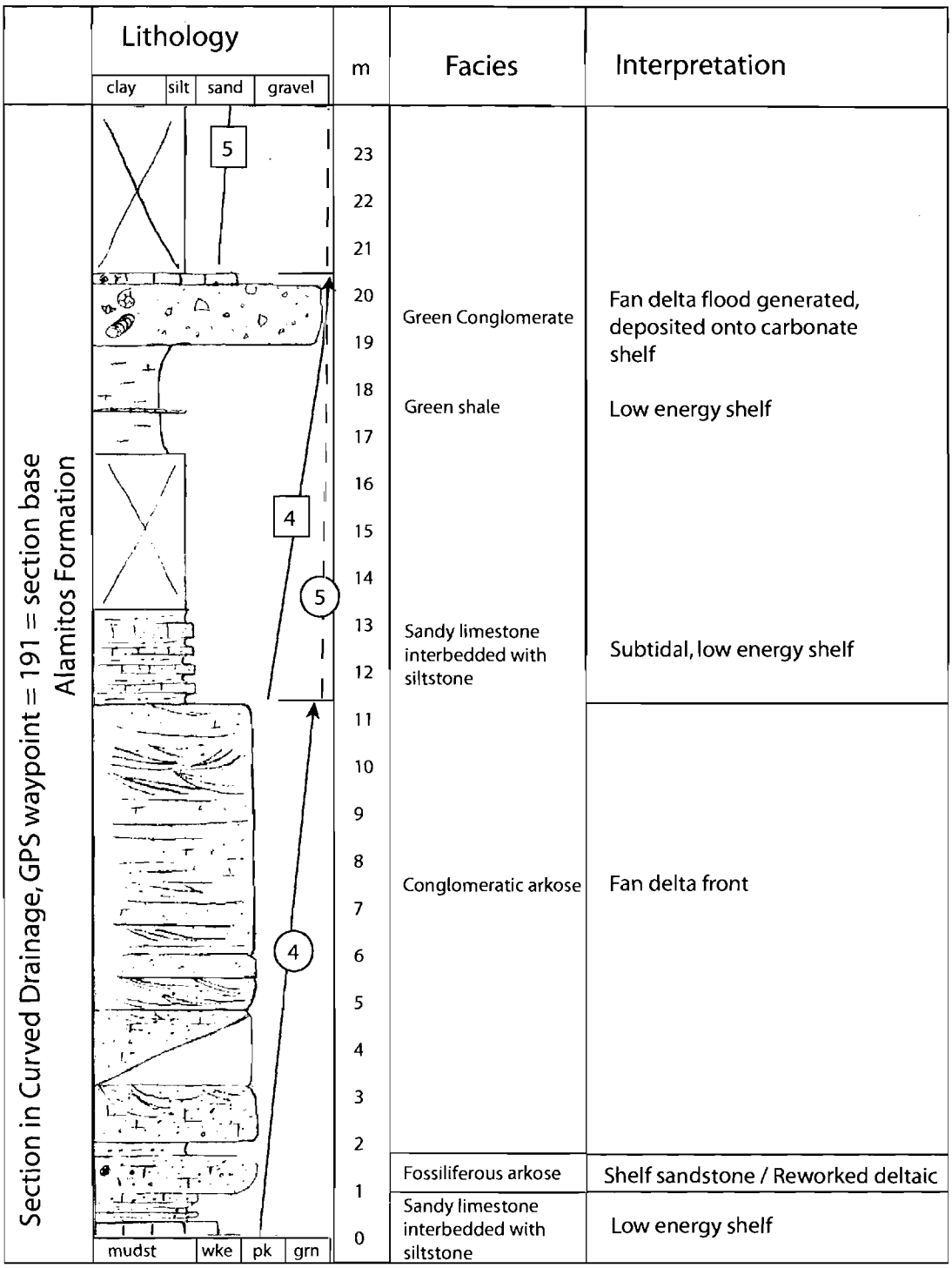

Figure 2.16. Section in Curved Drainage. Arrows with circled numbers indicate shallowing upward cycles. Dashed lines show intervals where shallowing cycles are not well defined. (Dashed line continues upward in the section.) Arrows with boxed numbers indicate gravity flow pluse intervals.

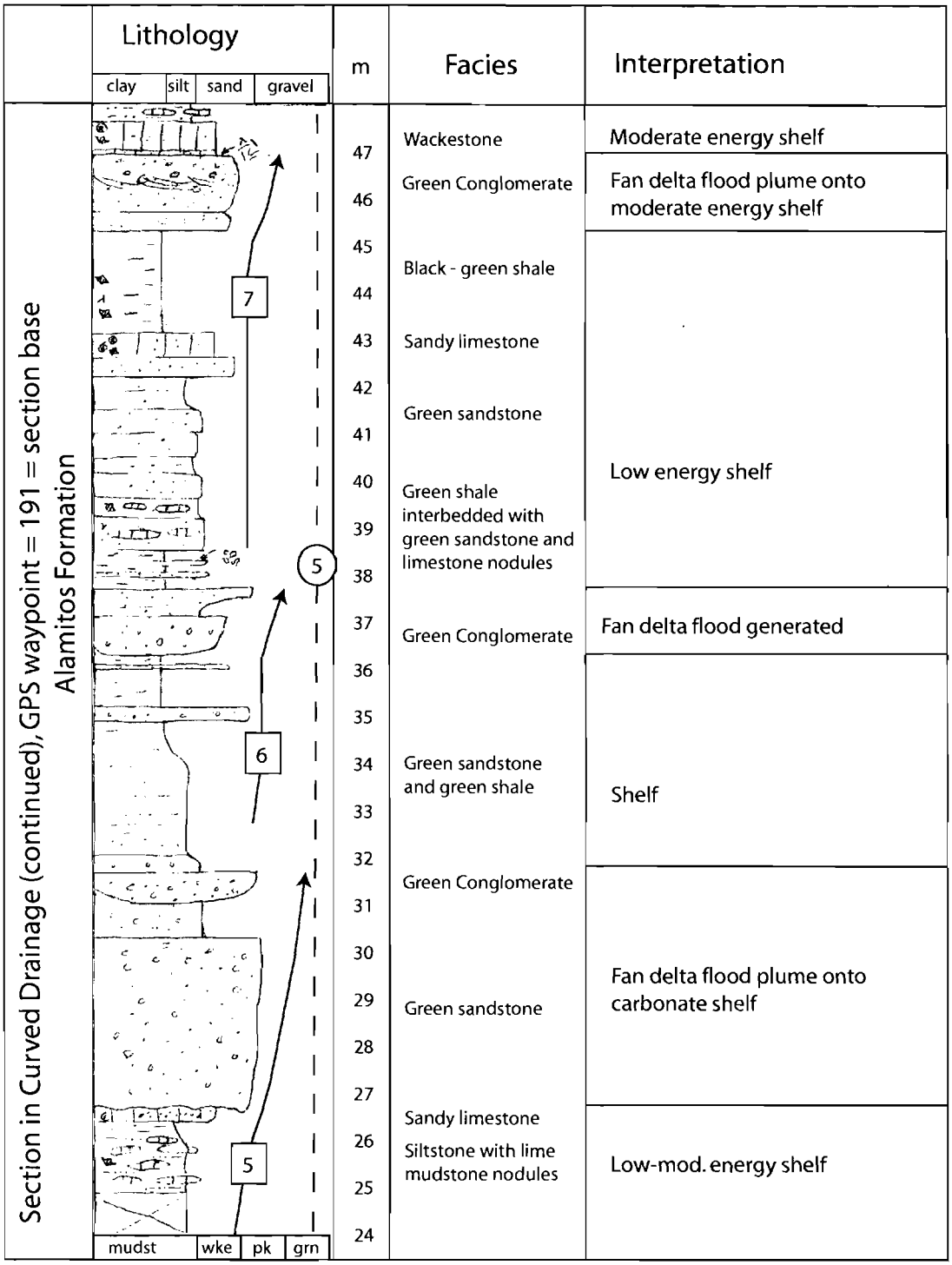

Figure 2.16. (continued)

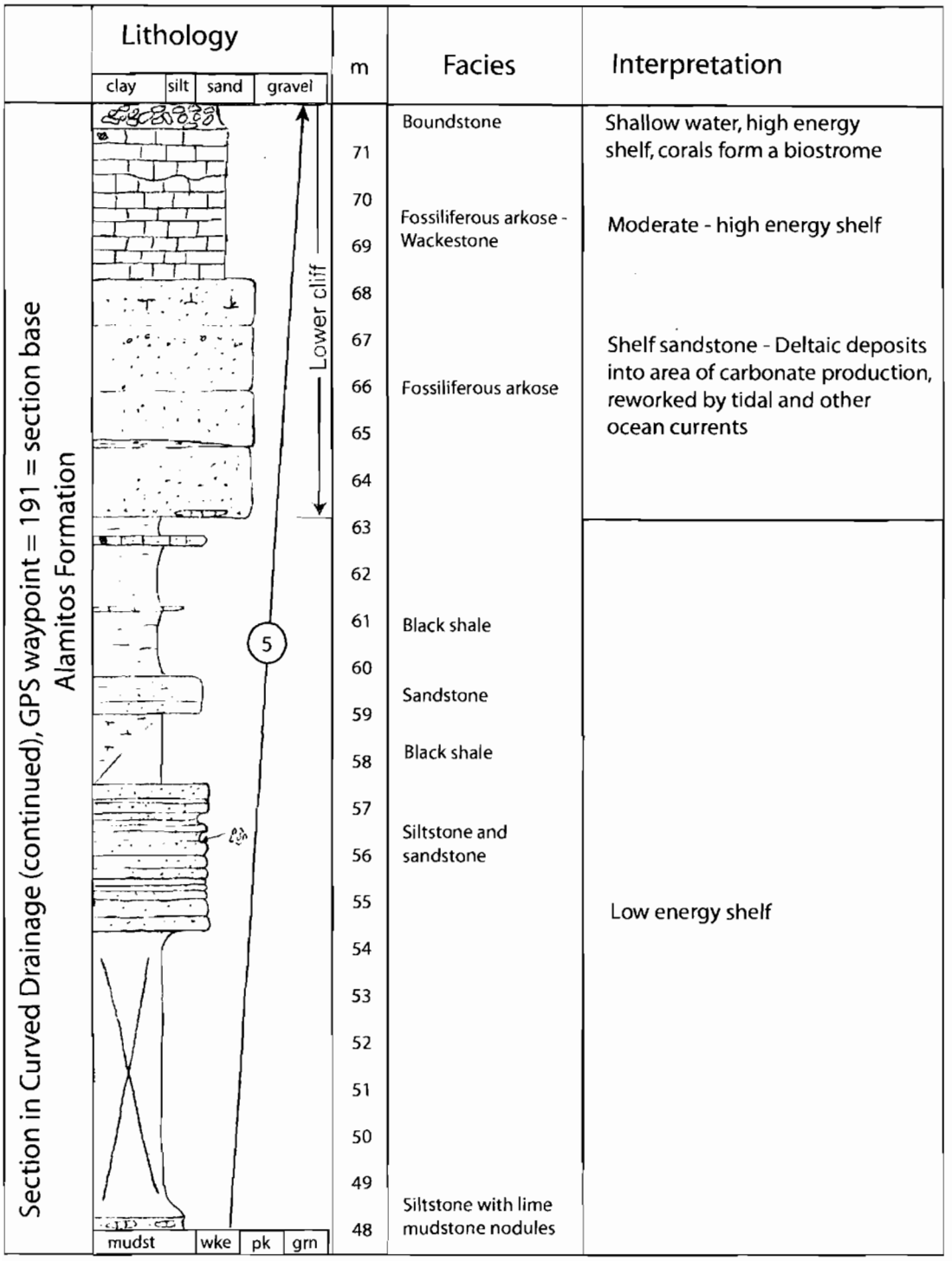

Figure 2.16. (continued).

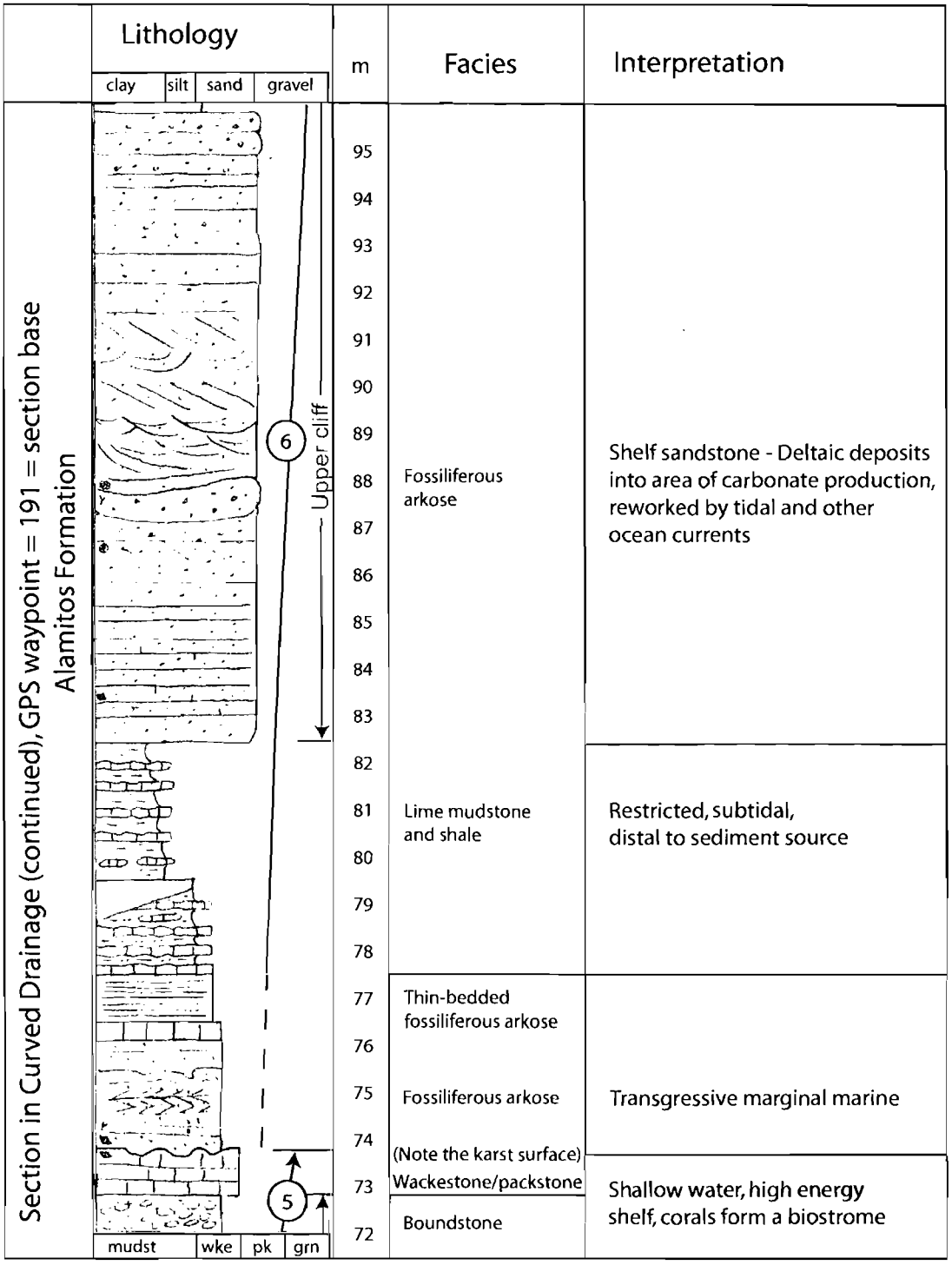

Figure 2.16. (continued).

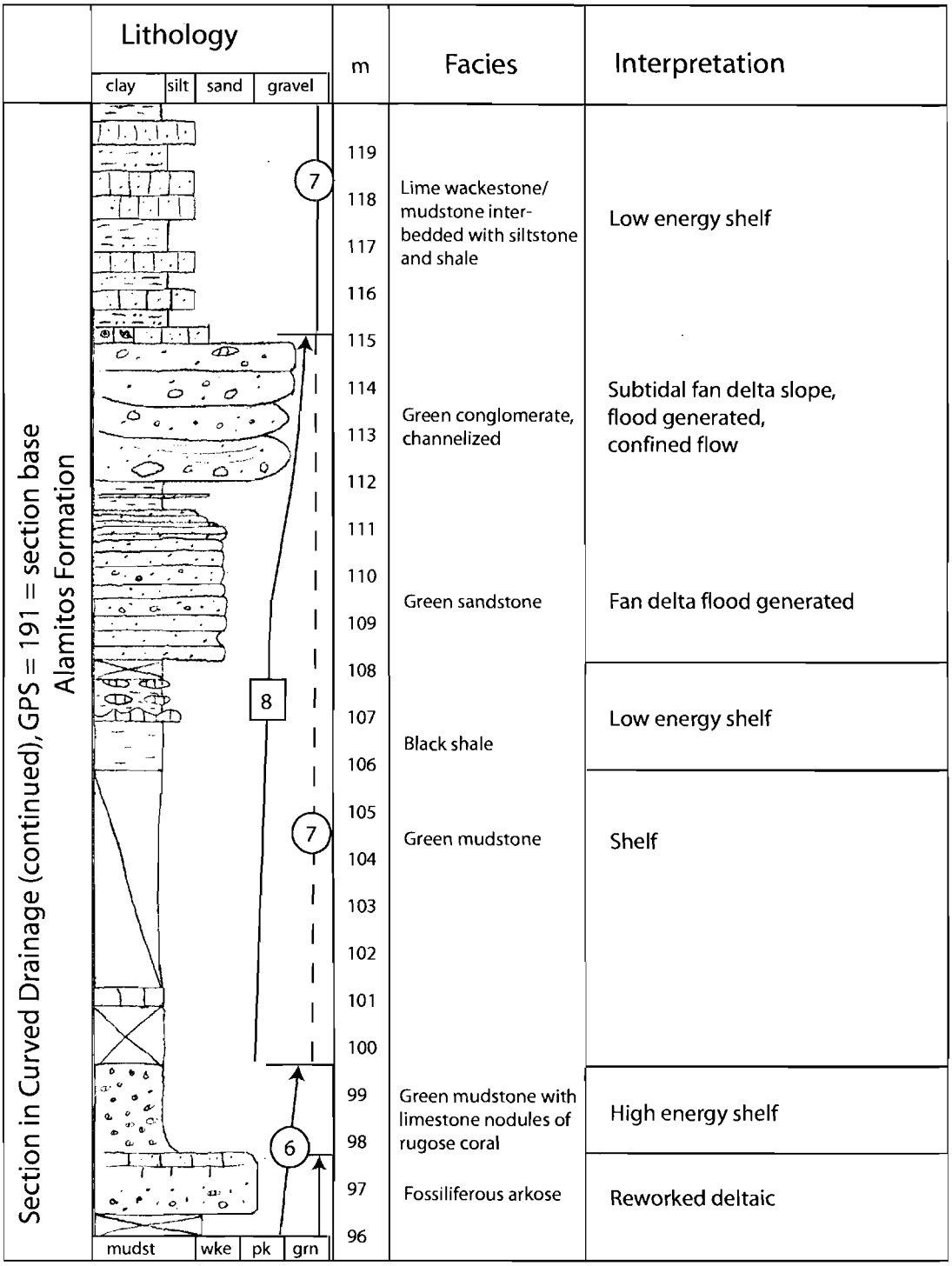

Figure 2.16. (continued).

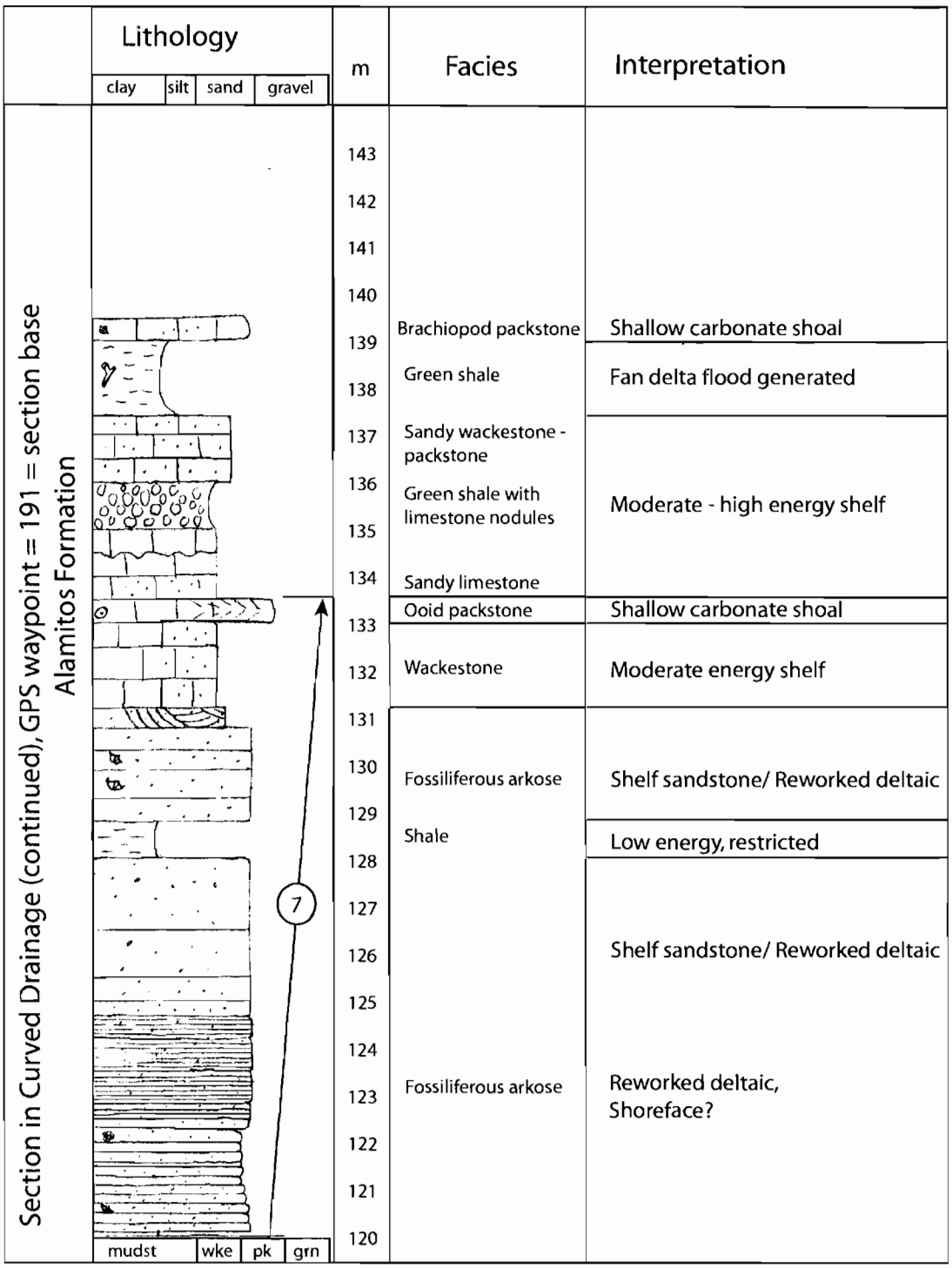

Figure 2.16. (continued).

shallowing upward parasequences [*Van Wagoner et al.*, 1988]. A typical shallowing upward cycle in this area consists of (in ascending stratigraphic order) low energy shelf facies such as black shale, lime mudstone and shale, or sandy limestone and siltstone, followed by fossiliferous arkose, followed by shallow water/shallow marine carbonates such as carbonate shoals, coral biostromes, or phylloid algae. The gravity flow pluse intervals represent periods of quiescence followed by sediment pulses from the Ancestral Highland and consist of low energy shelf facies followed by high energy flood-plume facies including green conglomerate, green sandstone, and/or green and red mudstone.

A total of seven shallowing upward cycles (arrows with circled numbers) and at least eight gravity flow pluses (arrows with boxed numbers) are identified in the 203 m of composite section. Gravity flow pulses are embedded within shallowing upward cycles. The dashed line on shallowing upward cycles indicates intervals where the shallowing upward cycles are not well defined. Facies in these intervals indicate no significant change in water depth (i.e., all subtidal). It is important to note that more shoaling events may have occurred, but are not recorded in the strata at Pecos, e.g., water depth may have been sufficiently deep to exceed the amplitude of eustatic oscillations [*Gong*, 1992]. Cyclothems are discussed further in Section 2.4.2.

Original stratigraphic sections with detailed lithologic descriptions are included in Appendix C. Table 2.6 shows the stratigraphic order and meter intervals of the measured sections that were used to create the composite section (Figure 2.8).

Table 2.6. Stratigraphic order and intervals of sections used for the composite section.

Strati-graphic Order	Section Name	Meter interval used in composite section	Cumulative meters (composite section)
4th	Section in Curved Drainage	0 - 139.5 (entire section)	63.5 - 203
3rd	S. Section on Hwy. 63 Roadcut	0 - 15.4	48.1 - 63.5
2nd	N. Section on Hwy. 63 Roadcut	0 - 13.1	35 - 48.1
1st	Section on Knob	0 - 35 (entire section)	0 - 35

Paleocurrent data show scattered and bidirectional paleocurrents in most of the study area (Figure 2.17). Paleocurrents in the northwest section of the study area are uniformly orientated in a southerly direction. Although all paleocurrent data is plotted on Figure 2.17, most measurements are from the fossiliferous arkose facies (specifically the upper and lower cliffs). Only a few paleocurrents were obtained from the green conglomerate facies because it lacks visible internal stratification in most locations. Paleocurrent measurements and paleogeography are discussed further in Section 2.4.3.

2.4 Discussion

2.4.1 Depositional environment

2.4.1.1 Regional environment

The Ancestral Rocky mountains undoubtedly provided the source of clastic sediment in the study area. Stratigraphic and paleocurrent data from this study indicate that the Ancestral Rocky mountain front may have resided near the Pecos-Picuris fault, which is approximately 6 km from the northwest edge of the study area [*Miller et al.*, 1963; *Baltz and Myers*, 1999; *Ude*, 1992; *Gong*, 1992; *Casey*, 1980; *De Voto*, 1972] (see paleogeographic discussion, Section 2.4.3). Facies in this study suggest that the regional depositional environment consisted of a series of braided streams or alluvial fans radiating from the mountain front (a bajada) feeding braid or fan deltas, which in turn were depositing coarse grained sediment onto a carbonate platform (Figure 2.18).

The definitions delineated by *Miall* [1990] for braid and fan deltas are implemented in this study. A braid delta consists of a delta fed by braided streams with a distant source area, and a fan delta consists of a delta fed by an alluvial fan. Due to the absence of subaerial deposits in the study area, it is difficult to classify the delta type on the basis of direct evidence. Alluvial fan (bajada) and braided-river alluvial plain subaerial deposits are documented along the margins of the Central Colorado trough, the Paradox Basin, the Denver basin, and the northern Taos Trough [*Casey*, 1980; *De Voto*, 1972] (Figure 2.3). Fan delta deposits are documented in the

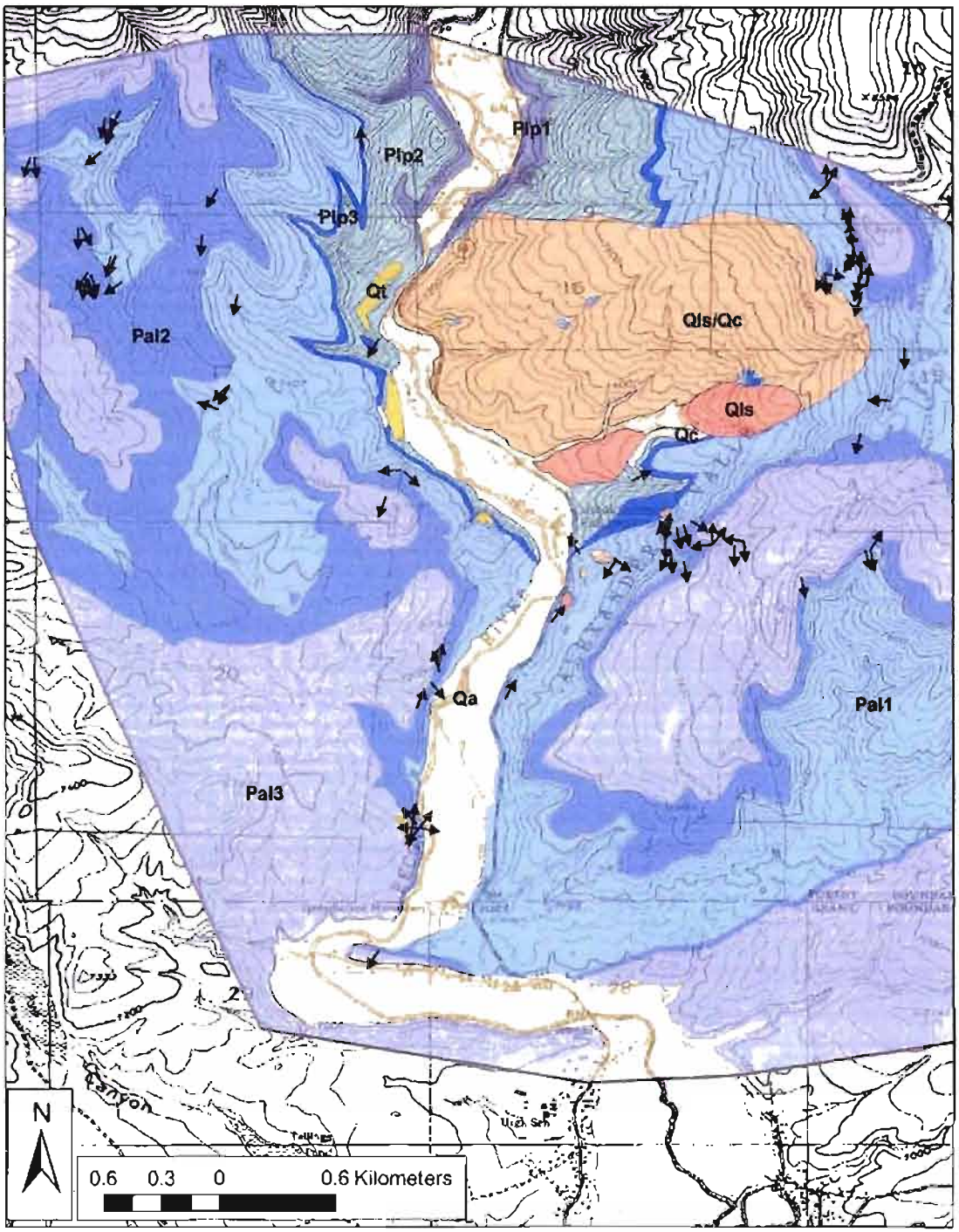

Figure 2.17. All paleocurrent data (small arrows) superimposed on a topographic map with colored geologic units (see color legend Figure 2.6 and Figure 2.8). Arrow start marks the measurement location.

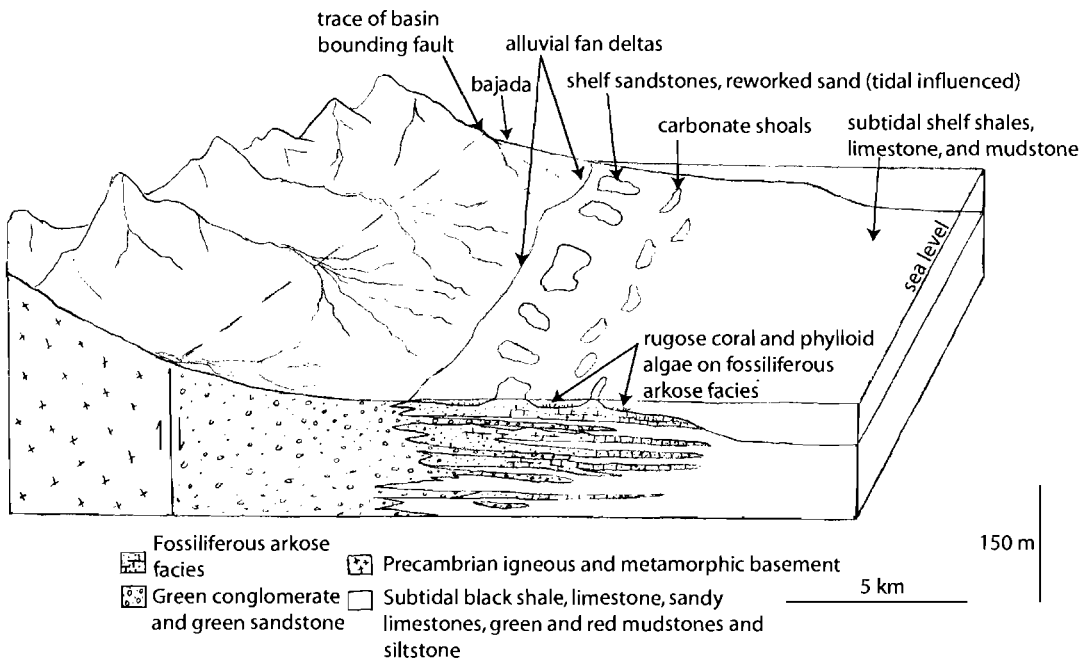

Figure 2.18. Regional depositional environment and distribution of facies for the Desmoinesian Pecos Platform. (Highlands not drawn to scale)

northern Taos Trough and Paradox basin [*Casey*, 1980; *De Voto*, 1972]. A fan delta interpretation is favored for the Pecos Platform because of the presumed proximity of the source area and similarity of the deposits found in the study area to well-documented modern and ancient fan delta deposits (Section 2.4.5).

2.4.1.2 Facies

Deposition of clastic material into an area of carbonate production results in a large number and variety of lithologies. Seventeen descriptive facies were designated in this study. Several facies that are important to the interpretation of depositional environment are further described and discussed here.

The green conglomerate facies was likely deposited during flood events by a process that involved debris flows from the nearby Uncompahgre Uplift entering the ocean via a fan delta. The conglomerates are polymictic and characteristically green from allogenic and authigenic chlorite [*Ude*, 1992]. The clast composition of

this facies predominately consists of granite, rhyolite, and quartzite. Limestone, siltstone, and sandstone intraclasts are also present. In several places, Pennsylvanian marine fauna were incorporated into the conglomeratic flows. Figure 2.9 shows Pennsylvanian ammonoids and a nautiloid in a green conglomerate outcrop. The green conglomerate facies grades laterally into several other facies: green sandstone facies, green and red mudstone facies, and lime packstone facies. A general lack of internal stratification and presence of *Helminthoida crassa* (Figure 2.10a), *Planolites*, and *Zoophycos* indicate that the green conglomerate and sandstone were deposited below wave base in relatively deep water. *Casey* [1980] also documented *Helminthoida* and *Zoophycos* trace fossils in the northern Taos Trough and speculated that water depth rarely exceeded 30 m for the associated facies.

The conglomeratic lime packstone facies that occurs gradational to the green conglomerate is a conglomerate composed primarily of skeletal carbonate grains but has abundant intraclasts of green and red mudstone and large (up to 6 cm) igneous and metamorphic clasts (Figure 2.10c, d, e, and f). The presence of this packstone conglomerate facies presents additional evidence of flood plumes onto a carbonate shelf. The packstone conglomerate facies was likely deposited by high energy currents of low turbidity water that passed through carbonate shoals, thereby picking up and redepositing the carbonate material. The gradational relationship of the packstone conglomerate facies with the green conglomerate facies suggests that it was deposited during the same flood events. In several places the green conglomerate grades vertically into the packstone conglomerate facies; here, the packstone conglomerate marks the end of a sediment gravity flow.

The fossiliferous arkose facies may have been deposited by smaller flood events into or adjacent to an area of carbonate production on the fan delta front and then reworked by shallow marine processes resulting in a mixed carbonate-siliciclastic sediment (Figure 2.11a and b). Deposition of the fossiliferous arkose by smaller flood events seems plausible since the fossiliferous arkose has smaller clasts in comparison to those of the green conglomerate. However, variations in sediment

supply would also explain the difference in observed clast size. The largest clasts of the green conglomerate (15 cm) are entrained by a critical current velocity of 5 m/sec according to Hjulstrom's diagram as modified by Sundborg [*Hjulstrom*, 1939], whereas the largest clasts of the fossiliferous arkose facies (3 cm) are entrained by a critical current velocity of 2.5 m/sec.

Tidal influence in the fossiliferous arkose facies is evidenced by mud drapes and reactivation surfaces from current reversal (Figure 2.11)d. Figure 2.11e shows large (up to 5 m) tabular crossbedding in the upper and lower cliff (fossiliferous arkose facies). These large dunes are present in the northeast part of the study area, indicating that the area may have been subject to strong tidal currents. Other ocean currents such as longshore or rip currents could have influenced this area or even amplified the tidal currents. One to 3 m tidal bundles are observed at the same stratigraphic interval in other parts of the study area.

Presence of relatively pure carbonates within the siliciclastic sequence at the study area implies that input of clastics fluctuated greatly during accumulation of carbonates on the Pecos platform. Episodic deposition of clastics is a process that supports the fan delta flood plume interpretation. The diversity of Pennsylvanian fauna at the study area indicates an open marine environment with waters of normal marine salinity [*Sutherland*, 1963]. The shallow marine carbonates such as the boundstone and coral packstone, skeletal packstone, and phylloid packstone (Figure 2.12f) facies commonly occur on top of the fossiliferous arkose facies. The presence of these carbonates denotes a period of abandonment of sedimentation in the area, which may have been caused by stream or channel avulsion, a lack of storms to generate siliciclastic material, or a relative rise in sea level. *Casey* [1980] also documented shallow marine limestones on top of fan delta deposits in the northern Taos Trough that he attributed to delta abandonment.

2.4.1.3 Climate

Middle Pennsylvanian evaporite deposits are present in nearby Ancestral Rocky Mountain basins such as the Paradox basin and Central Colorado Trough [*De Voto*,

1972], indicating that the climate at this time was regionally arid or semiarid. Abundant plant debris was observed by *Casey* [1980] in the prodelta sediments of the northern Taos trough during early to middle Pennsylvanian time, suggesting that the climate was at least not extremely arid. Abundant plant debris is not observed at Pecos. Due to the absence of subaerial deposits in the study area, it is difficult to classify the climate on the basis of direct evidence. The arid or semiarid climate indicated by deposits in other Ancestral Rocky Mountain basins would promote the debris flow/flood processes interpreted as responsible for deposition of the green conglomerate facies.

2.4.2 Cycles

Pennsylvanian cyclothems are observed world wide [*Ross and Ross*, 1988; *Merriam*, 1964; *Wanless and Weller*, 1932]. Their origin in North America has been controversial, attributing them to either glacial-eustatic sea-level fluctuation (midcontinent and Ancestral Rocky Mountain basins) or to episodic tectonism (Appalachian and Ancestral Rocky Mountain basins and midcontinent) [*Tankard*, 1986; *Algeo*, 1991; *Gong*, 1992; *Gong and Humphrey*, 1991; *Wiberg and Smith*, 1991; *Klein and Willard*, 1989; *Klein and Kupperman*, 1992]. *Casey* [1980] attributes coarsening upward cycles in the northern Taos Trough to progradation associated with tectonic uplift. In southern Taos Trough (Pecos platform), *Gong* [1992] concluded that tectonism dominates cycles proximal to the Ancestral Rocky Mountain front, while glacial-eustatic fluctuation controlled cycle development distal to the basin-bounding fault. Gong's criteria to distinguish tectonic versus eustatic controls are based on the number of cyclothems observed proximal and distal to the basin-bounding fault. Approximately 33 km from the basin-bounding fault, Gong observed 21 Desmoinesian cyclothems. Twenty-nine Desmoinesian shale-evaporite cyclothems are recognized in the Paradox Basin [*De Voto*, 1972]. *Klein and Kupperman* [1992] distinguished glacial-eustatic influence from tectonic influence on sea-level fluctuation using tectonic subsidence data for the midcontinent. Ten to 20 m thick coarsening upward cycles are observed in a Pennsylvanian-Permian fan

delta sequence in western Spitsbergen [*Kleinspehn et al.*, 1984]. At Spitsbergen, a combination of intrabasinal and extrabasinal controls determine sequence evolution. Although tectonism and corresponding relative sea-level changes influence fan evolution, avulsion of fluvial channels, lateral migration of barriers, aggradation of mouth bars, and modification by tidal, wave, and storm currents exert primary control on the character of delta front deposits. In the southwestern Paradox basin, coarsening upward cycles associated with fan deltas in the Desmoinesian Honaker Trail Formation are interpreted to record a history of shifting centers of deltaic sedimentation [*De Voto*, 1972].

At Pecos, an interplay of allogenic (extrabasinal) and autogenic (intrabasinal) processes produced seven shoaling upward cycles (11 - 25 m thick) and eight gravity flow pluse intervals (5.5 - 15 m thick) in the studied section (Figure 2.19). Similar to the fan delta at Spitsbergen, these allogenic and autogenic processes may include eustatic sea-level fluctuation, tectonic subsidence, progradation, local climate, avulsion of fluvial channels, lateral migration of barriers and shoals, and delta front/shelf modification by tidal, wave, and storm-driven currents. The clastic sediments at Pecos were deposited in close proximity to their source area, thus, local effects, e.g., storm-generated floods, likely play an important role in the sedimentologic record.

Meter interval 75 to 111, Figure 2.19 (meter interval 12 to 48 in the Section in Curved Drainage, Figure 2.16), shows a thick interval (36 m) of primarily green mudstone, green sandstone, green conglomerate, sandy limestone, green and black shale, and siltstone with lime mudstone nodules that may be interpreted with several models. There are four intervals delineated in this part of the section (marked with arrows and boxed numbers 4 - 7) that are 9, 12, 5.5, and 9.5 m thick. The facies in this section represent a low to moderate energy shelf environment with recurrent flood plumes from a fan delta; thus, the intervals are called gravity flow pluses. One interpretation of this section portion is that the pulses are the result of hiatuses between flood events where gradual subsidence was occurring to accommodate the volume of sediments. Another interpretation involves the hiatus

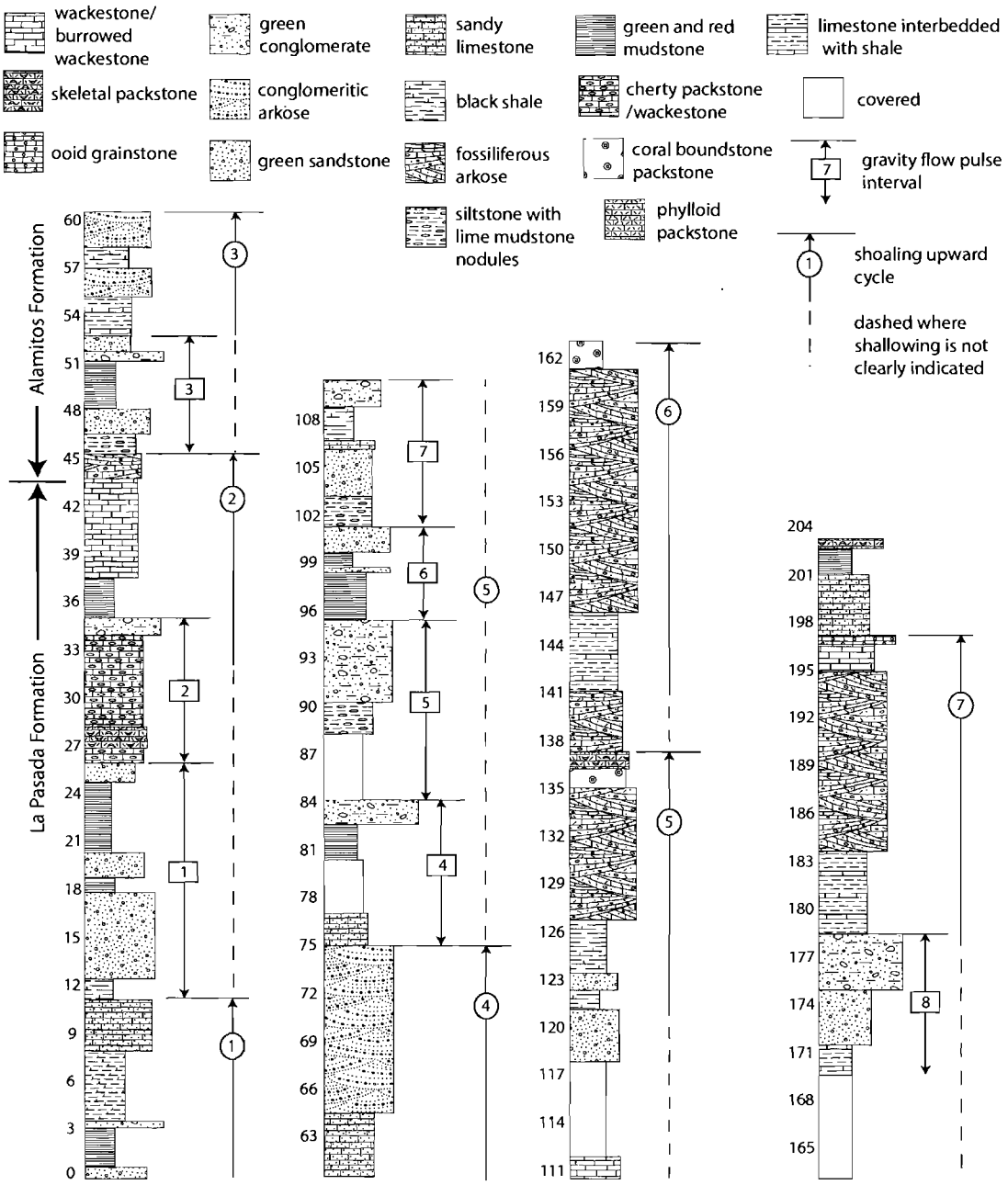

Figure 2.19. Generalized stratigraphic section. Circled numbers designate shoaling upward cycles and boxed numbers designate gravity flow pluses. Dashed lines show intervals where shoaling cycles are not well defined. See text for descriptions and discussion.

between high-energy sediment gravity flows being the result of fluvial avulsion on a fan delta. *Casey* [1980] documented avulsion in fan delta channels in the northern Taos Trough. Yet a third viable interpretation is that the cycles are the result of sporadic fault movements associated with uplift of the Ancestral Rocky mountain source area. In all cases, eustatic sea level fluctuation was unlikely a primary factor producing these gravity flow pluses because of the proximity to the source area and a lack of evidence supporting a major change in sea level during deposition. Fossils and trace fossils found in the gravity flow pulse intervals indicate a consistent subtidal shelf water depth during deposition (Section 2.3). Meter interval 164 to 178 and 12 to 35, Figure 2.19 (meter intervals 100 to 115 in the Section in Curved Drainage and meter interval 12 to 35 in the Section on Knob, Figure 2.13), show similar gravity flow pulses that are 15, 13, and 9 m thick.

Intervals marked with arrows and circled numbers on the stratigraphic sections are interpreted as shallowing upward cycles indicated by changes in depositional environment. Meter interval 111 to 137, Figure 2.19 (meter interval 48 to 73 in the Section in Curved Drainage, Figure 2.16), is an example of one of these cycles. The shallowing upward cycle here consists of (in ascending stratigraphic order): black shale, sandstone and siltstone, additional black shale, a thick sequence ($\sim$10 m) of fossiliferous arkose, followed by coral boundstone/packstone and skeletal packstone. At other localities, the fossiliferous arkose is capped by phylloid algae packstones or ooid grainstones. Thus, a shallowing transition from a deeper shelf environment (black shale facies) to a tidal-infuenced subtidal environment (fossiliferous arkose facies) to a shallow shoal environment (skeletal packstone facies and ooid grainstone facies) is observed.

The seven shallowing upward cycles observed in the strata are approximately 11, 11, 15, 15, 25, 22 and 18 m thick (excluding the thickness of embedded gravity flow intervals). The thickness of cycles at Pecos are comparable to those observed by *Gong* [1992]. Relative sea-level changes due to either tectonics or eustatics produced the cycles. Allocyclic sea-level fluctuation (a eustatic fall) in the Pecos stratigraphic section is evidenced by a karst surface (photo in Figure 2.20) above

Figure 2.20. Karst surface between the upper and lower cliffs (arrow).

the 5th cycle. Subsidence combined with avulsion of fluvial channels or lateral migration of barriers could have also produced the shallowing upward cycles containing the fossiliferous arkose facies, but these interpretations are not favored due to the large lateral extent of the fossiliferous arkose facies.

In the section at Pecos, eustatic sea-level fluctuation, punctuated tectonic subsidence, and gradual subsidence combined with avulsion of fluvial channels are processes that can each produce a shallowing upward cycle. Primary controls on sedimentation such as climate and lateral migration of channels, barriers, and shoals can produce simple coarsening upward cycles which could be mistaken for shallowing upward cycles. As a result, determining which process or combination of processes are controlling the cycles observed in fan deltas in an actively subsiding basin can be difficult with limited outcrop. As seen in this study, an understanding of depositional environments and lateral facies relationships enables distinction of at least some of these processes. Correlation of the strata over a region large enough to encompass several basins would enable complete distinction of extrabasinal controls

on sedimentation from intrabasinal controls on sedimentation. Because only seven Desmoinesian shallowing upward cycles are observed in the study area, and 21 Desmoinesian cycles are observed 25 km east-northeast of the study area (*Gong* [1992]) further from the basin bounding fault, distance from the basin-bounding fault appears to play an important role in cycle development. Tectonic subsidence associated with movement of this fault may have at times created a deeper environment close to the fault; therefore, a eustatic sea level fluctuation was not recorded in the stata, whereas the same eustatic fluctuation resulted in deposition of a cycle distal to the fault where the basin water depth was shallow. Additional discussion of cyclothems observed at the Pecos Platform is in Section 2.4.4.

Whether punctuated or gradual, basin subsidence is necessary to accommodate the volume of sediments on the Pecos platform. Evidence for punctuated subsidence in the Central Colorado trough and Paradox basin includes abrupt thickness and facies variations over short distances in proximity to faults and uplift blocks *De Voto* [1972]. In this study, a basin subsidence calculation conducted using a program called BasinMod indicates that there has been ~450 m of tectonic subsidence on the Pecos platform throughout the Pennsylvanian and ~165 m during the Desmoinesian interval of the Pennsylvanian (Appendix D). Factors such as sediment compaction and subsidence due to sediment and water weight are accounted for in this calculation. Appendix D contains a description of subsidence modeling and model inputs, as well as a graphical display and discussion of results. The large amount of tectonic subsidence during deposition of the studied interval and difference in number of shallowing upward cycles proximal and distal to the basin bounding fault show that tectonics had an influence on the succession of strata at Pecos.

2.4.3 Paleogeography

Figure 2.21 is a schematic cross-section showing several correlated sections. The cross-section runs along an approximate west - east line across the study area (Figure 2.6). All sections are hung on the karst surface above the fifth shallowing upward cycle (Figure 2.16) as it likely represents a reasonable chronologic datum.

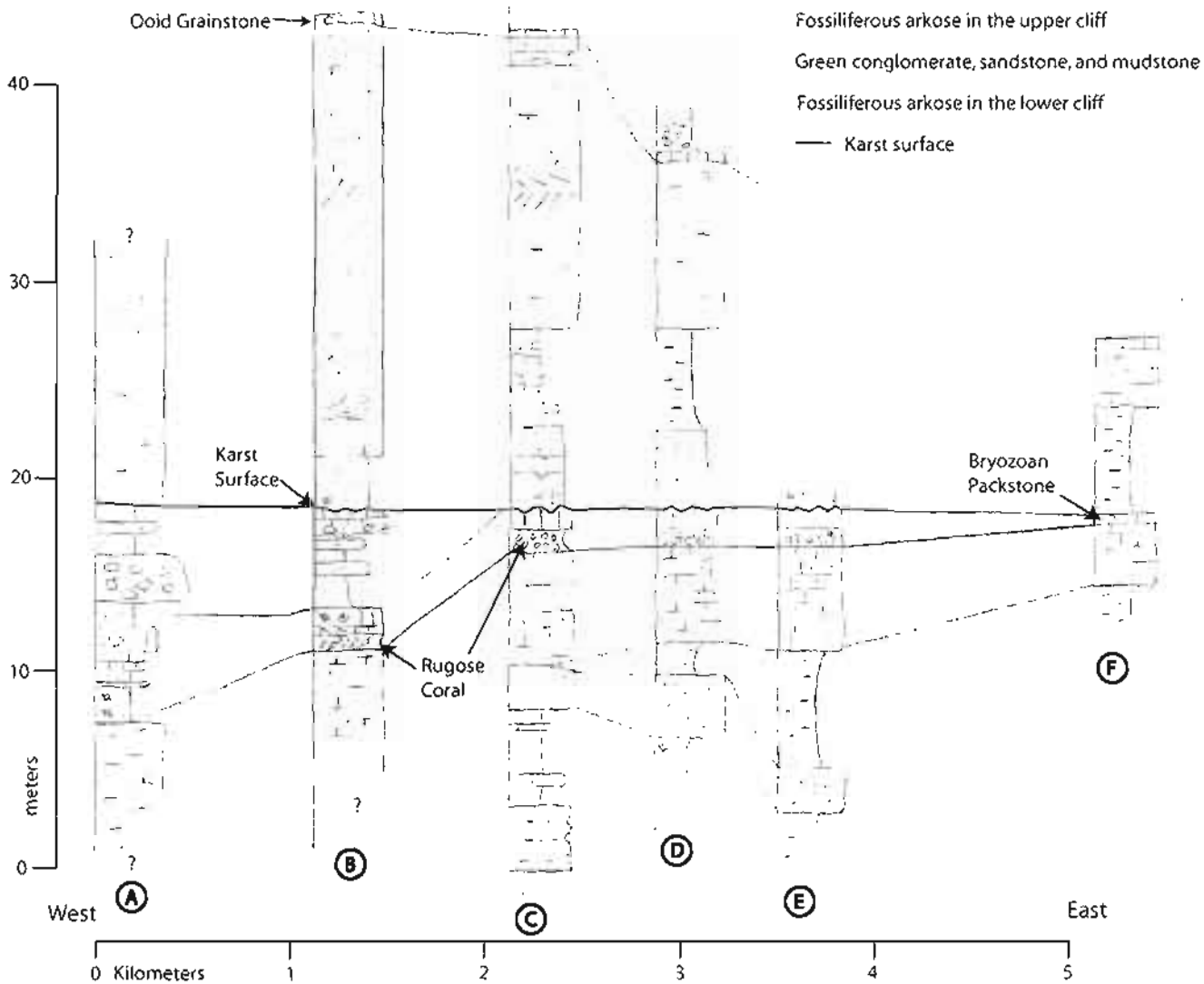

Figure 2.21. Correlated sections. Letters show section locations on Figure 2.6.

To emphasize thickness changes on the color-coded correlation section, the lower cliff fossiliferous arkose is colored blue, the upper cliff fossiliferous arkose is colored pink, and green conglomerate is colored green. The correlation section shows that the siliciclastic units thin toward the east. The upper cliff thins most dramatically from 20 m to 5 m over a distance of 5 km. In addition, the upper and lower cliff fossiliferous arkoses become lime rich toward the east and siliciclastic rich toward the northwest. Construction of the cross-section on a northwest to southeast line would yield the same result. Green conglomerates at other parts of the section also thin to the east or southeast. This thickness and compositional data are persuasive evidence that the ancestral highland was located west or northwest of the study area.

The Pecos-Picuris fault lies approximately 6 km northwest of the study area; thus, it may have been a major basin-bounding fault (Figure 2.3). *Miller et al.* [1963] postulated that the Pecos-Picuris fault was originally active in the Precambrian, reactivated in the Pennsylvanian, and reactivated again during the Laramide Orogeny. *Miller et al.* [1963]'s basis involves the current location of the fault, the fault's relationship with Laramide age folding, the distribution and composition of Precambrian rock east and west of the fault, and thickness and provenance data for Pennsylvanian rocks. *Bauer and Ralser* [1995] also report a complicated history of repeated activation for the Pecos-Picuris fault.

Precambrian igneous and metamorphic rocks west of the Pecos-Picuris fault consist of granite, metagranite, quartzite, amphibolite, granodiorite, and diorite. The granitic rocks are collectively called the Embudo Granite [*Sutherland*, 1963]. These lithologies are reasonable provenance rocks, given the similarities of arkosic composition and clast types in the sedimentary rocks observed in the study area. An outcrop of Precambrian gneissic diorite and biotite feldspar gneiss weathering to a green soil was observed in a road cut west of the Pecos-Picuris fault near the Santa Fe ski area (Hwy 475). Thin sections of rocks from this location reveal biotite and amphibole altering to chlorite. Precambrian diorites, gneiss, and amphibolites

may have provided the source of allogenic chlorite observed in the green sandstones, mudstones, and conglomerates in the study area.

As discussed previously, the fossiliferous arkose facies in the upper and lower cliffs show reworking by tidal currents. Asymmetric tidal currents produced large-scale tabular planar crossbedding with a unimodal paleocurrent trend. More symmetrical tidal flow produced medium to small scale trough crossbedding with a bidirectional paleocurrent trend as well as bidirectional tabular crossbedding. The upper and lower cliffs show primarily asymmetric tidal currents, but both types are observed. Figures 2.22 and 2.23 show paleocurrent and interpreted depositional environment maps for the lower and upper cliffs respectively.

The paleocurrents for the lower cliff, Figure 2.22(a), are dominantly asymmetric tidal currents directed to the south. With the exception of the northwest corner of the study area, the upper cliff shows bidirectional and asymmetric tidal currents, but the asymmetric currents are directed to the north (Figure 2.23(a)). In modern tidal seas, tidal currents flow perpendicular or parallel to shorelines [*Banks*, 1973; *Lanckneus and de Moor*, 1995]. It is difficult to determine the orientation of tidal current flow relative to the shoreline landward of the study area due to uncertainty in the orientation of this shoreline. The north - south elongated and possibly constricted shape of the Taos Trough (Figure 2.3) may have promoted tidal flow parallel to parts of the shorelines.

In the southwest side of the study area, a two to three meter thick discontinuous interval of the black shale exists at the top of the lower cliff. The shale contains abundant productid brachiopods in growth positions. The shale pinches out abruptly to the north and east, but its western and southern extent is not known. This outcrop may represent a lagoonal environment protected by a barrier bar of the fossiliferous arkose facies but its unknown extent leaves this interpretation in question (Figure 2.22(b)).

For both the upper and lower cliffs, paleocurrents in the northwest section of the study area are more uniformly directed to the south (Figures 2.22 and 2.23). The upper and lower cliffs contain a lower carbonate fraction in this area. The lower

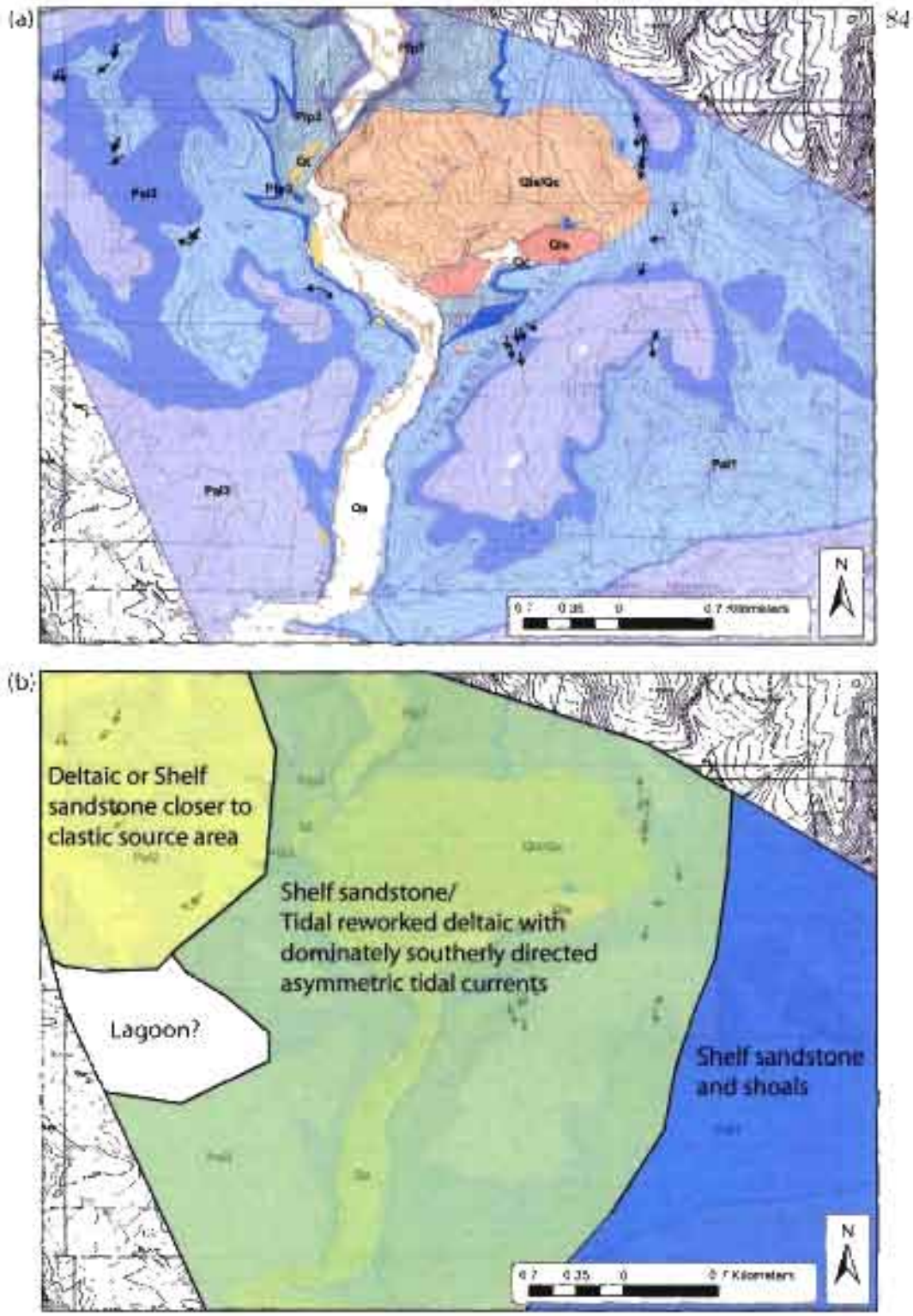

Figure 2.22. Alamitos Formation lower cliff paleocurrent and paleogeographic maps. (a) Lower cliff paleocurrent data overlain on a topographic map with colored geologic units (see legend Figure 2.6). Arrow start marks the measurement location. (b) Paleogeographic/depositional environment interpretation during deposition of the lower cliff overlain on map (a).

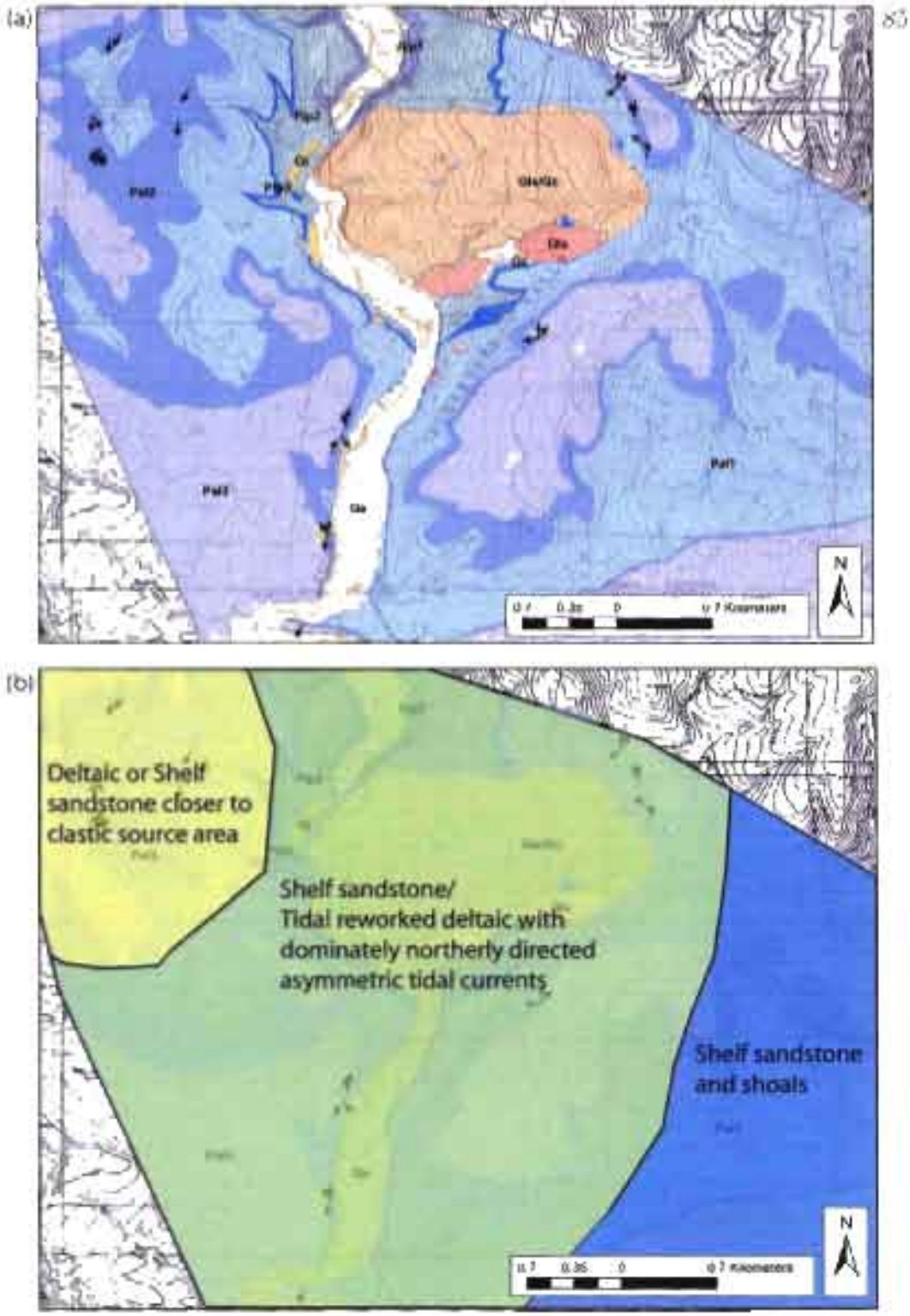

Figure 2.23 Alamitos Formation upper cliff paleocurrent and paleogeographic maps. (a) Upper cliff paleocurrent data overlain on a topographic map with colored geologic units (see legend Figure 2.6). Arrow start marks the measurement location. (b) Paleogeographic/depositional environment interpretation during deposition of the upper cliff overlain on map (a).

cliff is chlorite rich (similar to the green sandstone facies) and becomes clearly channelized in this area. Paleocurrents for the upper cliff in this area originate from large south-directed trough crossbeds. These sedimentary features may be an indicator of less tidal reworking and more of a fluvial-deltaic influence moving paleogeographically toward the Ancestral Rocky Mountain front (Figures 2.22(b) and 2.23(b)). The stratigraphic data presented in this section indicate that the Uncompahgre Uplift (Figure 2.3) provided the source of clastic sediment found in the study area.

2.4.4 Comparison with previous studies

Ude [1992] studied the upper and lower cliffs at Benedictine Monastery at the southern end of the study area. Ude conducted a facies analysis similar to that of this study. His interpretation of depositional environment does not differ widely from the interpretations in this study. Ude places the upper and lower cliffs in a sequence stratigraphic framework using allocyclic sea level changes to explain the vertical succession of strata. A combination of intrabasinal and extrabasinal controls (discussed in Section 2.4.2) more likely determines the organization of the strata. Local climate and steam avulsion may have played an important role in the time-space relationship for the fan delta system.

Ude [1992] suggests that the green conglomerate and green sandstone facies were deposited during a sea-level lowstand. Evidence in this study (Section 2.3) suggests that the green conglomerate/green sandstone facies were deposited in water that was relatively deep compared to other facies in the section. Thus, the green conglomerate must have been deposited during a period of relatively high sea level such as a eustatic highstand or period of rapid basin subsidence.

Gong [1992] conducted a sedimentological study at Dalton Bluff, just north of the Pecos study area, and at Johnson Mesa, 25 km east of Dalton Bluff. Gong also observed shallowing upward sequences (cyclothems) in Middle Pennsylvanian strata. He determined that there are 21 cyclothems throughout the Desmoinesian at Johnson Mesa, and calculated a periodicity of 315 ky with an interpreted origin

of glacial-eustatic sea level fluctuation. Gong concluded that cycles at Dalton Bluff were poorly developed. In this study, a mixed carbonate-siliciclastic facies (fossiliferous arkose facies) is interpreted as the product of reworking by shallow marine processes. Gong presented a conflicting interpretation of a mixed bioclastic/siliciclastic facies at Dalton Bluff as the product of sediment gravity flows into relatively deep water. Gong based this interpretation primarily on a lack of observed crossbedding and presence of massive bedding, whereas in Pecos, the bioclastic/siliciclastic facies is also massive but commonly crossbedded. Gong concluded that sedimentation at Dalton Bluff occurred primarily under deep water conditions and that tectonism was the primary control on sedimentation, while eustatic influences were masked by the deep water conditions. Even if the mixed bioclastic/siliciclastic facies at Dalton Bluff is a shallow water deposit instead of a deep water deposit, there would be at most four Desmoinesian shallowing upward cycles at Dalton Bluff. Combined with the remaining Desmoinesian shallowing upward cycles observed in this study (seven), this would result in a total of 11 shallowing upward cycles for the Desmoinesian Pecos Platform, still far less than the number of shallowing upward cycles observed (21) distal to the basin bounding fault. Thus, even with this altered depositional environment interpretation, Gong's overall conclusion would remain unchanged: tectonics plays a major role in sedimentation proximal to the basin bounding fault.

Using methods similar to this study, *Klein and Kupperman* [1992] calculated tectonic subsidence for Midcontinent Pennsylvanian stratigraphic sections. They then calculated the tectonic subsidence per cyclothem for each time series. The subsidence per cycle for the Desmoinesian series ranged from 13 to 26 m. They concluded that Desmoinesian cycles show a large tectonically induced sea level change. The subsidence per cycle for the Desmoinesian cycles of the Pecos Platform would be $\frac{165\text{ m}}{11\text{ cycles}}$ or 15 m. This falls within the range reported by *Klein and Kupperman* [1992]; thus, further indicating that tectonics plays an important role at Pecos.

Although this study in some ways supports the conclusions of *Ude* [1992] and *Gong* [1992] for the Pecos Platform, Ude's research focused on interpretation of depositional environments and Gong's research mainly focused on tectonic and eustatic control on cyclothems. The contributions from this research combine aspects of both interpretation of depositional environment and addressing the origin of cyclic deposits on the Pecos Platform with new stratigraphic data. This study was the first to consider the degree of tectonic subsidence for the Pecos Platform using a tectonic subsidence calculation. The extent of tidal influence initially indicated by Ude was expanded by the results of this study. In addition, detailed geologic mapping required correlation of strata resulting in an understanding of lateral stratigraphic variations. A combined mapping, stratigraphic, and sedimentologic study is the first of its kind in the field area.

2.4.5 Modern and Ancient Analogs

The Fly River delta and Torres Strait in Papua New Guinea/Northeast Australia are examined as a comparative modern analog to the Pecos sediments. The Fly River delta is a tidal-modified delta prograding onto carbonate sediments of the northern part of the Great Barrier Reef and has a transitional zone of mixed carbonate-siliciclastic sediment at the delta front [*Cole et al.*, 1995]. Unlike the Pecos sediments, the Fly River deltaic sediments are fine-grained because the Fly delta is far (>300 km) from its sediment source area. Large tidal dunes like those in the upper and lower cliffs at Pecos are not uncommon. The shallow seaway (<20 m deep) adjacent to the Fly River delta, the Torres Strait, is rimmed by large (5.4 m high) coarse-grained carbonate dunes that have formed as a result of tidal currents [*Keene and Harris*, 1995]. Large (>4 m) tidal sand dunes also occur in the North Sea and English channel [*Lanckneus and de Moor*, 1995]. *Banks* [1973] attributed formation of large coarse-grained tabular and trough cross beds of marine origin in Cambrian strata to tidal processes.

Zones of carbonate-clastic mixing currently occur where siliciclastic detritus is dispersed by currents driven by trade winds (shelf east of Nicaragua), by monsoons

(Sunda Shelf of Java Sea), or by storms and tides [*Miall*, 1990; *Mount*, 1984]. On the inner shelf of Venezuela and on several fan deltas in the Red Sea, influx of siliciclastic sediment is a rare event, so benthic carbonate communities become well established. The communities are disrupted by storm events and the resulting deposition of siliciclastics, but they can recover during fair-weather conditions [*Mount*, 1984; *Weiss et al.*, 1978]. This scenario may also be true for the Pecos platform, where storm/flood events were likely responsible for deposition of the green conglomerate and green sandstone facies; the interbedded carbonates may reflect times of fair weather.

The Gulf of Suez and Gulf of Elat are places where active rifting has led to the development of steep-sided, fault-bounded basins where marine dispersal mechanisms are weak. Carbonate-clastic transitions occur there over lateral distances as little as a few tens of meters where reefs have developed fringing on the outer margins of small fan deltas [*Miall*, 1990]. The carbonate-clastic transition at Pecos occurs over a lateral distance of over 5 km; thus, the deltas at Pecos may have been larger, lower-gradient fans, and marine dispersal mechanisms were most likely involved.

Several ancient Pennsylvanian-Permian shelf deposits contain mixed carbonate-clastic successions. *Galloway and Brown* [1973] and *Hanford and Dutton* [1980] describe examples from north-central Texas and northernmost Texas, respectively. The system studied by *Galloway and Brown* [1973] consists of widespread shelf limestones that alternate with deltaic clastic sheets. The deltaic system prograded onto a stable shelf and distributary channels incise into the underlying deposits. They concluded that the association of carbonates and clastics may reflect regular changes in sea level, with the clastic phase representing low sea level and the carbonate phase representing high sea level. The Pecos study area does not have clastic distributary channels that incise into underlying carbonate deposits. Although sea-level was fluctuating during deposition of the succession of sediments in the Pecos study area, this model alone does not explain the association of carbonate and

clastic sediment. As discussed earlier, much of the carbonate and clastic sediment at Pecos was deposited contemporaneously or penecontemporaneously.

A Pennsylvanian-Permian fan delta sequence in western Spitsbergen [*Kleinspehn et al.*, 1984] provides a good ancient analog to the Pecos sediments. Channel mouth conglomerates observed at Spitsbergen are texturally similar to the green conglomerate facies at Pecos. *Kleinspehn et al.* [1984] suggest that preservation of subaqueous channel mouth conglomerates is indicative of a subsidence and burial rate sufficiently high to protect those deposits from reworking. This may be true for the green conglomerate facies at Pecos as well. The strata at Spitsbergen represent a section more proximal to the aluvial fan than the strata at Pecos because at Spitsbergen, fluvial conglomerates are domumented and there are fewer carbonates. The fan delta at Spitsbergen is catagorized as a fluvial-wave dominated delta, whereas the Pecos fan deltas were tidal dominated. Similar to Pecos, the fan delta sediments of Spitsbergen do not suggest deposition on a steep avalanche face.

2.5 Conclusions

The Pennsylvanian La Pasada and Alamitos Formations record primarily subtidal and shallow water marine sedimentation on the Pecos platform at the edge of an actively subsiding tectonic basin. The 203 m of strata measured in the study area consist of 59% siltstone, sandstone, and conglomerate, 25% carbonate, and 16% shale with 42% of the sandstone of mixed carbonate-siliciclastic composition. Evidence of tectonism is reflected in the abundance of coarse clastic sediment, and basin subsidence is necessary to create the accomodation space for this sediment. Approximately 165 m of tectonic subsidence occured on the Pecos platform during the Desmoinesian interval of the Pennsylvanian. The large amount of tectonic subsidence during deposition of the studied interval and difference in number of shallowing upward cycles proximal and distal to the basin bounding fault show that tectonics had a definite influence on the succession of strata at Pecos. In addition to tectonics, local climate and avulsion of fluvial channels are intrabasinal controls that could have produced eight gravity flow pluses in the section. Relative sea-level

changes due to either intrabasinal tectonics or extrabasinal eustatics produced seven shallowing upward cycles in the section. A well-developed karst surface shows evidence of eustatic sea level fall. Because a combination of intrabasinal and extrabasinal controls determines the organization of the Pecos strata, their distinction is difficult, and a model that relies on a single process is likely unrepresentative.

Thickness data show that several clastic units pinch out or thin from east to west or from the northwest toward the southeast. Lithologic data show that the upper and lower cliff fossiliferous arkoses become lime rich toward the southeast and siliciclastic rich toward the northwest. These lateral stratigraphic variations indicate that the Ancestral Rocky highland was located northwest of the study area, supporting the idea that the Pecos-Picuris fault may have been an active basin-bounding fault at this time (Figure 2.3).

Facies analysis was completed for the upper 43 m of the La Pasada Formation and the lower 160 m of the Alamitos Formation. Paleocurrents show bidirectional north and south transport in mixed siliciclastic-carbonate sediment of the fossiliferous arkose facies. This facies is interpreted as a shelf sandstone and likely represents tidal and storm reworked deltaic deposits. The arkosic composition of sandstones and abundance of granitic and metamorphic clasts in the conglomerates reveal basement uplift of igneous and metamorphic provenance. Stacked channels and large clasts in the green conglomerate facies indicate high-energy sediment pulses from flood plumes and rapidly shifting channels in close proximity to the basement uplift. The presence of open marine Pennsylvanian invertebrate fossils and trace fossils in many of these clastic deposits and interbedded carbonates shows deposition onto a carbonate platform. Thus, the clastic sediments are interpreted as tidal influenced fan-delta deposits on the carbonate Pecos platform, southeast of the Uncompahgre highlands of the Ancestral Rocky Mountains. This study provides insight into mixed carbonate-clastic facies, depositional environments of the Pecos platform, and the role of Ancestral Rockies in Pennsylvanian paleogeography.

2.6 Future Directions

Middle to Late Pennsylvanian outcrops cover much of the region surrounding the study area. Study of additional outcrops may lead to new insights concerning the depositional environment and paleogeography of the region. An attempt to correlate the strata over a very large region may enable distinction of extrabasinal controls on sedimentation from intrabasinal controls on sedimentation and development of a robust sequence stratigraphic model. Age dating on the Pecos-Picuris fault may confirm whether it was active in the Pennsylvanian. Paleomagnetic measurements of the sediments would allow placement of the strata in an absolute time reference, which would aid studies concerning basin history/evolution, sedimentation rates, and the periodicity of cyclothems.

APPENDIX A

ELECTRONIC DATA

Paleocurrent, waypoint, sample, and geologic GIS database files are included on the CD-ROM in ArcGIS 9 format. A notated list of waypoints including samples, paleocurrent, and geologic data is included in Excel and tab-delimited text format. Sample photos, the geologic map, cross section, waypoint map, and sample map in pdf and png formats are also included on the CD-ROM.

APPENDIX B

DETAILED CHARACTERISTICS OF MAJOR FACIES

Table B.1. Additional Carbonate Facies Characteristics

Facies Name	Color[b]	Characteristics of Siliciclastic portion	Bed Thickness
lime mudstone and shale	shale is dark gray N3, lime mudstone is medium gray N4 - dark gray N3 and yellowish gray[a] 5Y6/2	N/A	0.1 - 0.3 m
boundstone and coral packstone	light olive gray 5Y5/2, medium gray N5	N/A	0.2 m - 0.45 m
wackestone	medium olive gray 5Y5/1, medium light gray[a] N6, olive gray 5Y4/1, yellowish gray[a] 5Y7/2, dusky yellow[a] 5Y5/4	<10% detrital quartz, plag., silt size, rare igneous lithic fragments	0.5 - 1.5 m
phylloid packstone	olive gray 5Y4/1, medium gray[a] N5	N/A	0.3 m
cherty wackestone-packstone	very light gray N8	N/A	6 m total, 0.1 m beds
siltstone with lime mudstone nodules	medium gray N5 to medium dark gray N4 to olive gray 5Y4/2 limestone nodules and yellowish gray 5Y7/2 to dusky yellow 5Y6/4 or pale olive 10Y6/2 silt	grain size ranges from clay - f. sand	1.3 m total, 2-4 cm nodules
burrowed wackestone	yellowish gray 5Y7/2 silt, medium light gray N6 limestone	grain size ranges from clay - vf. sand	5.2 m total, 0.3 - 0.7 m beds
skeletal packstone	light gray N7 - light olive gray 5Y6/1, medium light gray[a] N6, moderate yellowish brown[a] 10YR5/4	in places gradational with green conglomerate, abundant 1-2 cm mudstone clasts, 6 cm max clast size	0 - 1 m
sandy limestone	brownish gray 5YR4/1, dark yellowish brown[a] 10YR5/2	vf., subangular, well sorted, grain size ranges from silt to <5% c. grains, abundant biotite	0.2 - 0.3 m
ooid grainstone	medium gray N5, yellowish gray 5Y8/1, light gray[a] N7	few angular-subangular grains of c. quartz	0.2 - 0.5 m

[a]Weathered color.
[b]Classified according to a Rock Color Chart [*Goddard et al.*, 1979].
c. = coarse, f. = fine, vf. = very fine.

Table B.2. Additional Clastic Facies Characteristics

Facies Name	Color[a]	Primary Cements	Secondary Cements	Bed Thickness	Vertical Relationships
green conglomerate	pale olive 10Y6/2, grayish olive 10Y5/2	chlorite	calcite	0 - 2 m	grades to lime packstone, interbedded with green sandstone and green and red mudstone
green sandstone	pale olive 10Y6/2, greenish gray 5GY6/1, moderate olive brown 5Y4/4, light olive gray 5Y5/2, dusky yellow green 5GY6/2	chlorite	calcite	0.1 - 0.5 m	interbedded with green conglomerate, and green and red mudstone
green and red mudstone	red mudstone is grayish brown YR3/2 - blackish red 5R2/2, green mudstone is dusky yellow 5Y6/4	chlorite	calcite	0.5 cm	interbedded with green conglomerate and green sandstone, gradational with black shale
conglomeratic arkose	grayish yellow 5Y7/4, yellowish gray 5Y8/1, pale olive10Y6/2, pinkish gray 5YR8/1(rare)	calcite, quartz overgrowths	N/A	1 - 5.4 m	none significant
fossiliferous arkose	yellowish gray 5Y7/2, 5Y7/1, 5Y8/1, 5Y6/2, dusky yellow 5Y6/4	calcite	N/A	5 m - 13 m total thickness with 2 mm - 0.6 m beds	sharp contact with underlying shale, can grade to limestone (lower cliff)
burrowed arkose	dusky yellow 5Y6/4, pale olive 10Y6/2	calcite, quartz overgrowths	N/A	0.4 m	overlain by siltstone with limestone nodules
black shale	grayish black N2, olive black 5Y2/1, olive gray 5Y4/1	N/A	N/A	0.2 - 3.2 m total	gradational with green shales

[a]Classified according to a Rock Color Chart [*Goddard et al.*, 1979].

APPENDIX C

ORIGINAL STRATIGRAPHIC SECTIONS

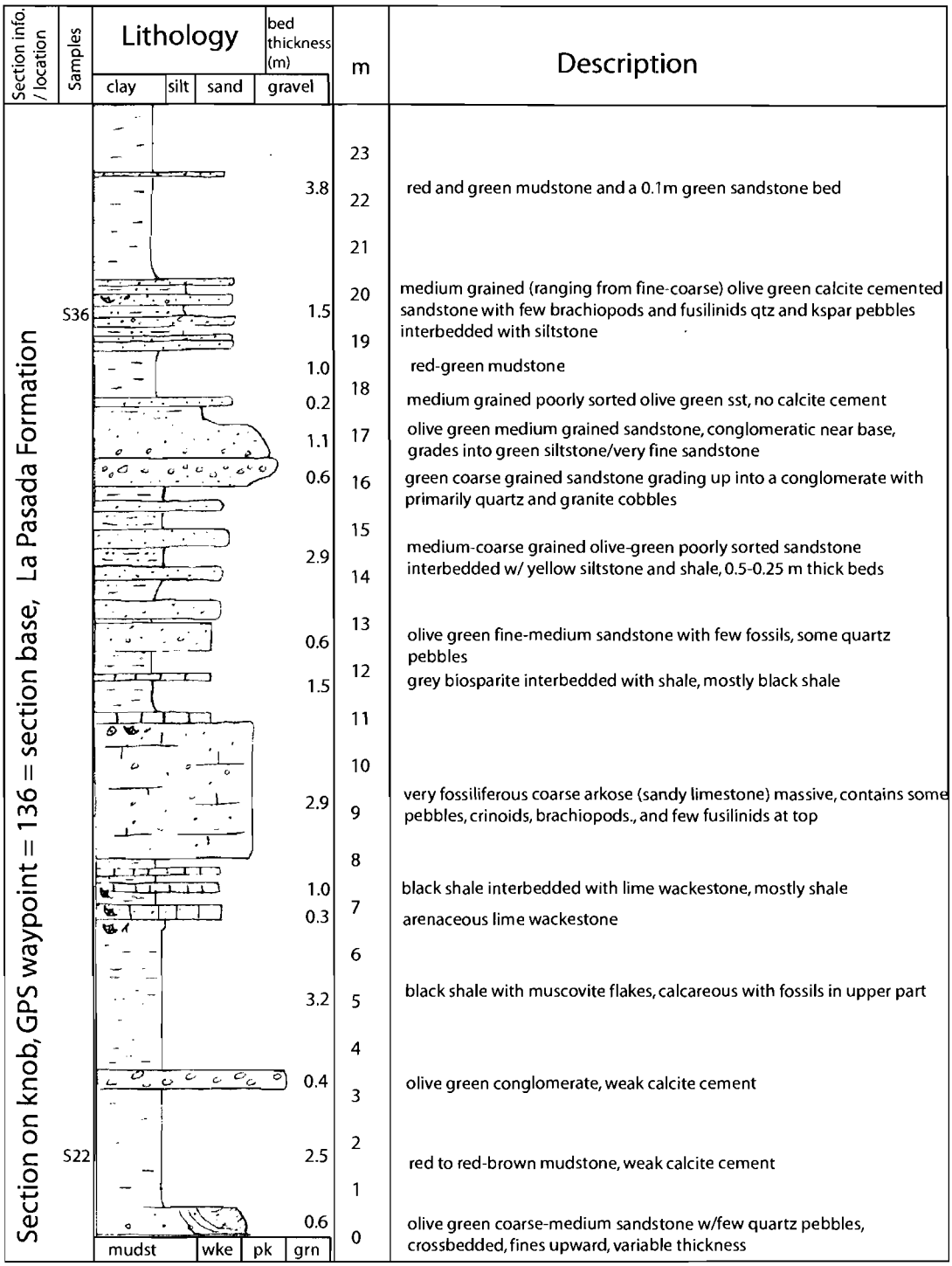

Figure C.1. Section on Knob.

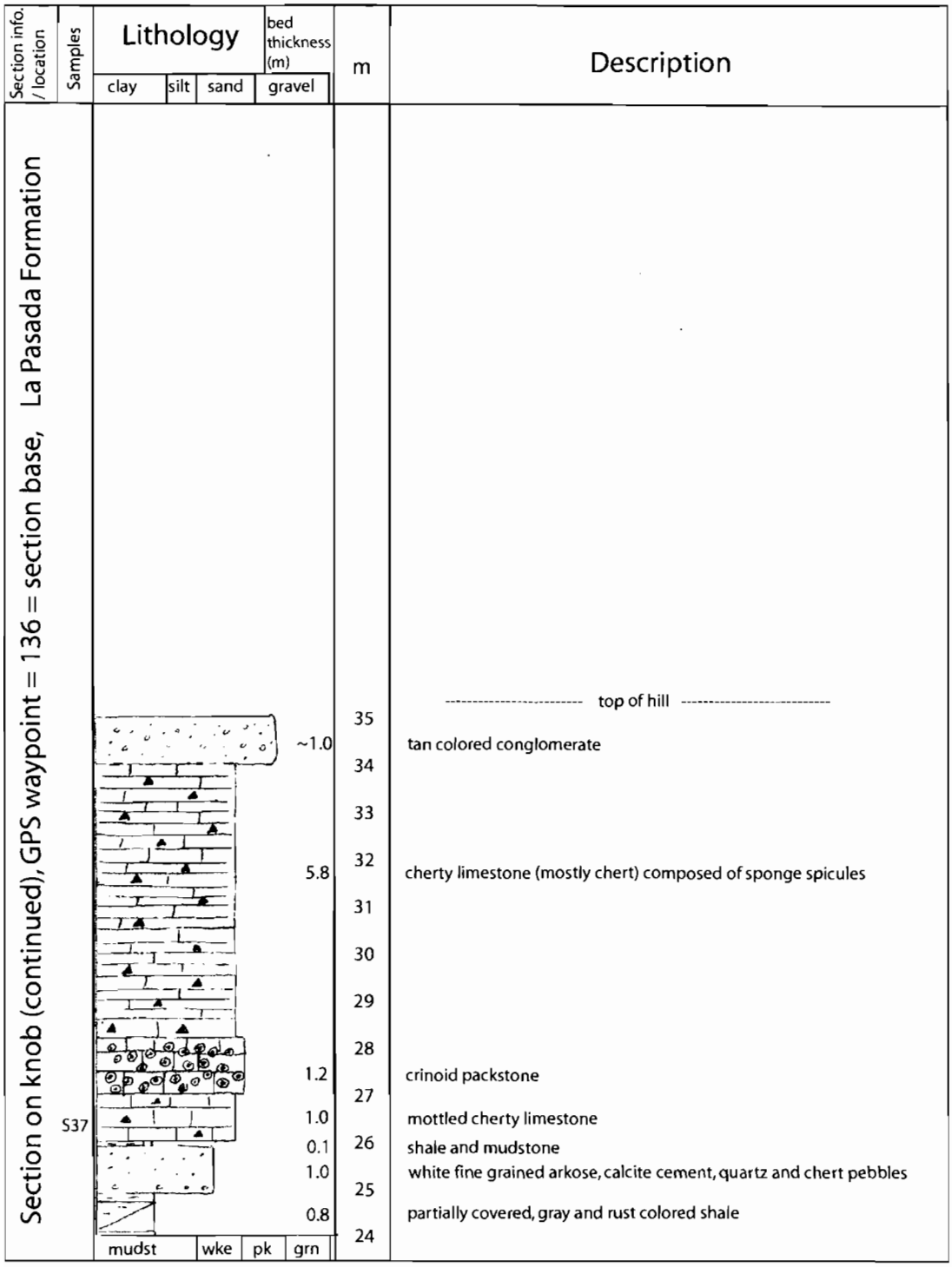

Figure C.1. (continued).

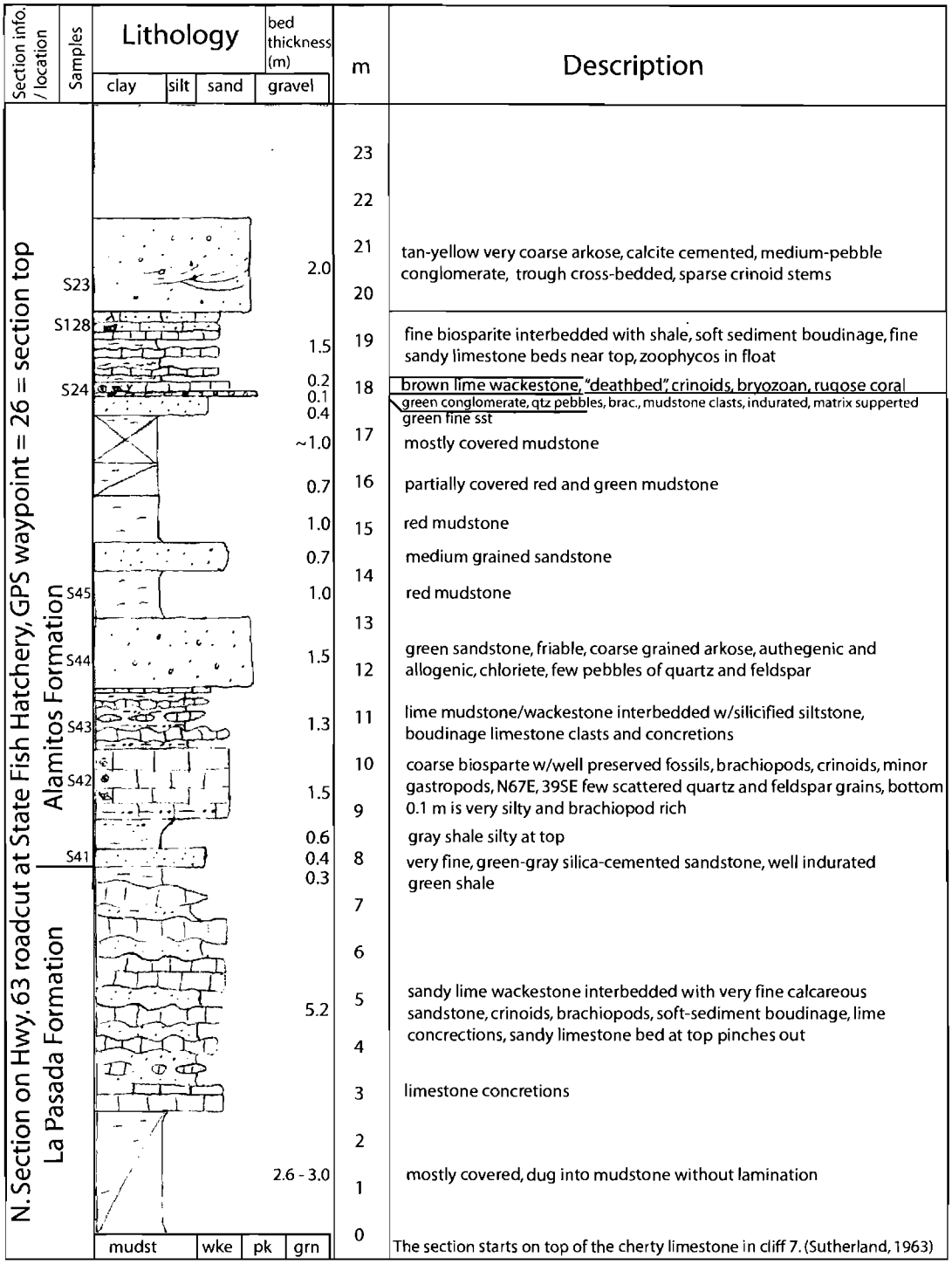

Figure C.2. N. Section on Hwy 63 Roadcut.

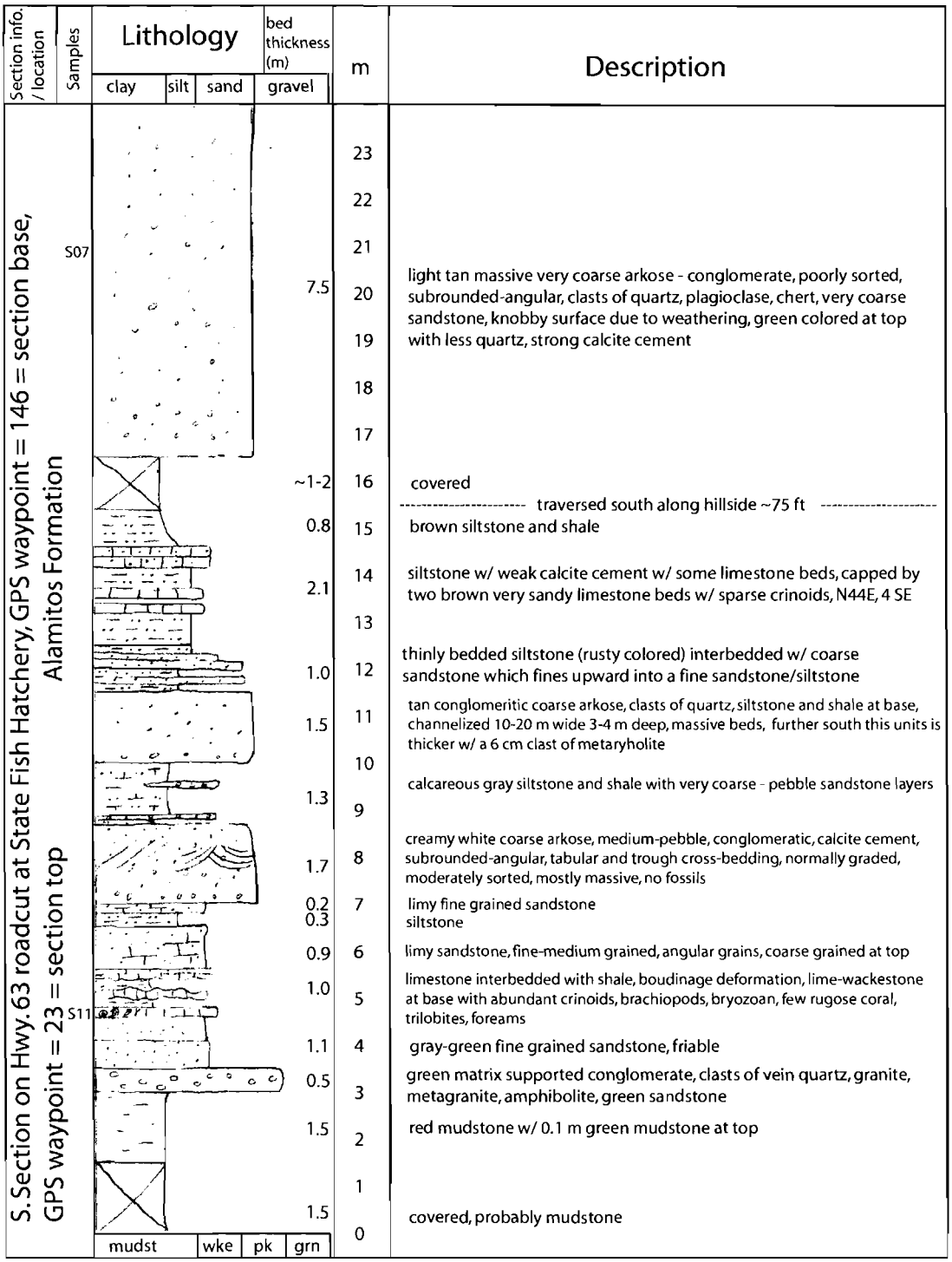

Figure C.3. S. Section on Hwy 63 Roadcut.

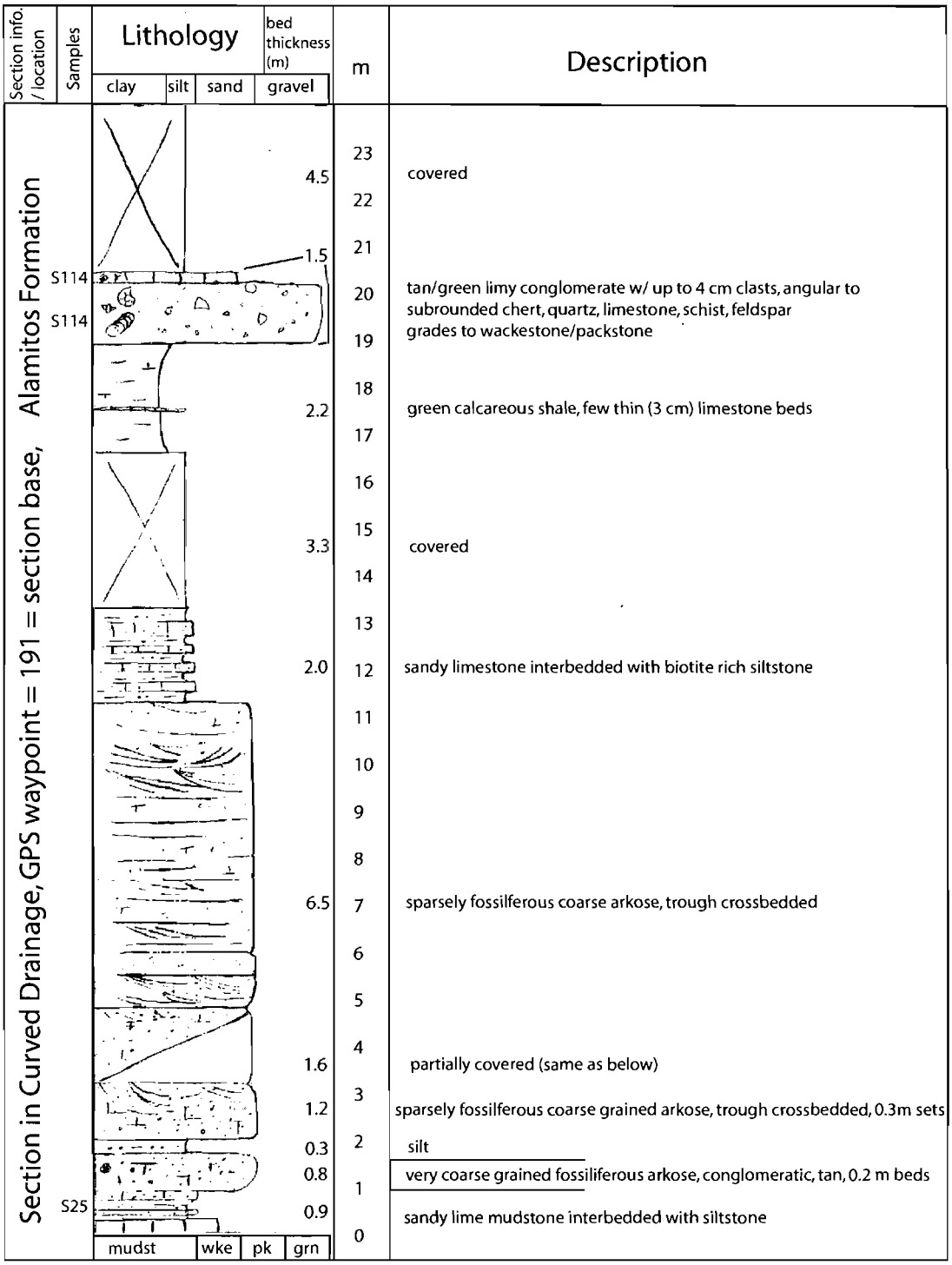

Figure C.4. Section in Curved Drainage.

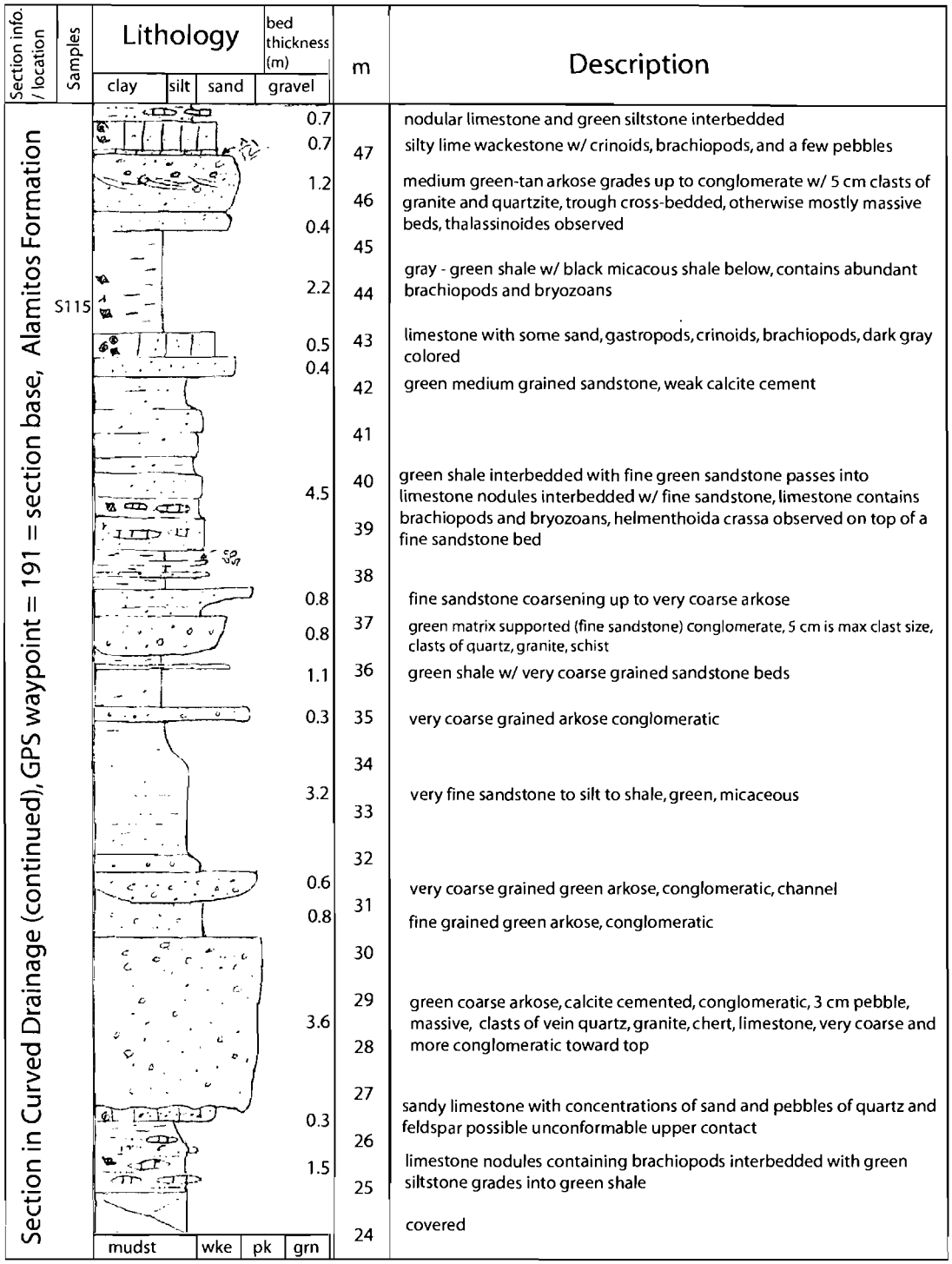

Figure C.4. (continued).

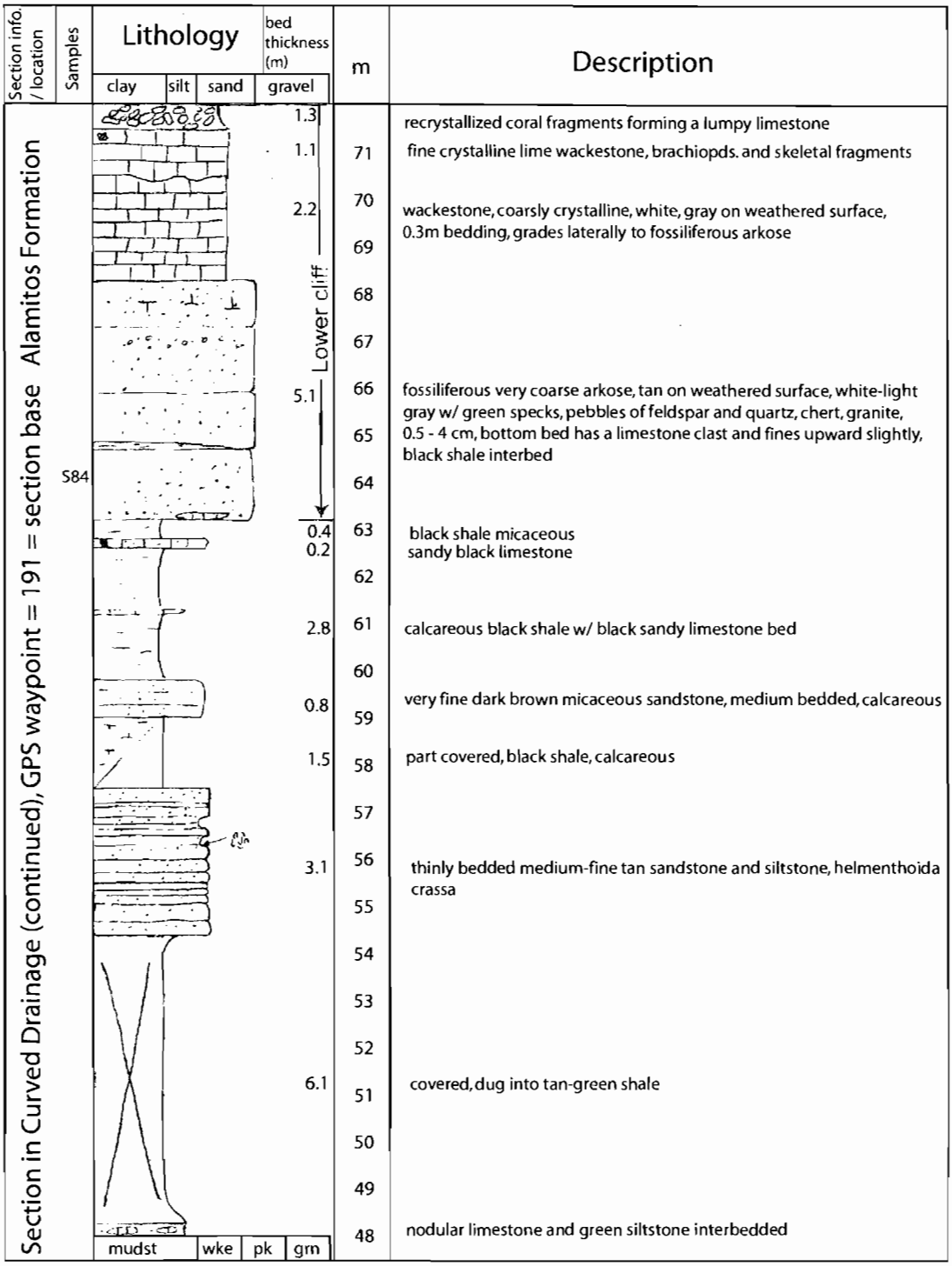

Figure C.4. (continued).

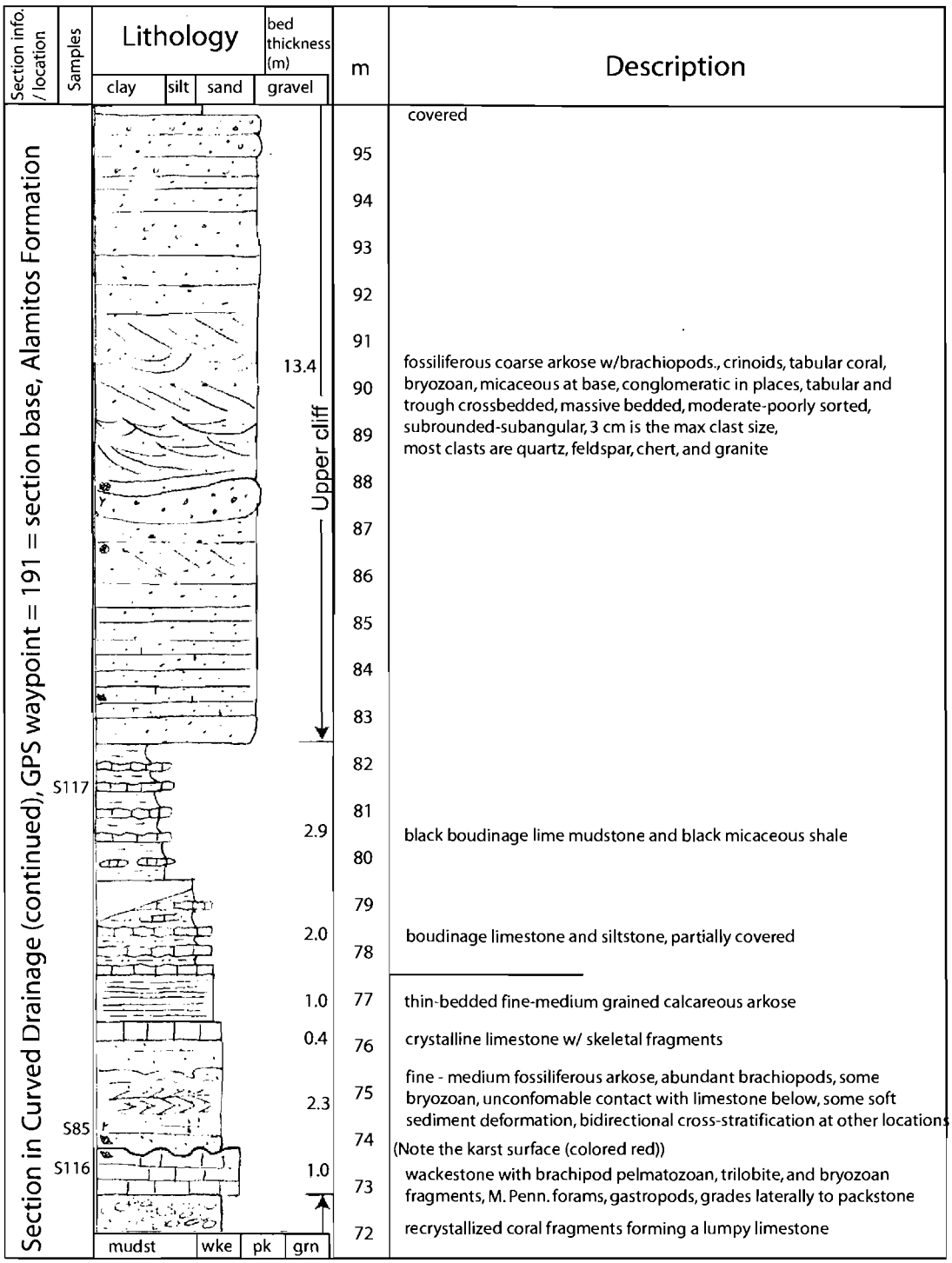

Figure C.4. (continued).

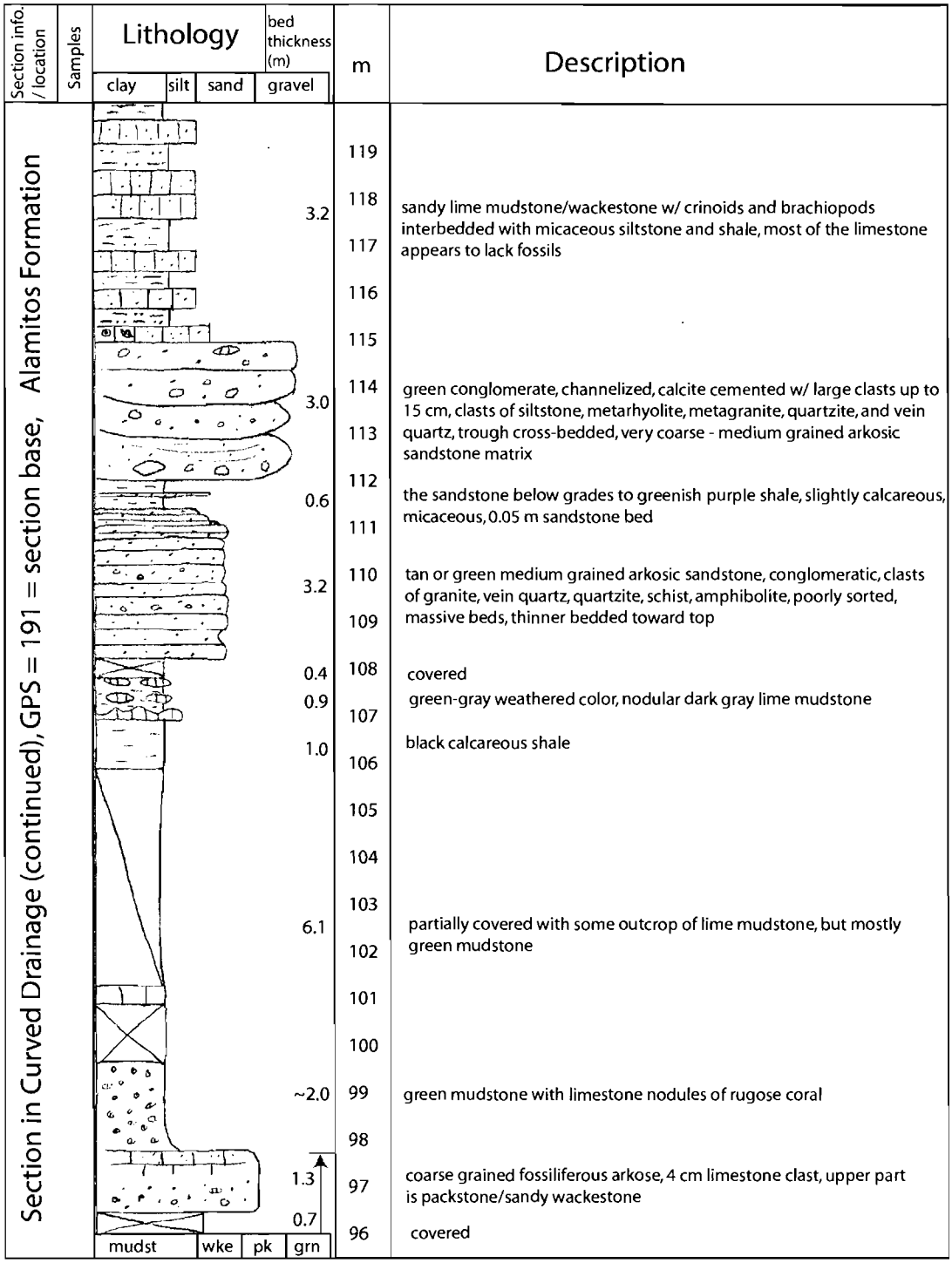

Figure C.4. (continued).

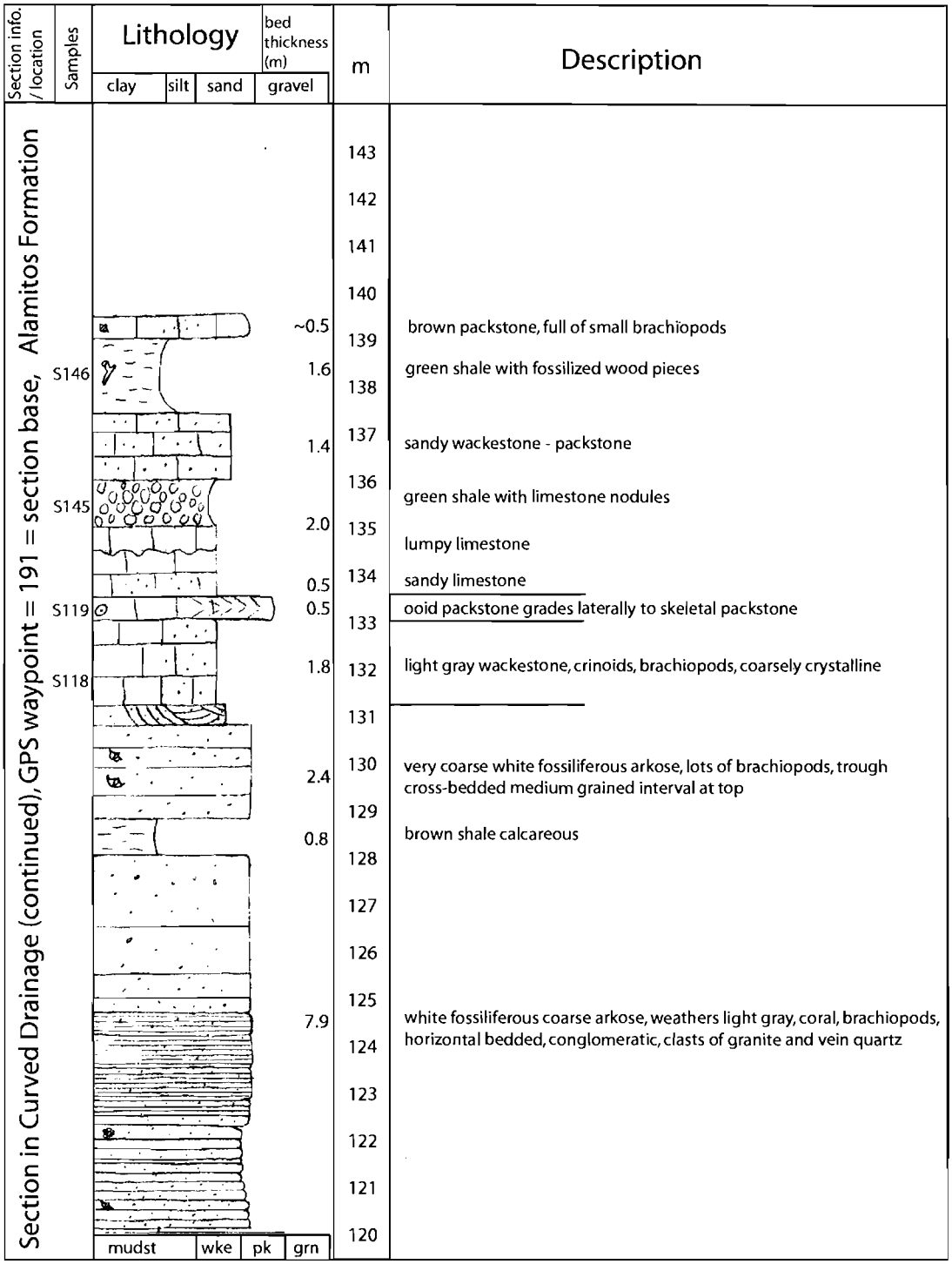

Figure C.4. (continued).

APPENDIX D

PLATFORM SUBSIDENCE

Subsidence and geohistory modeling is useful for determining tectonic subsidence history of sedimentary basins. A geohistory analysis was performed in this study to calculate the amount of tectonic subsidence on the Pecos platform. The Pecos platform was located at the southern end of the Taos Trough, an actively subsiding intracratonic basin in the Pennsylvanian.

Sequential methods for geohistory analysis include the following:

1. First, stratigraphic data necessary for the analysis are gathered for the basin of interest. These data include lithologies, age, thickness, and paleobathymetry.

2. The thickness and age data are used to construct a sediment accumulation curve, i.e., a plot of total basin sediment thickness over time.

3. A correction for sediment compaction effects is applied to determine the 'true' thickness of strata in the basin.

4. Finally, subsidence due to isostatic effects, the load of sediments and oceanic water, are removed to construct a 'residual' or tectonic subsidence curve.

Stratigraphic data necessary for subsidence modeling of the Pecos Platform (model inputs) are summarized in Table D.1. These data were obtained from type-sections of the Alamitos and La Pasada Formation measured by *Sutherland* [1963]. Paleobathemetry values are estimated based on Sutherland's interpreted depositional environments. The stratigraphic data were modeled without paleobathemetric information, and results show that removing this data has little effect on the resulting tectonic subsidence curve.

Table D.1. Stratigraphic data used for subsidence modeling at the Pecos platform [*Sutherland*, 1963]. In modeling, a constant sedimentation rate is assumed for each formation division shown in this table.

Formation Name	Relative Age	Age at beginning of deposition (Ma)	Thickness (m)	Lithology (%)			Estimated paleobathemetry (m)	Depositional environment
				Sandstone and conglomerate	Limestone	Shale and siltstone		
La Pasada	Morrowan	322	62	23	27	50	5	Shallow marine with less common non-marine intervals
La Pasada	Atokan	311	57	18	39	43	20	Shallow marine with less common non-marine intervals
La Pasada	Desmoinesian	307	178	9	67	24	70	Neritic, off-shore marine with infrequent near-shore marine and nonmarine
Alamitos	Middle Desmoinesian to Virgillian	303	389	50	21	29	15	Shallow marine to shelf
Sangre De Cristo	Permian	290						Continental and fluvial

The program BasinMod 1-D [*Platte River Associates, Inc.*, 2006] was used for subsidence modeling. Both the sediment accumulation curve corrected for compaction and the resulting tectonic subsidence curve for the Pecos platform are shown in Figure D.1. Model results show that ~450 meters of tectonic subsidence occurred on the Pecos platform by the end of the Pennsylvanian and ~165 m during the Desmoinesian interval of the Pennsylvanian. The shape of the subsidence curve indicates that gradual subsidence began in Morrowan time and increased to a higher and sustained rate at the beginning of the Atokan series.

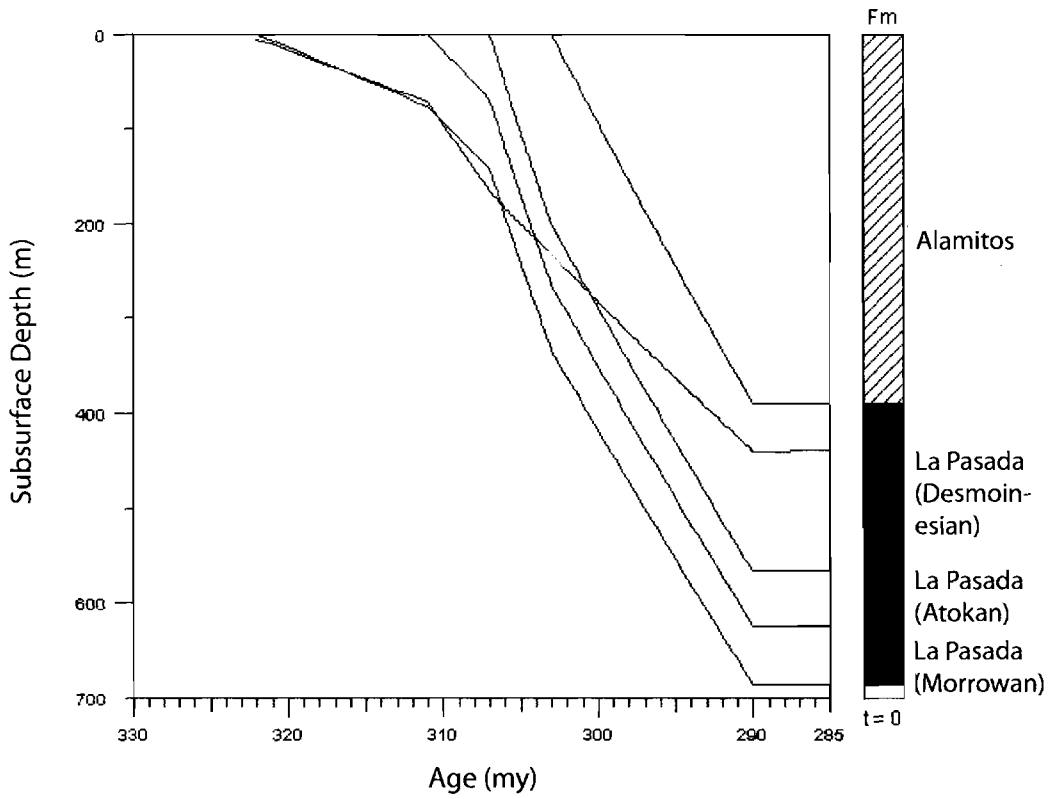

Figure D.1. Subsidence history model of the Pecos platform. Blue dashed line indicates tectonic subsidence. Solid black lines depict the total basin subsidence (total sediment thickness) for each of the formations or formation parts. At any given time, the distance between the lowest black line and the blue dashed line represents the subsidence due to sediment load.

REFERENCES

Algeo, T. J. (1991), Lower-Middle Pennsylvanian Gobbler Formation: Eustatic and tectonic controls on carbonate shelf cyclicity, *Geological Society of America, Rocky Mountain Section, Abstracts with Programs*, *23*(4), 2.

Allen, J. R. L. (1980), Sand waves: a model of origin and internal structure, *Sedimentary Geology*, *26*, 281–328.

Baltz, E. H., and G. O. Bachman (1956), Notes of the geology of the southeastern Sangre de Cristo Mountains, New Mexico, *New Mexico Geological Society Guidebook, 7th Field Conf.*, pp. 96–108.

Baltz, E. H., and D. A. Myers (1984), Porvenir formation (new name) and other revisions of nomenclature of Mississippian, Pennsylvanian, and lower Permian rocks, southeastern Sangre De Cristo Mountains, New Mexico, *U.S. Geological Survey Bullitin 1537-B*, 39pp.

Baltz, E. H., and D. A. Myers (1999), *Stratigraphic framework of upper Paleozoic rocks, southeastern Sangre De Cristo Mountains, New Mexico, with a section on speculations and implications for regional interpretation of Ancestral Rocky Mountains paleotectonics*, New Mexico Bureau of Mines and Mineral Resources, 269pp.

Banks, N. L. (1973), Tide-dominated offshore sedimentation, Lower Cambrian, north Norway, *Sedimentology*, pp. 213–228.

Bauer, P. W., and S. Ralser (1995), The picuris-pecos fault; repeatedly reactivated, from Proterozoic to Neogene, *New Mexico Geological Society Guidebook*, *46*, 111–115.

Bauer, P. W., S. Ralser, S. Kelley, and J. Marcoline (1997), 100-km scale, long-lived fault systems in the southern Sangre de Cristo Mountains, New Mexico, *Geological Society of America, Abstracts with Programs*, *29*(6), 276.

Blakey, R. (2006), Global plate tectonics and paleogeography, Northern Arizona University, Department of Geology.

Brill, K. G. (1952), Stratigraphy in the Permo-Pennylvanian zeugogeosyncline of Colorado and northern New Mexico, *Geological Society of America Bulletin*, *63*, 809–880.

Casey, J. M. (1980), Depositional systems and basin evolution of the late Paleozoic Taos Trough, northern New Mexico, Ph.D. thesis, University of Texas, Austin.

Casey, J. M., and G. O. Bachman (1979), Pennsylvanian coarse-grained fan deltas associated with the Uncompahgre Uplift, Talpa, New Mexico, *New Mexico Geological Society Guidebook, 30th Field Conf.*, pp. 96–108.

Cather, S. M., W. C. McIntosh, and S. A. Kelley (2004), *Tectonics, geochrology, and volcanism in the Southern Rocky Mountains and Rio Grande Rift*, vol. Bulletin 160, New Mexico Bureau of Geology and Mineral Resources.

Cole, A. R., P. T. Harris, and J. B. Keene (1995), *Foramininifers as facies indicators in a tropical, macrotidal environment: Torres Strait-Fly River delta, Papua New Guinea*, pp. 213–223, Blackwell Science.

De Voto, R. H. (1972), Pennsylvanian and Permian stratigraphy and tectonism in central Colorado, *Colorado School of Mines Quarterly, 67*, 139–185.

Dunham, R. J. (1962), *Classification of carbonate rocks according to depositional tecture*, pp. 108–121, American Association of Petroleum Geologists.

French, B. M. (1998), *Traces of Catastrophe: A Handbook of Shock-Metamorphic Effects in Terrestrial Meteorite Impact Structures*, Lunar and Planetary Institute, Houston, 120pp.

Galloway, W. E., and L. F. Brown (1973), Depositional systems and shelf-slope relations on cratonic basin margin, uppermost Pennsylvanian of north-central Texas, *Association of Petroleum Geologists Bulletin*, pp. 1185–1218.

Goddard, E. N., P. D. Trask, R. K. D. Ford, O. N. Rove, J. T. Singewald Jr., and R. M. Overbeck (1979), *Rock-Color Chart*, Huyskes-Enschede.

Gong, S. Y. (1992), Sedimentological studies of Pennsylvanian carbonates of the southern Sangre De Cristo Mountians, New Mexico, Ph.D. thesis, University of Texas, Dallas.

Gong, S. Y., and J. D. Humphrey (1991), Eustatic versus tectonic conrols on carbonate cycles of the La Pasada Formation (Pennsylvanian), southern Sangre de Cristo Mountains, New Mexico, *Abstracts with Programs - Geological Society of America, Rocky Mountain Section, 23*(4), 25.

Hamblin, W. K. (1965), Internal structures of "homogeneous" sandstones, *Kansas Geological Survey Bulletin, 175*, 1–37.

Hanford, C. R., and S. P. Dutton (1980), Pennsylvanian-early Permian depositional systems and shelf-margin evolution, Palo Duro Basin, Texas, *Association of Petroleum Geologists Bulletin*, pp. 88–106.

Hjulstrom, F. (1939), *Transportation of detritus in moving water*, pp. 5–31, American Association of Petroleum Geologists.

Johnson, R. B. (1973), *Geologic Map of the Pecos Quadrangle, San Miguel and Santa Fe Counties, New Mexico*, United States Geological Survey.

Keene, J. B., and P. T. Harris (1995), *Submarine cementation in tide-generated bioclastic sand dunes:epicontinental seaway, Torres Strait, north-east Australia*, pp. 225–236, Blackwell Science.

Klein, G. d., and J. B. Kupperman (1992), Pennsylvanian cyclothems: Methods of distinguishing tectonically induced changes in sea level from climatically induced changes, *Geological Society of America Bulletin*, pp. 166–175.

Klein, G. d., and D. A. Willard (1989), Origin of Pennsylvanian coal-bearing cyclothems of North America, *Geology*, pp. 152–155.

Kleinspehn, K. L., R. J. Steel, E. Johannessen, and A. Netland (1984), Conglomeratic fan-delta sequences, late Carboniferous - carly Permian, western Spitsbergen, *Canadian Society of Petroleum Geologists Memoir 10*, pp. 279–294.

Lanckneus, J., and G. de Moor (1995), *Bedforms on the Middelkerke Bank, southern North Sea*, pp. 33–51, Blackwell Science.

Lowe, D. (1982), Sediment gravity flows: II. Depostional models with specific reference to the deposits of high-density turbidity currents, *Journal of Sedimentary Petrology*, pp. 279–297.

Merriam, D. F. (1964), Symposium on cyclic sedimentation, *Kansas Geological Survey Bulletin.*

Miall, A. D. (1990), *Principles of Sedimentary Basin Analysis*, Springer-Verlag, 668pp.

Miller, J. P., P. K. Sutherland, and A. Montgomery (1963), *Geology of part of the southern Sangre De Cristo Mountains, New Mexico*, State Bureau of Mines and Mineral Resources New Mexico Institute of Mining and Technology, 103pp.

Miller, K. B., and R. R. West (1993), Reevaluation of Wolfcampian cyclothems in northeastern Kansas: Significance of subaerial exposure and flooding surfaces, *Current Research on Kansas Geology, Bulletin 235*, pp. 1–26.

Mount, J. (1984), Mixing of siliciclastic and carbonate sediments in shallow shelf environments, *Geoology, 12*, 432–435.

Mount, J. (1985), Mixed siliciclastic and carbonate sediments: a proposed first order textural and compositional classification, *Sedimentology, 32*, 445–442.

New Mexico Geological Society (1996), *New Mexico Highway Geologic Map*, New Mexico Geological Society, Inc.

Nio, S. D., and C. S. Yang (1991), Diagnostic attributes of clastic tidal deposits: a review, *Canadian Society of Petroleum Geologists Memoir 16*, pp. 3–28.

Platte River Associates, Inc. (2006), BasinMod 1-D, http://www.platte.com.

Reed, A., and G. Rawling (2002), *Geology of Pecos 7.5 Minute Quadrangle*, New Mexico Bureau of Geology and Mineral Resources.

Reed, C. B., and G. H. Wood (1947), Distribution and correlation of Pennsylvanian rocks in late Paleozoic sedimentary basins of northern New Mexico, *Geology, 55*, 220–236.

Ross, C. A., and J. R. P. Ross (1988), *Late Paleozoic transgressive-regressive deposition*, pp. 227–247, Society of Economic Paleontologists and Mineralogists Special Publication 42.

Soegaard, K. (1990), Fan-delta and braid-delta systems in Pennsylvanian Sandia Formation, Taos Trough, northern New Mexico; depositional and tectonic implications, *Geological Society of America Bulletin, 102*(10), 1325–1343.

Sutherland, P. K. (1963), *Paleozoic Rocks*, pp. 22–46, State Bureau of Mines and Mineral Resources New Mexico Institute of Mining and Technology.

Sutherland, P. K., and F. H. Harlow (1973), *Pennsylvanian brachiopods and biostratigraphy in southern Sangre de Cristo Mountains, New Mexico*, New Mexico Bureau of Mines and Mineral Resources, 173pp.

Tankard, A. J. (1986), *On the depositional response to thrusting and lithospheric flexure: Examples from the Appalachian and Rocky Mountain basins*, pp. 369–392, International Association of Sedimentologists Special Publication 8.

Thompson, M. L. (1942), Pennsylvanian System in New Mexico, *New Mexico State Bureau of Mines Bullitin, 17.*

Tweto, O. (1980), Summary of Laramide Orogeny in Colorado, *Rocky Mountain Association of Geologists*, pp. 129–134.

Ude, S. C. (1992), Depositional styles of the middle Pennsylvanian upper Madera formation, Taos Trough, northern New Mexico, Master's thesis, University of Texas, Dallas.

United States Geological Survey (1961), *Pecos Quadrangle, New Mexico 7.5 Minute Series (Topographic)*, United States Geological Survey.

Van Wagoner, J. C., H. W. Posamentier, R. M. . Mitchem, P. R. Vail, J. F. Sarg, T. S. Loutit, and J. Hardenbol (1988), *An overview of the fundamentals of sequence stratigraphy and key definitions*, pp. 39–45, Society of Economic Paleontologists and Mineralogists Special Publication 42.

Wanless, H. R., and J. M. Weller (1932), Correlation and extent of Pennsylvanian cyclothems, *Geological Society of America*, pp. 1003–1016.

Weiss, M. P., P. A. Goddard, and X. Picard (1978), Marine geology of reefs and inner shelf, Chichiriviche, Estado Falcon, Venesuela, *Marine Geology, 28*, 210–244.

Wiberg, T. L., and G. A. Smith (1991), Cyclic sedimentation on a middle pennsylvanian (desmoinesian) carbonate-clastic ramp, Sandia Mountains, north-central New Mexico, *Abstracts with Programs - Geological Society of America, Rocky Mountain Section*, *23*(4), 105.

Young Jr., J. A. (1945), Paleontology and stratigraphy of the Pennsylvanian strata near Taos, New Mexico, Ph.D. thesis, Harvard University.